Solar radiation, longwave radiation and daylight

Annex to CIBSE Guide A chapter 2

January 2015

Contents

Solar radiation, longwave radiation and daylight

0 Introduction

This annex contains information on the creation of solar and illuminance data for building design as previously included in CIBSE Guide J (2002) (now withdrawn).

Section 1 provides a general introduction to radiation and illuminance.

Section 2 concentrates on the provision of design data derived directly from observed shortwave radiation and sunshine, using mainly UK observed data. It provides the essential knowledge needed to calculate the underlying solar geometry and to estimate solar radiation from sunshine and cloud amount. It includes a full description of the recommended accurate methodology for converting an observed time series of hourly global and diffuse horizontal irradiation data into the corresponding time series for any inclined plane. It also supports the monthly mean and design 97.5 percentile exceedence global radiation and associated diffuse radiation tables in CIBSE Guide A, chapter 2, for 14 UK sites.

Section 3 considers the theoretical estimation of solar radiation on a world-wide basis and provides the basis for the world clear sky irradiance tables.

Section 4 considers longwave radiation exchanges with the atmosphere and the ground.

Section 5 deals with illuminance.

Appendix A1 discusses quality control of global solar irradiation data.

Appendix A2 provides a detailed explanation of the processes used to fill gaps in hourly diffuse irradiation records.

Appendix A3 describes the various algorithms used in the development of the solar data

1 General

The radiation received at the surface of the earth is conveniently divided into shortwave radiation with wavelengths between about 0.29 and 4 μm, and thermal longwave radiation emitted from the terrestrial atmosphere with wavelengths between 4 and 100 μm. The shortwave solar radiation spectrum can be further broken down into three bands:

— ultra-violet: wavelengths between 0.29 and 0.4 μm

— visible: wavelengths between 0.4 and 0.7 μm

— shortwave infra-red band: wavelengths between 0.70 to 2.6 μm.

There is very little energy in the solar spectrum at wavelengths beyond 2.6 μm. Ultra-violet radiation can be classified into UV-A (315–400 nm), UV-B (280–315 nm) and UV-C (100–280 nm). The statospheric ozone layer virtually eliminates UV irradiation below 290 nm. The magnitude of the damaging UV-B element in the external terrestrial environment is very strongly dependent on the amout of ozone in the atmosphere and also on the relative path lengths through the atmosphere. When compared with the UV-B impacts, changes in ozone make only relatively small impacts on UV-A irradiation.

While, theoretically, the illuminance may be derived from knowledge of the spectral irradiance in the visible region by applying the CIE $V(\lambda)$ function, such continuous observed spectral data are not available. The derivation of UK illuminance data in this annex is based on the use of observed hourly global and diffuse irradiation data in conjunction with luminous efficacy algorithms. The luminous efficacy algorithms used are based on simultaneous UK observations of global illuminance and global irradiance and also of diffuse illuminance and diffuse irradiance.

2 Solar radiation estimates based on meteorological observations

2.1 Fundamental concepts

The distinction between irradiance and irradiation is important. The instantaneous flux of solar radiation on any surface is termed the solar irradiance. It is the flow of radiant energy per unit time falling on unit area ($W \cdot m^{-2}$). The solar energy received per unit area over a stated period of time is known as the solar irradiation. Irradiation data are usually presented by meteorological services in megajoules per square metre ($MJ \cdot m^{-2}$). However, in this document, irradiation data are presented in kilowatt-hours per square metre ($W \cdot h \cdot m^{-2}$).
(*Note*: 1 $W \cdot h = 3.6 \times 10^{-3}$ MJ.)

The shortwave solar radiation falling on any surface can be divided into three components:

— direct beam radiation (B) received from the sun

— diffuse radiation (D) received at the surface from the sky vault after scattering and inter-reflection within the atmosphere (including reflection from clouds)

— reflected diffuse radiation (R).

The surface reflected component (R) arises from inter-reflection of beam and diffuse sky radiation, both from the ground and also from the surrounding natural and human constructed obstructions. In addition to scattering there is considerable atmospheric absorption of the solar beam by gases such as carbon dioxide and by water vapour. These shortwave absorption effects are particularly important in the shortwave infrared region, i.e. at wavelengths beyond 0.7 μm. There are a number of quite deep absorption bands in the infrared region due to absorption by water vapour and by carbon dioxide. There is very little solar radiation at wavelengths beyond 2.6 μm.

A significant proportion of incoming shortwave radiation passing through a cloudless sky is scattered by the molecules and larger particles in the atmosphere and arrives at the surface of the earth as diffuse irradiation. The atmospheric molecular scattering is inversely proportional to the fourth power of the wavelength. It is this wavelength dependence that causes the sky to appear blue. Particulates and water drops in the atmosphere absorb some of, and scatter some of the incoming energy. The additional scattering under clear sky conditions adds to the diffuse energy coming from the clear sky, but is less blue-rich than the light due to molecular scattering. The wavelength dependence of this additional scattered diffuse energy typically is inversely proportional to the wavelength to the power 1.3. The colour of the of the cloudless sky changes from deep blue to pale blue, or even near white, in hot humid climates as this scattering increases. When present, clouds produce a stronger scattering across the whole shortwave radiation spectrum. Their presence shifts the balance between beam and diffuse sky radiation. Simultaneously the diffuse sky radiation spectrum changes, becoming far whiter. The sum of the beam irradiance and the two components of diffuse irradiance on any plane of tilt β and orientation α is termed the global irradiance $G(\beta,\alpha)$ on that plane. Thus:

$$G(\beta,\alpha) = B(\beta,\alpha) + D(\beta,\alpha) + R(\beta,\alpha) \quad (1)$$

where $G(\beta,\alpha)$ is the global irradiance ($W \cdot m^{-2}$) on a plane of orientation α (°) and tilt β (°), $B(\beta,\alpha)$ is the beam irradiance on the plane ($W \cdot m^{-2}$), $D(\beta,\alpha)$ is the diffuse irradiance on the plane ($W \cdot m^{-2}$) and $R(\beta,\alpha)$ is the reflected irradiance on the plane ($W \cdot m^{-2}$).

While the shape of the extraterrestrial spectral irradiance curve is fairly close to that of a black body at 5900 K, the solar spectrum at the surface is far more complex, as shown in Figure 1. The dips in the curve indicate absorption due to various atmospheric constituents. In the infra-red region, the deep dips are due mainly to water vapour and carbon dioxide.

There are two useful spectral computational models for estimating the cloudless day global and diffuse spectral irradiance on horizontal surfaces in the public domain, available through the Internet (Spectrl2 and Smart2). US resources may be accessed through the Solar Radiation Resource Information website (http://www.nrel.gov/rredc/). These resources include the *National Renewable Energy Laboratory (NREL) Spectral Solar Radiation Data Base*, the *Solar Radiation Data Manual for Buildings*, and the *Solar Spectral Model for Clear Days*.

The calculations also take into account absorption by ozone. The amount of ozone exerts a strong influence on the amount of UV-B radiation received at the earth's surface. UV-B radiation is particularly damaging biologically, due to the high energy of the photons.

Figure 1 below shows the calculated (using Spectrl2) global and diffuse spectral irradiances for cloudless conditions on horizontal surfaces at sea level against wavelength, with the sun at 30 degrees at mean solar distance. The precipitable water vapour in the atmosphere was set as 2 cm, typical of summer in the UK. The Angstrom turbidity at 1000 nm β_A was set at 0.083. (Typical observed values in Europe are 0.05 for rural sites and 0.1 for urbam sites.) The value 0.083 was chosen to yield a calculated Linke turbidity factor of 3.5, for consistency with the radiation tables given in this Guide. Figure 2 below gives the corresponding ratio of spectral diffuse to spectral global irradiance for horizontal surfaces, D_λ / G_λ , as a function of wavelength. Note that the clear sky ultra-violet irradiance is predominantly diffuse and the clear sky infra-red irradiance on horizontal surfaces is predominantly beam irradiation. The corresponding values of the luminous efficacy are given in the caption. Note that the luminous efficacy of the blue sky is greater than the luminous efficacy of the global radiation because its infra-red content is relatively low.

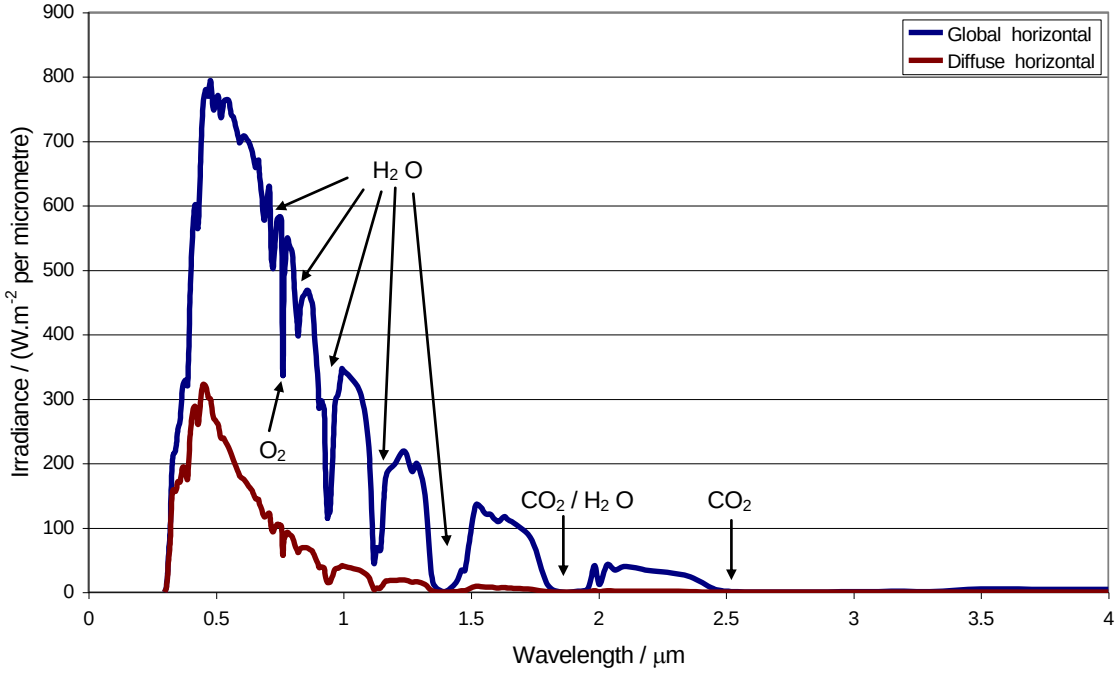

Figure 1 Calculated clear sky global and diffuse irradiances on a horizontal surface for solar altitude of 30° (global irradiance: 476 W·m^{-2}; diffuse irradiance: 144 W·m^{-2}; global luminous efficacy: 113 lumen·W^{-1}; diffuse luminous efficacy: 104 lumen·W^{-1})

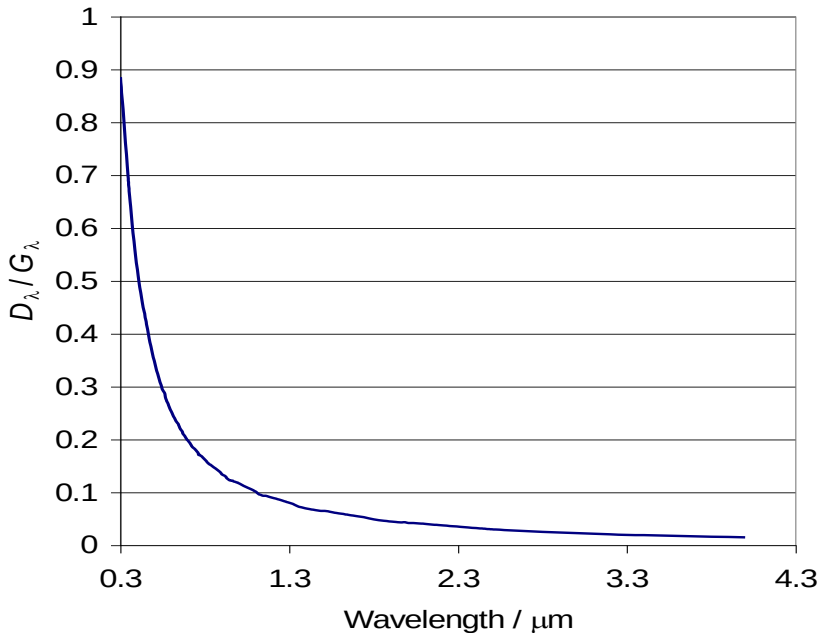

Figure 2 Ratio of the clear sky diffuse spectral irradiance on a horizontal surface (D_λ) to the spectral global irradiance on a horizontal surface (G_λ) for the spectrum shown in Figure 1; note the dominance of diffuse irradiation in the ultra-violet region and of beam radiation in the infra-red region

2.2 Solar radiation notation

The notation used within this document follows that adopted in the 4th edition of the *European Solar Radiation Atlas*[1]. This project was funded by the European Commission.

Common integration periods used for compiling shortwave radiation observations are the month, the day and the hour. It is sound practice to state the integration period. The symbol convention for these periods used in this document follows European Union practice. The subscripts used to identify the integration periods are 'm' for monthly integration, 'd' for daily integration and 'h' for hourly integration. No subscript is used when referring to irradiances. Additional subscripts 'c' are used to denote clear sky conditions and 'b' to denote overcast conditions (i.e. 'bewolken'). A monthly mean hourly value is presented in the form $(G_h)_m$, in this case the monthly mean hourly global irradiation on a horizontal surface. The irradiation on a sloping surface is indicated by the addition of (β,α) to describe the slope tilt β and the slope azimuth angle α, refer to Figure 3, see section 2.7. Thus $(G_h(\beta,\alpha))_m$ is the monthly mean hourly global irradiation on an inclined plane. The absence of (β,α) always indicates a horizontal plane. The subscript 'n' is used for normal incidence, i.e. B_n solar beam irradiance normal to the rays of the sun.

2.3 Solar radiation measurements and their accuracy

Ground based measurements of global shortwave radiation (G) are made using hemispherically sensitive instruments, called pyranometers, which measure the downward solar radiation flux falling on horizontal surfaces. These measurements combine the beam (B) and diffuse irradiance (D) components. In the UK, operational pyranometers of high quality are used in the Met Office networks and significant attention is given to maintaining calibration standards. Such shortwave pyranometer measurements provide the basis of all the tabulated observed UK irradiation and illuminance data, which have been statistically processed for this document. Illuminance data have been derived from shortwave hourly irradiation using luminous efficacy relationships, see section 5.3.

The diffuse radiation on horizontal surfaces is measured in the UK radiation network using suitably designed shading rings so mounted as to shield the receiving surface of the pyranometer from the direct rays of the sun. The position of the shadow band has to be adjusted regularly as the declination changes. Serious overestimates will occur if observers fail to ensure accurate day-by-day adjustment. Suitable corrections have to be applied to allow for the shading effects of shadow bands themselves on the diffuse component[(2)]. The Met Office applies what is known as the isotropic correction. This is calculated from the geometry of the shadow band assuming a sky of uniform radiance. Additional non-isotropic shade ring corrections have not been applied.

At a few sites, radiation measurement instruments with a very narrow angular band of acceptance, called pyrheliometers, are used in conjunction with sun-following trackers to measure the direct beam irradiation as a separate element. However all estimates of measured direct beam irradiation in this document have been formed from the differences between the measured global, and measured diffuse horizontal irradiation in conjunction with algorithmic estimates of the associated solar geometry, normally calculated at the mid-hour of the observation period. Unfortunately at low solar elevations this procedure gives estimates of irradiance normal to the beam of limited accuracy. Therefore all records obtained at low solar altitudes should be checked to ensure that the estimated normal incidence beam irradiation lies within acceptable limits. Values of solar irradiation at low solar altitudes that may cause computational problems must be replaced with acceptable values using theoretical models in conjunction with observed cloud amounts.

Observed irradiance values are not normally available from meteorological services; irradiation values are normally provided. The estimation of observed irradiation is achieved by integrating the observed irradiance values with respect to time over a stated time interval. This time interval must be stated. Usually, hourly integration periods are used in published records. Observed solar irradiation data and sunshine data are assembled by the Met Office for publication as irradiation values integrated over each integral hour in local apparent time (LAT) (i.e. solar time). Published UK irradiation values thus run from 10:00 to 11:00, 11:00 to 12:00 LAT etc. This is common international but not universal meteorological practice. All radiation data in this document are presented using LAT, see section 2.6.

2.4 Angular movements of the sun during the seasons

The angular movements of the sun as seen from any point on the surface of the earth depend on the latitude of the site, the date in the year and the time of day. The key input variable in the estimation of the solar geometry is the solar declination, i.e. the angle between the direction of the centre of the solar disk and the equatorial plane. The declination is a continuously varying function of time. The summer and winter solstices, i.e. the longest and shortest days, occur when the declination reaches its maximum and minimium values, respectively, for that hemisphere. The declination on any given day in the southern hemisphere has the opposite sign to that in the northern hemisphere on that same day.

2.5 Time systems used in conjunction with solar geometry and solar radiation predictions

It is strongly recommended that all calculations of the solar geometry are carried out in solar time, usually called local apparent time (LAT). Solar noon at any place is defined as the instant the sun crosses the north-south meridian. For trigonometric calculations, solar time is converted to its angular form, the ‘solar hour angle’, referenced to solar noon. The earth rotates through 15 degrees in each hour. Therefore, 14:00 h LAT represents an hour angle of 30° and 10:00 h LAT represents an hour angle of –30°.

In this document, observed irradiation data are presented in LAT on an hour-ending basis. Thus irradiation data for 11:00 to 12:00 hours are identified as 12:00 h in the tables. In contrast calculated irradiance and illuminance data are calculated in this document as mid-hour values, except for the sunrise and sunset hour. The tabulated time is the actual calculation time except in the sunrise and sunset hour, see footnotes to tables.

Theoretical estimates of solar irradiation are achieved through the calculation of irradiance at specific time intervals. The irradiation values are estimated by numerical integration of such irradiance estimates over defined time periods, usually one hour. It is assumed here that the irradiation can be regarded as being approximately equal to the mid-hour irradiance. The irradiance data presented in this document are normally calculated at the mid-point of the standard irradiation integration period. Thus, for hours when the sun is up for the whole hour, the calculations have been performed on the half-hour, i.e. 10:30, 11:30 LAT etc. For the hours during which sunrise and sunset occur, the solar geometry has been calculated using as input data, for the morning, the solar time midway between sunrise and the end of the first sunlit hour of the day and, for the evening, midway between the beginning of the last hour and sunset in the last sunlit hour of the day. The irradiance values for these two hours are estimated using the solar geometry corresponding to the mid-point of the integration interval. In the sunrise and sunset hours, the estimation of irradiation involves integration over periods of less than one hour. Thus the assumption that the calculated global irradiance is a good approximation to the hourly irradiation does not hold for these beginning and end of daylight hours. The appropriate integration procedure is discussed in section 3.3.6.

2.6 Conversion of local mean time to local apparent time (solar time)

Local mean time (LMT), often called ‘clock time’ or ‘civil time’, differs from local apparent time (LAT), or ‘solar time’, by an amount varying with the longitude of the place, the reference longitude of the time system in use and the time of year. Most climate observations in the UK are made in synoptic time, i.e. Greenwich Mean Time (GMT). Summertime is not adopted for making meteorological measurements. Important exceptions are solar irradiation and bright sunshine measurements, which are normally summarised in LAT. As climatic data are provided in two different systems of time, it is sometimes important to be able to inter-relate the two time systems, especially in the case of simulation studies. In general, as the solar irradiance is a discontinuous function at sunrise and sunset and the synoptic weather variables are continuous, it is more accurate to interpolate synoptic values into solar time than to interpolate irradiation values into synoptic time, when compiling consistent data sets for simulation.

Conversion requires knowledge both of the longitude of the site and the reference longitude of the time system being used. The conversion also requires application of the equation of time, which accounts for certain perturbations in the rotation of the earth about its polar axis. In the UK, LMT is Greenwich Mean Time (GMT) in winter and British Summer Time (BST) in summer. Many countries in the west of the European Union use West European Time (WET) and its summer time variants. Based on longitude 15°E, these nearby countries have time systems generally one hour ahead of GMT and BST. Telephone directories and airline timetables are useful sources of current time systems in use in different zones of different countries and also the existence or otherwise of summer time. It is European Union policy that the dates of the changes to and from summer time should be harmonised within the EU.

The conversion between the two systems of time requires the value of the equation of time for that day. The equation of time at noon at Greenwich is the difference in time between solar noon at longitude 0° and 12:00 GMT.

2.6.1 Formulae for conversion of time systems

The calculation of the value of the equation of time requires the day number in the year. This is converted into a day angle in the year. Note the day numbers and day angles are also used for other algorithmic procedures that are presented in this document.

Days are numbered continuously through the year to produce a Julian day number, J. January 1 = 1, February 1 = 32, March 1 = 57 in a non-leap year and 58 in a leap year etc. Each day in the year can be expressed in an angular form as a day angle, J', in degrees by multiplying J by 360/365.25.
The equation of time (EOT) is calculated as:

$$\text{EOT} = -0.128 \sin (J' - 2.80°) - 0.165 \sin (2J' + 19.7°) \quad (2)$$

Then:

$$\text{LAT} = \text{LMT} + (\lambda - \lambda_R) / 15 + \text{EOT} - c \quad (3)$$

where LAT is local apparent time (h), J' is the day angle in the year (°), λ is the longitude of the site (°) (positive values denote east), λ_R is the longitude of the time zone in which the site is situated (°) (positive values denote east), EOT is the equation of time (h) and c is the correction for summer time (h). Values of the equation of time for selected dates are given in Table 1.

Table 1 Equation of time (EOT) values associated with recommended CIBSE radiation calculation design dates expressed in decimal hours and in minutes (Source: *European Solar Radiation Atlas*[1])

Equation of time (EOT) expressed in hours and minutes for stated design day						
(*a*) Northern hemisphere (for clear day design days)						
Date	Jan 29	Feb 26	Mar 29	Apr 28	May 29	Jun 21
EOT (h)	–0.216	–0.255	–0.084	+0.042	+0.043	–0.029
EOT (min)	–13.0	– 13.5	– 5.1	+ 2.5	+ 2.6	–1.8
Date	Jul 4	Aug 4	Sep 4	Oct 4	Nov 4	Dec 4
EOT (h)	–0.072	+0.099	+0.027	+0.205	+0.274	+0.149
EOT (min)	–4.3	–5.9	+1.6	+12.3	+16.4	+8.9
(*b*) Southern hemisphere (for clear day design days)						
Date	Jan 4	Feb 4	Mar 4	Apr 4	May 4	Jun 4
EOT (h)	–0.079	–0.232	–0.204	–0.053	+0.054	+0.027
EOT (min)	–4.7	– 13.9	– 12.3	–3.2	+ 3.3	+1.6
Date	Jul 29	Aug 29	Sep 28	Oct 29	Nov 28	Dec 22
EOT (h)	–0.105	–0.007	+0.173	+0.276	+0.187	–0.195
EOT (min)	–6.32	–0.4	+10.4	+16.6	+11.2	–11.7
(*c*) Northern and southern hemispheres (mid–month design dates)						
Date	Jan. 17	Feb. 15	Mar.16	Apr. 15	May 15	Jun. 11
EOT (h)	–0.163	–0.241	–0.157	–0.006	+0.061	+0.009
EOT (min)	– 9.8	– 14.5	– 9.4	– 0.3	+ 3.7	+0.5
Date	Jul. 17	Aug.16	Sep. 16	Oct.16	Nov.15	Dec. 11
EOT (h)	–0.099	–0.070	+0.094	+0.250	+0.252	+0.106
EOT (min)	–5.9	–4.2	+5.6	+15.0	+15.1	+6.4

Example 1

Estimate the time of occurrence in British Summer Time of solar noon at Belfast on August 4.

Longitude of Belfast is 6° 13' W. The time system is BST. The time zone reference longitude is Greenwich 0° 0'; westward displacement is 6° 13' (i.e. 6.217°), hence:

$$(\lambda - \lambda_R) / 15 = (-6.217 - 0.0) / 15 = -0.414 \text{ hours} = -24.9 \text{ minutes}$$

LAT is 12:00. From Table 1, the EOT on August 4 is –5.9 minutes.

Therefore, in LMT, solar noon will occur at 12:00 – (–00:24.9) – (–00:05.9) minutes, i.e. 12:31 GMT or 13:31 BST.

2.7 Solar geometry

2.7.1 Angles describing solar geometry

Two angles are used to define the angular position of the sun as seen from a given point on the surface of the earth, see Figure 3. These are:

— Solar altitude, γ_s: the angular elevation of the centre of the solar disk above the horizontal plane.

— Solar azimuth, α_s: the horizontal angle between the vertical plane containing the centre of the solar disk and the vertical plane running in a true north–south direction. Solar azimuth is measured clockwise from due south in the northern hemisphere and anti-clockwise measured from due north in the southern hemisphere. Values are negative before solar noon and positive after solar noon. In the region of the equator, between the Tropic of Cancer and the Tropic of Capricorn, the sun will pass to the north at noon at some times of the year and to the south at noon at other times of the year.

Five other important angles for solar geometry are:

— Solar incidence angle on a plane of tilt α and slope β, $\nu(\beta,\alpha)$: the angle between the normal to the plane on which the sun is shining and the line from the surface passing through the centre of the solar disk. The cosine of $\nu(\beta,\alpha)$ is used to estimate the incident beam irradiance on a surface from the irradiance normal to the beam.

— Vertical shadow angle, sometimes called the vertical profile angle, γ_p: the angular direction of the centre of the solar disk, as it appears on a drawn vertical section of specified orientation see Figure 4.

— Wall solar azimuth angle, sometimes called the horizontal shadow angle, α_f: the angle between the vertical plane containing the normal to the surface and the vertical plane passing through the centre of the solar disk, i.e. the resolved angle on the horizontal plane between the direction of the sun and the direction of the normal to the surface, see Figure 4.

— Sunset hour angle, ω_s: the azimuth angle at astronomical sunset, used in certain algorithmic procedures.

— Declination angle, δ: the angle that the sun's rays make with the equatorial plane at any instant.

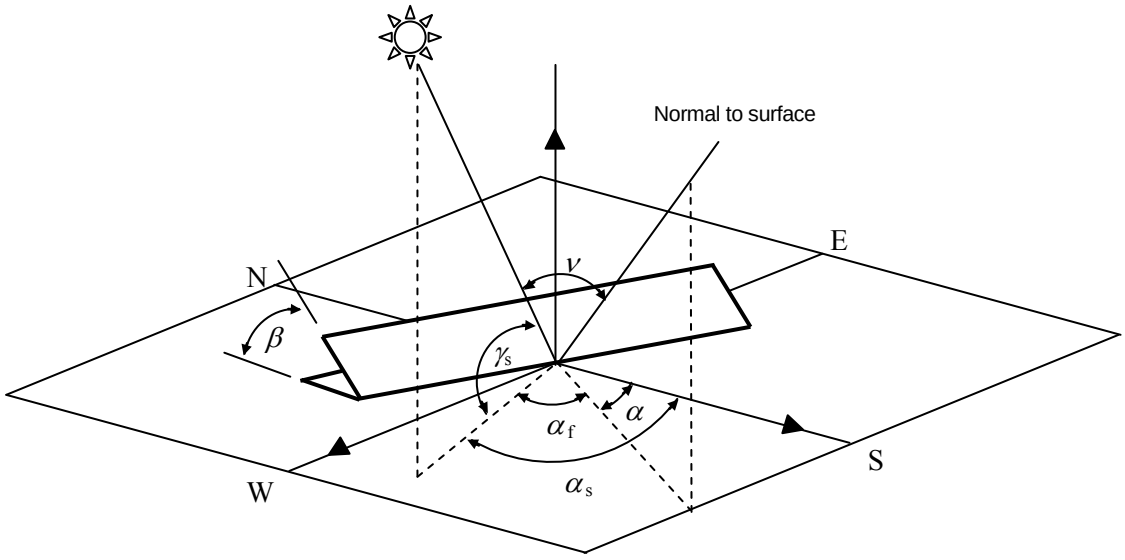

Figure 3 Definition of angles used to describe solar position (γ_s and α_s), orientation and tilt of the irradiated plane (α and β), angle of incidence (ν) and horizontal shadow angle (α_f)

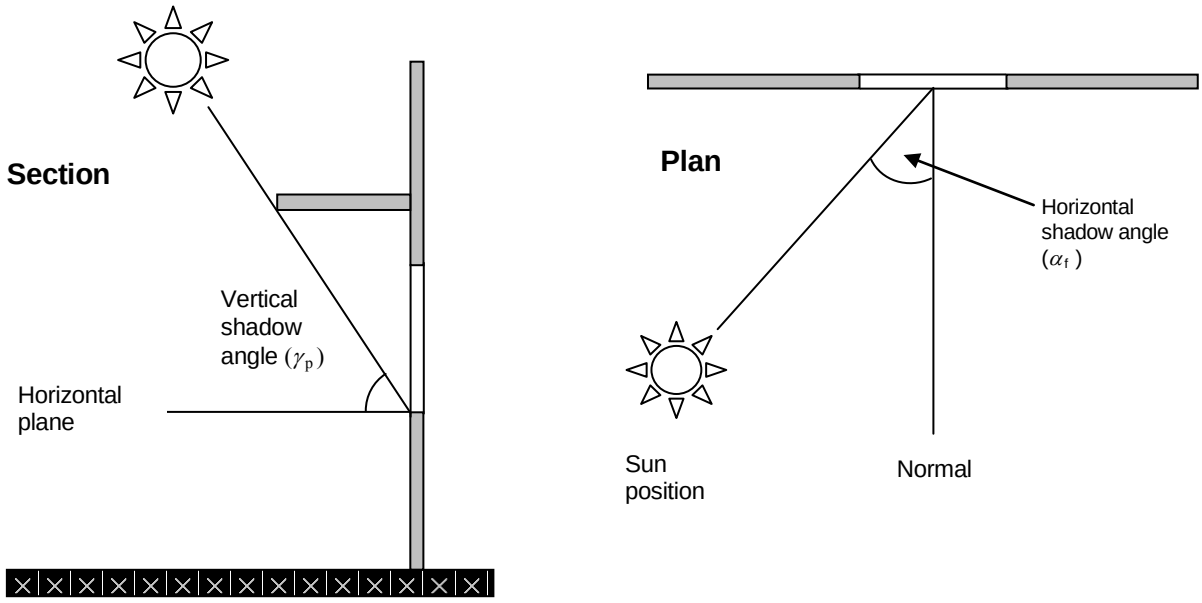

Figure 4 Vertical shadow angle, γ_p, (left) and horizontal shadow angle, α_f (right)

2.7.2 Estimating the solar geometry

Climatological algorithms for estimating declination

The solar year is approximately 365.25 days long. The calendar is kept reasonably synchronous with the solar driven seasons through the introduction of leap years. This leap year cycle means that the precise declination for any selected day varies according to the position of the day within the four-year leap cycle. For calculations involving climatological radiation data averaged over several years, it is appropriate to use long-term mean value formulae to estimate the declination, accepting a 365-day year for all years. In contrast, if observed data for specifically identifiable days in specific years are available, it is logical to use more accurate declination formulae to calculate the declination for that day and longitude, for example in developing the solar geometry to use with simulation tapes. More accurate formulae have to take account of the varying number of days between years. Usually the noon declination values are used. This gives sufficient accuracy for practical calculations.

Mean value formulae for calculating the solar declination

The day number J may be converted to a day angle J' (assuming an average year length of 365.25 days within the 4-year leap year cycle) as: J (360/365.25) degrees = J (360/365.25) (π/180) radians.

The formula used in the *European Solar Radiation Atlas*[1] to compute representative values of the declination based on a 365-day year:

$$\delta = \sin^{-1} \{0.3978 \sin [J' - 1.400 + 0.0355 \sin (J' - 0.0489)]\} \quad (4)$$

where J' is the day angle in radians.

By integrating the daily declination values over each day of each month, monthly mean declination values can be derived for each month, together with a monthly mean representative design date. Table 2 tabulates the recommended climatological values of the mean declination for use at the monthly mean level. It includes the day in the month when the declination is closest to the long term monthly mean value.

Table 2 gives a second set of design dates for clear sky conditions. These dates have been selected to match typical dates of occurrence of monthly maximum daily global horizontal irradiation. In the northern hemisphere, the days of observed maximum daily global irradiation on horizontal planes tend to cluster towards the end of the month in the first half of the year and towards the beginning of the month in the second half of the year. The opposite relationship applies for the southern hemisphere. This choice of date facilitates the statistical comparison of measured monthly maximum data and predicted maximum irradiation in any month. These clear day design dates have been used systematically in this document to select the declination values underlying the solar geometry of all tables based on clear sky conditions. Table 2 thus tabulates, for both hemispheres, the recommended design declinations to match statistically the typical dates of occurrence of the highest daily global radiation in each month.

Accurate formulae for calculating the solar declination

The Bourges algorithm[3] is recommended for use by engineers to obtain an accurate assessment of the declination on specific days in specific years. Details of this algorithm are given in section 2.10.3. An alternative algorithm by Yallop[4] is somewhat more difficult for inexperienced users to handle. The latter algorithm has been used in the processing of UK observed solar radiation tapes to provide the underlying solar geometry used in this document, see Appendix A3.2.

Table 2 Recommended representative values of the solar declination, δ, in radians and in decimal degrees at different design dates in the year

Solar declination, δ, expressed in radians and in degrees for stated design days

(*a*) Northern hemisphere (monthly design dates based on monthly mean declination)

Date	Jan 17	Feb 15	Mar 16	Apr 15	May 15	Jun 11
Radians	–0.3615	–0.2236	–0.0314	+0.1705	+0.3286	+0.4027
Degrees	–20.71	–12.81	–1.80	+ 9.77	+18.83	+23.07
Date	Jul 17	Aug 16	Sep 16	Oct 16	Nov 15	Dec 11
Radians	+0.3693	+0.2382	+0.0504	–0.1522	–0.3206	–0.4013
Degrees	+21.16	+13.65	+ 2.89	– 8.72	–18.37	–22.99

(*b*) Southern hemisphere (monthly design dates based on monthly mean declination)

Date	Jan 17	Feb 15	Mar 16	Apr 15	May 15	Jun 11
Radians	+0.3615	+0.2236	+0.0314	–0.1705	–0.3286	–0.4027
Degrees	+20.71	+12.81	+1.80	– 9.77	–18.83	–23.07
Date	Jul 17	Aug 16	Sep 16	Oct 16	Nov 15	Dec 11
Radians	–0.3693	–0.2382	–0.0504	+0.1522	+0.3206	+0.4013
Degrees	–21.16	–13.65	– 2.89	+ 8.72	+18.37	+22.99

(*c*) Northern hemisphere (for clear day design days)

Date	Jan 29	Feb 26	Mar 29	Apr 28	May 29	Jun 21
Radians	–0.3169	–0.1577	+0.0599	+0.2477	+0.3777	+0.4089
Degrees	–18.16	– 9.04	+ 3.43	+ 14.19	+ 21.64	+ 23.43
Date	Jul 4	Aug 4	Sep 4	Oct 4	Nov 4	Dec 4
Radians	+0.3992	+0.3006	+0.1248	–0.0766	–0.2691	–0.3883
Degrees	+ 22.87	+17.22	+7.15	– 4.39	– 15.42	–22.25

(*d*) Southern hemisphere (for clear day design days)

Date	Jan 4	Feb 4	Mar 4	Apr 4	May 4	Jun 4
Radians	+0.3979	+0.2876	+0.1115	–0.1002	–0.2793	–0.3918
Degrees	+22.80	+16.48	+ 6.39	–5.74	–16.00	–22.45
Date	Jul 29	Aug 29	Sep 28	Oct 29	Nov 28	Dec 22
Radians	–0.3269	–0.1698	+0.0360	+0.2356	+0.3721	+0.4095
Degrees	–18.73	–9.73	+ 2.06	+ 13.50	+ 21.32	+ 23.46

2.7.3 Calculation of solar altitude and azimuth angles and astronomical daylength

The solar altitude and azimuth angles are defined in section 2.7.1, see Figure 3. These angles are dependent on the time of day, t, as measured in hours LAT on the 24-hour clock. For the solar trigonometric calculations that follow, time is first expressed as an hour angle, given by:

$$\omega = 15\,(t - 12) \tag{5}$$

where ω is the hour angle (°).

The solar altitude angle is given by:

$$\sin \gamma_s = \sin \phi \sin \delta + \cos \phi \cos \delta \cos \omega \tag{6}$$

where γ_s is the solar altitude angle (°), ϕ is the latitude of the location (°), δ is the solar declination angle (°) and ω is the hour angle (°).

The solar azimuth angle is obtained from:

$$\cos \alpha_s = (\sin \phi \sin \gamma_s - \sin \delta) / (\cos \phi \cos \gamma_s) \tag{7}$$

$$\sin \alpha_s = \cos \delta \sin \omega / \cos \gamma_s \tag{8}$$

where α_s is the solar azimuth angle (°).

If $\sin \alpha_s < 0$, then $\alpha_s = -\cos^{-1} (\cos \alpha_s)$; if $\sin \alpha_s > 0$, then $\alpha_s = \cos^{-1} (\cos \alpha_s)$.

Both equations 7 and 8 are needed to resolve the azimuth angle into the correct quadrant in computer programmes.

The sunset hour angle is calculated by setting the solar altitude angle to zero in equation 6. Therefore:

$$\omega_s = \cos^{-1} (-\tan \phi \tan \delta) \tag{9}$$

where ω_s is the sunset hour angle (°).

The time of astronomical sunrise in LAT may be found as $(12 - \omega_s / 15)$ hours. The time of astronomical sunset in LAT may be found as $(12 + \omega_s / 15)$ hours. Note that these formulae do not allow for atmospheric refraction or the angular size of the sun. A better estimate of actual sunrise time is achieved by assuming an astronomical elevation of –50 minutes, an adjustment that considers both solar disk size and atmospheric refraction.

The astronomical daylength is therefore $(2\ \omega_s / 15)$ hours.

2.7.4 Calculation of angle of incidence and vertical and horizontal shadow angles

The angle of incidence of the solar beam, $\nu(\beta,\alpha)$, on a surface of tilt β and surface azimuth angle α, is calculated from the solar altitude and solar azimuth angles. The wall–solar azimuth angle, α_f, must first be calculated using equation 10. The sign convention adopted for wall solar azimuth angle is the same as that used for the solar azimuth angle. The angle is referred to due south in the northern hemisphere and to due north in the southern hemisphere. Values to the east of the north–south meridian are negative and values to the west are positive.

$$\alpha_f = \alpha_s - \alpha \tag{10}$$

where α_f is the wall–solar azimuth angle (°), α_s is the solar azimuth angle (°) and α is the azimuth angle of the surface (°).

If $\alpha_f > 180°$, then $\alpha_f = \alpha_f - 360°$; if $\alpha_f < 180°$, then $\alpha_f = \alpha_f + 360°$.

Once the wall–solar azimuth angle has been calculated, the angle of incidence $\nu(\beta,\alpha)$ may be calculated using equation 11. A negative value implies the sun is behind the surface and then the value is usually set to zero.

$$\nu(\beta,\alpha) = \cos^{-1}(\cos\gamma_s \cos\alpha_f \sin\beta + \sin\gamma_s \cos\beta) \quad (11)$$

where $\nu(\beta,\alpha)$ is the angle of incidence (°) on a surface of tilt β (°) and surface azimuth angle α (°), γ_s is the solar altitude angle (°), α_f is the wall–solar azimuth angle of the surface and β is the angle of inclination of the surface (°).

The vertical shadow angle is given by:

$$\gamma_p = \tan^{-1}(\tan\gamma_s / \cos\alpha_f) \quad (12)$$

where γ_p is the vertical shadow angle γ_s is the solar altitude angle (°) and α_f is the wall–solar azimuth angle of the surface (°). If $\gamma_p < 0$, $\gamma_p = 180 + \gamma_p$.

For a vertical surface, if $\gamma_p > 90°$, then the sun is falling on the opposite parallel vertical surface. The horizontal shadow angle is identical to α_f.

2.7.5 Presentation of solar altitude and azimuth angle data

Data on sun position may be presented in graphical or tabular forms. Sun-path diagrams are useful for visualising the course of the sun during the year and are used in various graphical methods for analysing the effects of solar shading, whether due to external obstructions, building features or window position. Various projections may be used but the simplest projection for any given latitude is to plot the hourly solar altitude as a function of the hourly solar bearing for a range of declinations covering the year. Figure 5 below shows an example sun-path diagram for latitude 52°N.

The tables of solar altitude angles and bearings give numerical values of to the nearest degree for a range of latitudes. The tables have been calculated at 10-degree intervals of latitude from 0° to 60° with an additional table for latitude 55°. Linear interpolation can be used for intermediate latitudes. The solar azimuth angles, structured for the northern hemisphere, have been converted into bearings measured from true north. The tabulated values have been calculated month by month, using the northern hemisphere clear day design declination values given in Table 2. The tables are applicable in both hemispheres, but care must be taken to use the correct dates for the hemisphere concerned as given in the table headings. Also, when considering the southern hemisphere, the bearings must be adjusted to that hemisphere, as explained in the table footnotes.

Except for the sunrise and sunset hours, the angles have been calculated on the half-hour using LAT. In the astronomical sunrise hours, the solar geometry has been calculated for the solar time midway between sunrise and the end of the first sunlit hour of the day. In the sunset hours, the time midway between the beginning of the last hour and astronomical sunset has been used. The values for the sunrise and sunset hour are italicised to distinguish them from the normal mid-hour values.

Direct calculation of solar angles provide values for a specific time and place, so is more flexible and precise than is the use of diagrams or tables.

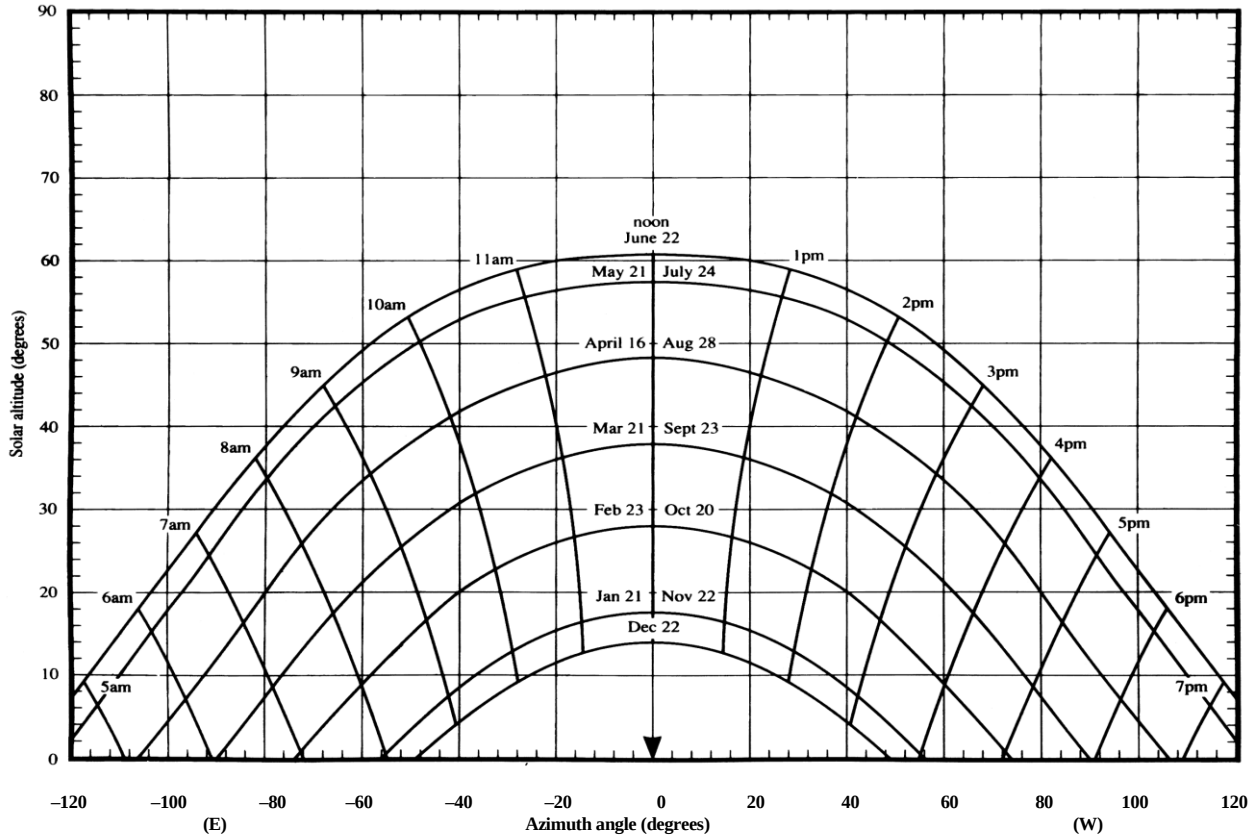

Figure 5 Sun-path diagram for latitude 52°N; times of day, defined by near-vertical lines, are express in LAT; note that in early and late parts of the day, the sun lies to the north of the building during the period between the spring and autumn equinoxes

2.8 Solar radiation outside the atmosphere

2.8.1 Solar constant (I_o)

Before considering solar radiation at the surface of the earth, it is useful to consider the effects of latitude and date in the year on the solar radiation on a horizontal surface outside the atmosphere. The solar constant (I_o) is the value of the extraterrestrial irradiance normal to the beam at mean solar distance. The internationally accepted value is 1367 W·m^{-2}. This value has been used in the preparation of this document, serving as a reference value in the checking measured data and as input data in estimating replacements for missing or doubtful data using dimensional analysis. It serves both as an absolute upper limit and as the critical variable in dimensionless algorithms for assessing the attenuation of the atmosphere.

2.8.2 Effect of distance between sun and earth

The orbit of the earth around the sun is elliptical with a small degree of eccentricity. So the sun–earth distance varies slightly during the year. This variation influences the extra-terrestrial irradiance being received on any specific day. The extra-terrestrial irradiance varies around its mean value by about ±3.5% during the year.

The correction factor to allow for the varying solar distance (ε_j) is calculated from:

$$\varepsilon_j = 1.0 + 0.03344 \cos (J' - 2.80) \quad (13)$$

where ε_j is the correction factor for solar distance, J' is the day angle in degrees (see section 2.6.1).

Table 3 gives values of ε_j for the computational dates recommended in Table 2. The extra-terrestrial beam irradiance on a horizontal plane is given by ($\varepsilon_j \times 1367 \sin \gamma_s$) where ε_j is the correction to mean solar distance, see equation 13, and γ_s is the solar altitude.

Table 3 Correction for changes in solar distance corresponding to recommended design dates (applied as a multiplier to values calculated at mean solar distance)

Correction factor for variation in solar distance, ε_j, for stated design days						
(*a*) Northern hemisphere (monthly design dates based on monthly mean declination)						
Date	Jan 17	Feb 15	Mar 16	Apr 15	May 15	Jun 11
Value (ε_j)	1.032	1.025	1.011	0.944	0.978	0.969
Date	Jul 17	Aug 16	Sep 16	Oct 16	Nov 15	Dec 11
Value (ε_j)	0.967	0.975	0.990	1.007	1.022	1.031
(*b*) Southern hemisphere (monthly design dates based on monthly mean declination)						
Date	Jan 17	Feb 15	Mar 16	Apr 15	May 15	Jun 11
Value (ε_j)	1.032	1.025	1.011	0.944	0.978	0.969
Date	Jul 17	Aug 16	Sep 16	Oct 16	Nov 15	Dec 11
Value (ε_j)	0.967	0.975	0.990	1.007	1.022	1.031
(*c*) Northern hemisphere (for clear day design days)						
Date	Jan 29	Feb 26	Mar 29	Apr 28	May 29	Jun 21
Value (ε_j)	1.030	1.020	1.003	0.986	0.973	0.967
Date	Jul 4	Aug 4	Sep 4	Oct 4	Nov 4	Dec 4
Value (ε_j)	0.967	0.971	0.984	1.001	1.018	1.029
(*d*) Southern hemisphere (for clear day design days)						
Date	Jan 4	Feb 4	Mar 4	Apr 4	May 4	Jun 4
Value (ε_j)	1.033	1.028	1.017	1.000	0.983	0.971
Date	Jul 29	Aug 29	Sep 28	Oct 29	Nov 28	Dec 22
Value (ε_j)	0.970	0.981	0.997	1.015	1.028	1.033

2.8.3 Daily irradiation outside the atmosphere

The daily irradiation falling on a horizontal plane immediately outside the earth's atmosphere, G_{od}, can be estimated on any day of the year from:

$$G_{od} = (24 / \pi)\, \varepsilon_j\, I_o\, [(\omega_s\, \pi / 180) \sin \phi \sin \delta + \cos \phi \cos \delta \sin \omega_s] \quad (14)$$

where G_{od} is the daily irradiation falling on a horizontal plane immediately outside the earth's atmosphere ($W \cdot h \cdot m^{-2}$), ε_j is the correction to mean solar distance on day j, I_o is the solar constant (1367 $W \cdot m^{-2}$), ϕ is the latitude of the location (°), δ is the solar declination angle (°) and ω_s is the sunset hour angle (°), see equation 9.

Table 4, see below, gives monthly mean values of G_{od} for five UK sites. Lerwick is the most northerly UK radiation measurement site and Jersey Airport is the most southerly. Note the very steep latitudinal change in the monthly mean extraterrestrial daily horizontal irradiation found in winter at high latitudes. This extraterrestrial gradient is reflected in the irradiation reaching the surface. Note also the small gradient in summer. Values of G_{od} for intermediate UK latitudes can be obtained by interpolation or by direct calculation.

Table 4 Monthly mean values of the daily extraterrestrial irradiation on a horizontal surface, $(G_{od})_m$, for five UK sites

Site	Monthly mean extraterrestrial irradiation ($W \cdot h \cdot m^{-2}$) for stated month											
	Jan	Feb	Mar	Apr	May	Jun	Jul	Aug	Sep	Oct	Nov	Dec
Lerwick (60.13°N)	974	2408	4853	7759	10210	11383	10761	8632	5851	3184	1333	627
Mylnefield (56.45°N)	1524	3029	5439	8179	10405	11437	10885	8966	6380	3798	1908	1135
Aughton (53.55°N)	1984	3520	5886	8492	10552	11487	10982	9216	6780	4278	2380	1573
Bracknell (51.38°N)	2340	3886	6210	8714	10655	11522	11050	9393	7069	4632	2740	1917
Jersey (49.22°N)	2700	4249	6525	8926	10751	11522	11112	9559	7346	4979	3102	2268

2.8.4 Clearness index

It is convenient to base much algorithmic analysis of solar radiation in dimensionless terms. An important dimensionless quantity is the 'clearness index', often called the KT-value. The daily KT-value, KT_d, is found by dividing the daily irradiation G_d by the extraterrestrial daily irradiation G_{od}. The hourly KT-value, KT_h, is found by dividing the hourly irradiation G_h at the surface of the earth by the hourly extraterrestrial irradiation G_{oh}. However, this calculation becomes unreliable when the sun is below 6 degrees because energy is entering the curved atmosphere from the side, which not accounted for in the value of the incident horizontal extraterrestrial irradiation. It can be corrected for, refer Page[5].

The monthly mean daily KT-value $(KT_d)_m$ is found by dividing the monthly mean daily global irradiation $(G_d)_m$ by the monthly mean extraterrestrial irradiation $(G_{od})_m$.

Pixellated monthly maps of $(KT_d)_m$ covering the whole of Europe for the period 1981–90, on a grid of approximately 10 km × 10 km, are available on a CD-ROM[1]. The maps cover the area from 30° W to 70° E and from 25° N to 75° N.

2.9 Sunshine and cloud observations

2.9.1 Sunshine observations and solar radiation estimation

Sunshine data are the most widely available data relating to solar radiation. The instruments used measure the length of time the direct beam irradiance normal to the beam is above a critical burn threshold. The critical burn threshold for direct beam irradiance lies between 100–200 $W \cdot m^{-2}$ [6] with a mean value of about 150 $W \cdot m^{-2}$. The bright sunshine, i.e. the sunshine strong enough to burn the card, is estimated from the burn trace on the sunshine recorder card.

The Met Office first extracts the hourly sunshine, which is the proportion of each hour in LAT (solar time) during which the sun is shining with a beam irradiance above the reference threshold. These measured hourly sunshine data, S_h, are available on an hour-ending basis in LAT in the CIBSE UK weather datasets for building simulation*. These hourly values are then summed to obtain daily sunshine values, S_d. Finally, monthly means of daily sunshine, $(S_d)_m$ are obtained by summing the daily values in each month over the selected observation period and dividing by the number of days with complete daily records of sunshine in that month.

The daily sunshine is often converted to a dimensionless form by dividing S_d by the astronomical daylength, S_{od}, using equation 9, see section 2.7.3. The resulting ratio, extracted on a monthly basis, is called the monthly mean relative duration of bright sunshine, σ_d. One advantage of presenting relative sunshine duration values rather

* Available from Customer Centre, Powell Duffryn House, London Road, Bracknell, Berkshire RG12 2SX

than actual daily sunshine duration in hours is that the user can form an immediate impression of relative sunniness without the need to know the actual daylength, which varies greatly with time of year at high latitudes. Dimensionless analysis is often used to estimate monthly mean daily global irradiation on horizontal surfaces from monthly mean sunshine data using the Angström relationship.

$$(G_d)_m / (G_{od})_m = a_m + b_m (S_d / S_{od})_m \quad (15)$$

where $(G_d)_m$ is the monthly mean daily global irradiation ($W \cdot h \cdot m^{-2}$), $(G_{od})_m$ is the monthly mean daily horizontal extraterrestrial irradiation ($W \cdot h \cdot m^{-2}$), S_d the daily sunshine hours (h), S_{od} is the astronomical daylength (h), a_m and b_m are month-by-month regression coefficients.

The regression coefficients a_m and b_m are specific to the site and are determined on a month-by-month basis, obtained using daily data from reliable sites observing both global radiation and daily sunshine. Values of these coefficients for many European sites are available in the *European Solar Radiation Atlas*[1]. The same source includes monthly mean bright sunshine data for a large number of sites.

For other parts of the world, if local data are not available, a judgement must be reached on representative values for a_m and b_m. In temperate climates, if there is a lot of rainfall and cloud, a_m typically falls in the range 0.18–0.22. If there are very few overcast days in the month then a_m typically is about 0.24–0.26. Coefficient b_m typically ranges from about 0.40 to 0.50, increasing with increasing sky clarity.

The UN Food and Agricultural Organisation[8] used the following factors in the estimation of crop yields in tropical areas:

— dry tropical zones: $a_m = 0.25$; $b_m = 0.45$; $(a_m + b_m) = 0.70$

— humid tropical zones: $a_m = 0.29$; $b_m = 0.42$; $(a_m + b_m) = 0.71$

In very clear climates the sum $(a_m + b_m)$ may exceed 0.76. In very dirty or dusty climates the sum may fall below 0.68. Many climates are two-seasonal with a heavy dust burden in the dry months which is washed out in the wet months. Different regression coefficients may be appropriate in different months.

Monthly mean daily global irradiation data can be easily converted into hour-by-hour estimated monthly mean values of irradiation[1].

2.9.2 Estimating global hourly horizontal irradiation from hourly cloud data

Using observations for Hamburg, Kasten and Czeplak[9] have shown that:

$$G_h / G_{ch} = 1 - C (N / 8)^D \quad (16)$$

where G_h is the hourly global irradiation ($W \cdot h \cdot m^{-2}$), G_{ch} is the hourly clear sky global irradiation ($W \cdot h \cdot m^{-2}$), N is the hourly cloud amount (okta), C and D are regression coefficients.

The constants for Hamburg were $C = 0.75$ and $D = 3.4$. When $N = 8$, equation 5.16 yields a value of 0.25. Suitable values of G_{ch} for use with this equation can be obtained from the world clear sky irradiance tables described in section 5.3. Using data for the UK, Gul et. al.[10] derived values of C and D for the UK, which are given in Table 5.

Assuming a typical clear day transmittance of 0.70, equation 16 yields an overcast day KT-value of 0.20, which is in agreement with the typical Angström coefficient, a_m. However, these overcast values do not accord well with the overcast day values for the UK mapped by Cowley[11]. Work undertaken for this document has indicated the need to restrict equation 16 to cloud cover of 7 oktas or less. In the UK, for 8 oktas of cloud, it seems better to use the Cowley (1976) daily UK mapped values, which are lower. Cloud amount can be estimated from sunshine, see section 2.9.3.

Table 5 Regression coefficients *C* and *D* for use with equation 16, found from UK observational data[10]

Site	Latitude	Value of coefficient		Overcast
		C	*D*	
Stornoway	58.2° N	0.73	3.4	0.27
Aldergrove	54.6° N	0.70	3.1	0.30
Finningley	53.0° N	0.71	3.7	0.29
Aberporth	52.1° N	0.71	4.2	0.29
London	51.5° N	0.71	3.4	0.29

2.9.3 Relationship between cloud amount and bright sunshine.

Sunshine and cloud amounts are inter-related, but the relationship is non-linear. The rays of the sun may pass through the cloud with enough energy left still to burn the card, especially with thin, high cloud. The regression can only be established for hours when the sun is strong enough to burn the record card. Using observed hourly cloud and sunshine data for Bracknell and Aberporth, Page[12] found the regression as:

$$\sigma_h = a(0) + a(1)\, N_h + a(2)\, N_h^2 \qquad (17)$$

where σ_h is the sunshine duration in the hour (h), N_h is the hourly cloud amount (okta), $a(0)$ $a(1)$ and $a(2)$ are solar altitude-dependent regression coefficients, see Table 6.

Table 6 Regression coefficients $a(0)$, $a(1)$ and $a(2)$ for Aberporth and Bracknell[12]

Coefficient	Solar altitude band (°)					
	8 –15	15–25	25–35	35–45	45–55	> 55
Aberporth:						
$a(0)$	1.023	0.983	0.934	0.911	0.886	0.887
$a(1)$	–0.059	–0.002	0.082	0.102	0.147	0.140
$a(2)$	–0.009	–0.015	–0.025	–0.026	–0.031	–0.030
Bracknell:						
$a(0)$	1.041	0.980	0.970	0.943	0.908	0.903
$a(1)$	–0.088	–0.007	0.043	0.090	0.123	0.120
$a(2)$	–0.005	–0.014	–0.020	–0.026	–0.029	–0.028

2.10 Estimation of all-sky irradiation on inclined planes from hourly time series of horizontal irradiation

2.10.1 General

Section 2.10 provides guidance on the conversion of observed hourly time series of global and diffuse irradiation on horizontal surfaces into the corresponding hourly components of irradiation on inclined planes. The method assumes the availability of an hourly time series of global and diffuse horizontal irradiation obtained from a reliable meteorological source. If the time series is to be used for simulation, any gaps in the horizontal data should first be filled, using appropriate techniques, see Appendices A1 and A2.

2.10.2 Components of slope irradiation

The tilt of the irradiated surface from the horizontal plane is defined as β. This angle needs to be entered in radians for some of the algorithms used. The azimuth angle of the surface is α, see Figure 3. This is measured from due south in the northern hemisphere and from due north in the southern hemisphere. Directions to the west of N–S are positive and to the east are negative.

The inclined surface global irradiation for any hour is obtained by summation of three slope irradiation components:

— slope beam component, $B_h(\beta,\alpha)$

— slope sky diffuse component, $D_h(\beta,\alpha)$

— slope ground reflected component, $R_{gh}(\beta,\alpha)$.

Each component is estimated separately. Then:

$$G_h(\beta,\alpha) = B_h(\beta,\alpha) + D_h(\beta,\alpha) + R_{gh}(\beta,\alpha) \quad (18)$$

where G_h is the hourly global irradiation ($W \cdot h \cdot m^{-2}$) on a surface of azimuth α and tilt β.

The associated hour-by-hour solar geometry has to be developed first to provide a matching time series of solar geometric data in order to start the process. As data for specific hours are involved, an accurate formula for the declination should be used. The Bourges formula, see equation 19, is accurate and simple in engineering use.

2.10.3 Establishing accurate noon declination and accurate solar geometry

The Bourges formula[3] is simple to use. It is adequate to accept the noon declination as representative for the whole day.

$$\delta_{noon} = 0.3723 + 23.2567 \sin \omega_t + 0.1149 \sin (2\ \omega_t) - 0.1712 \sin (3\ \omega_t)$$
$$- 0.7580 \cos \omega_t + 0.3656 \cos (2\ \omega_t) - 0.2010 \cos (3\ \omega_t) \quad (19)$$

where δ_{noon} is the noon declination (°) and ω_t (°) is given by equation 20.

$$\omega_t = \omega_1 (J - t_1) \quad (20)$$

where $\omega_1 = (360 / 365.2422)$ (°), J is the Julian day number (running from 1 to 365 for non-leap years and 1 to 366 for leap years) and t_1 (days) is given by equation 21.

$$t_1 = -0.5 - (\lambda / 360) - n_o \quad (21)$$

where λ is the longitude (°) (positive measured eastward) and n_o (days) is given by equation 22.

$$n_o = 78.8946 + 0.2422\ (Y - 1957) - \text{Int}\ [(Y - 1957) / 4] \quad (22)$$

where Y is the year number in full and Int denotes the integer part of the bracketed expression.

Knowing the mid-hour observational times of the input data, the detailed solar geometry can be established using section 2.7, making appropriate adjustments in the sunrise and sunset hour. (The astronomical sunrise and sunset times must first be calculated for each day in order to do this.) The angle of incidence of the beam on the plane is also required, see equation 11.

The equivalent accurate formula by Yallop[4] has been used in some of the calculations for this document, refer to Appendix A3.2.

2.10.4 Direct beam irradiation on inclined planes

The estimation of the slope beam irradiance from the beam normal irradiance is straightforward, once the cosine of the angle of incidence of the solar beam for the inclined plane under consideration has been established.

$$B(\beta,\alpha) = B_n \cos \nu(\beta,\alpha) \text{ for } \cos \nu(\beta, \alpha) > 0; \text{ otherwise } B(\beta,\alpha) = 0 \quad (23)$$

where $B(\beta,\alpha)$ is the slope beam irradiance ($W \cdot m^{-2}$).

However, there are sometimes difficulties when using observed irradiation data summarised on an hour-by-hour basis. The sun is not necessarily on the selected surface for the whole of the summation period. Outside the sunrise and sunset hour, provided that the sun is on the surface for the whole hour, the hourly mean beam normal irradiation may be estimated from:

$$B_{nh} = (G_h - D_h) / \sin \gamma_s \quad (24)$$

where B_{nh} is the hourly mean beam normal irradiation ($W \cdot h \cdot m^{-2}$) and γ_s is the mid-hour solar altitude angle (°).

In the sunrise and sunset hours, account must be taken of the proportion of the hour when the sun is above the horizon. Then:

$$B_{nh} = (G_h - D_h)\, \Delta T / \sin \gamma_s \quad (25)$$

where γ_s is the solar altitude angle (°) at a time halfway between sunrise and the end of the sunrise hour or halfway between the beginning of the sunset hour and sunset and ΔT is the period during the sunrise or sunset hour during which the sun is above the horizon (symmetrical if LAT is used).

The accurate estimation of beam irradiation on inclined planes using standard observational time periods of 1 hour also raises complications because the sunlight may move off the surface during the hour in question. This will not be detected using the hour-by-hour calculation process. A simple irradiation approximation can be achieved for hours when the sun is on the surface for the whole hour by using the mid-hour angle of incidence and setting the hourly irradiation equal to the mid-hour irradiance. Thus:

$$B_h(\beta,\alpha) = B_{nh} \cos \nu(\beta,\alpha) \quad (26)$$

The appropriate correction procedures for partially sunlit hours on inclined planes are discussed in section 3.3.6. This refinement is overlooked in many simulation programmes, except sometimes in the sunrise and sunset hour.

2.10.5 Estimation of irradiation received from sky on inclined surfaces using hourly horizontal diffuse irradiation

This section is based on research by Muneer[13] and incorporates improvements by Muneer and by the team responsible for preparing the *European Solar Radiation Atlas*[1]. European tests showed that, for sun-facing surfaces, the model yields similar values to the Perez model[14] at the day-by-day hourly level but better results at the monthly mean level. It also gives more accurate values for surfaces facing away from the sun than the Perez algorithm[14], both for monthly mean hourly values and also for daily hour-by-hour values. For clear skies, the predictions are almost identical with the Littlefair–Page model used to produce the world clear sky irradiance tables described in section 3.

The method requires, as inputs, hourly values of global and diffuse horizontal irradiation, G_h and D_h. For sun-

facing surfaces, there are different algorithms for low sun angles (i.e. below 5.7°) and high sun angles (i.e. above 5.7°). For potentially insolated surfaces, a distinction is also made between overcast hours and non-overcast hours.

An overcast sky hour is defined as an hour having $(G_h - D_h) < 5$ W·h·m^{-2}.

A modulating function, K_b, is first calculated in order to express the horizontal beam irradiance as a ratio to the extraterrestrial horizontal irradiance, corrected to mean solar distance. This function is given by:

$$K_b = B_h / (\varepsilon_j I_o \sin \gamma_s) = (G_h - D_h) / (\varepsilon_j\ 1367 \sin \gamma_s) \quad (27)$$

where K_b is the modulating function, I_o is the solar constant (1367 W·m^{-2}), ε_j is the correction to mean solar distance on day j (see equation 13) and γ_s is the solar altitude angle (°).

A diffuse irradiation function $f(\beta)$ for slope β is then calculated. Note that β is expressed in degrees. Function $f(\beta)$ is given by:

$$f(\beta) = \{\cos^2 (\beta / 2) + [2\ b / \pi\ (3 + 2\ b)]\ [\sin \beta - (\beta\ \pi / 180) \cos \beta\ - \pi \sin^2 (\beta / 2)]\} \quad (28)$$

where $f(\beta)$ is the diffuse irradiation function for a surface with slope β, β is the slope of the surface (°) and b is a constant.

Values for constant b are as follows:

— shaded surface: $b = 5.73$

— sunlit surface under overcast sky: $b = 1.68$

— sunlit surface under non-overcast sky: $b = –0.62$

As an improvement, for certain specific areas where appropriate observed data exist, Muneer[13] has suggested an alternative way of evaluating $[2\ b / \pi\ (3 + 2\ b)]$ to be applied to the sunlit surface cases only. For northern Europe (represented by Bracknell), $[2\ b / \pi\ (3 + 2\ b)]$ is replaced by $(0.00333 – 0.4150\ K_b – 0.6987\ K_b^2)$ and, for southern Europe, by $(0.00263 – 0.7120\ K_b – 0.6883\ K_b^2)$.
For a vertical surface, equation 5.28 reduces to

$$f(\beta) = \{0.5 + [2\ b / \pi\ (3 + 2\ b)]\ (1 – 0.5\ \pi)\} \quad (29)$$

Evaluating equation 29 for the above values of constant b gives the following values for $f(\beta)$:

— sunlit vertical surface, under non-overcast sky conditions (i.e. $b = –0.62$): $f(\beta) = 0.628$

— potentially sunlit surface under an overcast sky (i.e. $b = 1.68$): $f(\beta) = 0.404$.

— vertical surface not potentially sunlit, i.e. $\cos\ \nu(\beta,\alpha)$ is zero or less (i.e. $b = 5.73$): $f(\beta) = 0.357$

For sunlit surfaces, with $\gamma_s > 5.7°$ degrees, $D_h(\beta,\alpha)$ is found using the following equation:

$$D_h(\beta,\alpha) / D_h = f(\beta)\ (1 – K_b) + K_b \cos\ \nu(\beta,\alpha) / \sin \gamma_s \quad (30)$$

Hence, for a vertical sunlit surface with $\gamma_s > 5.7°$:

$$D_h(\beta,\alpha) / D_h = 0.628\ (1 – K_b) + K_b \cos\ \nu(\beta,\alpha) / \sin \gamma_s \quad (31)$$

where D_h is the hourly diffuse irradiation on the horizontal plane (W·h·m^{-2}) and $\cos\ \nu(\beta,\alpha)$ is the angle of incidence on the surface (°).

For a potentially sunlit surface with an overcast sky, $K_b = 0$; therefore for all solar altitudes, for a vertical surface:

$$D_h(\beta,\alpha) / D_h = f(\beta) = 0.404 \quad (32)$$

For surfaces in shade (i.e. cos $\nu(\beta,\alpha) = 0$) and for all solar altitudes, for a vertical surface:

$$D_h(\beta,\alpha) / D_h = f(\beta) = 0.357 \quad (33)$$

As there is not a perfect conjunction in the functions at the instant the sun changes from being just on the surface to being just off the surface, a small adjustment was made in the programme for the CEC ESRA project[1] to ensure continuity in estimation. Linear interpolation was used to achieve a smooth transition in this zone, using a zone of 20 degrees width either side of the on-off sun switch position. This improvement has been used in the evolution of the monthly mean slope irradiation tables for 14 UK sites, Table 2.11 of CIBSE Guide A, chapter 2.

The Muneer algorithm[15] is not suitable for sunlit surfaces below a solar elevation of 5.7°. In this region, Muneer has proposed applying an adjustment based on the Temps and Coulson algorithms[16].

The original Temps and Coulson algorithm for cloudless skies is:

$$D_c(\beta,\alpha) / D_c = \cos^2(\beta/2)\ \{1 + \sin^3(\beta/2)\}\ [1 + \cos^2\nu(\beta,\alpha)\ \sin^3(90 - \gamma_s)] \quad (34)$$

This formula was modified by Klucher[17] to become an all-sky model by introducing a modulating function F2, which was set as $[1 - (D_h / G_h)^2]$. Muneer [13] substituted K_b in equation 5.33 to give:

$$D_c(\beta,\alpha) / D_c = \cos^2(\beta/2)\ \{1 + K_b \sin^3(\beta/2)\}\ [1 + K_b \cos^2\nu(\beta,\alpha)\ \sin^3(90 - \gamma_s)] \quad (35)$$

2.10.6 Ground reflected irradiation

Three assumptions are implicit in the method adopted for making estimates of the irradiation reflected from the ground:

— the ground surface reflects isotropically

— the ground surface is fully irradiated

— there is no reflected energy other than that directly reflected from the level ground.

The reflected hourly ground irradiation $R_{gh}(\beta,\alpha)$, which is assumed independent of orientation α, is estimated as:

$$R_{gh}(\beta,\alpha) = r_g\ \rho_g\ G_h \quad (36)$$

where $R_{gh}(\beta,\alpha)$ is the reflected irradiation ($W \cdot h \cdot m^{-2}$), ρ_g is the ground albedo, r_g is the ground slope factor and G_h is the hourly irradiation falling on the ground ($W \cdot h \cdot m^{-2}$).

The ground slope factor is given by:

$$r_g = (1 - \cos\beta) / 2 \quad (37)$$

A ground albedo of 0.2 has been adopted in the tables contained in this document. This value can be changed if better knowledge exists about the ground cover in different months. Table 7 provides typical values of the ground albedo for different types of surface. The most important albedo change is that due to snow cover. Table 7 also demonstrates the directional reflection characteristics of water surfaces at different solar altitudes. Late afternoon water reflected gains may be important in some locations. Additional information about ground reflected irradiation in the UK may be found in Saluja and Muneer[18].

Table 7 Typical albedo values for various ground types[1]

Surface type	Albedo
Grass (July, Aug. UK)	0.25
Lawns	0.18–0.23
Dry grass	0.28–0.32
Uncultivated fields	0.26
Bare soil	0.17
Macadam	0.18
Asphalt	0.15
Concrete new before weathering	0.55
Concrete weathered industrial city	0.20
Fresh snow	0.80–0.90
Old snow	0.45–0.70
Water surfaces:	
— $\gamma_s > 45^o$	0.05
— $\gamma_s = 30^o$	0.08
— $\gamma_s = 20^o$	0.12
— $\gamma_s = 10^o$	0.22

2.11 Monthly mean daily irradiation on inclined planes in the UK

Tables 2.12(a) to 2.12(n) in CIBSE Guide A, chapter 2, provide values of monthly mean daily irradiation on a range of inclined planes for 14 UK sites. These tables are calculated from quality controlled and filled data tapes using observed hourly global and diffuse horizontal irradiation values for the periods described in Table 2.4 of CIBSE Guide A, chapter 2, adopting a standard ground albedo (i.e. ground reflectance for the entire solar spectrum) of 0.2. The methodology for estimating monthly mean daily slope irradiation followed precisely the process described in section 2.10.

2.12 Near-extreme global irradiation with associated diffuse irradiation

Tables 2.13(a) to 2.13(n) in CIBSE Guide A, chapter 2, provide values of near-extreme hourly irradiation on a range of inclined planes for 14 UK sites. The tables provide mean hourly irradiation values associated with a known exceedence of daily global irradiation on horizontal surfaces and are intended for use in risk-based design applications. Note that they are not tables of hourly exceedence values.

Monthly mean hourly near-extreme values of global and diffuse horizontal irradiation were established using the hourly data for all days when the daily horizontal global daily irradiation data on that day fell into the category of the highest 5% of the days in each long-term monthly daily series. The tabulated hourly mean horizontal values are based on taking hourly averages for all the days in each month with a daily global irradiation above the 95% level. Therefore the tables may be considered to be representative of the 97.5 percentile daily global horizontal irradiation conditions month-by-month.

The mean hourly horizontal global and diffuse data for each month were then subjected to a quality control process to eliminate any risk of computational problems arising when making slope irradiation estimates in hours when the solar altitudes were very low. Some small adjustments were needed in the first two and last two observations in the day[19]. These were made using of the clear sky model described in section 3 to ensure quality

control of the two ends of the mean daily extreme horizontal distribution. The horizontal adjustments needed in daily energy terms were negligible.

Proper quality control of horizontal data is very important. Difficulties sometimes arise in building simulation at low solar elevations, because the horizontal beam irradiation is determined by the difference of two very small numbers, both of which are subject to considerable measurement errors. The resulting, relatively inaccurate, horizontal beam irradiance at low solar elevations may then be divided by another small number, the sine of the mid-period solar elevation, to determine the mid-period beam normal irradiance, which is used to calculate the beam slope irradiances. The large errors that can result may seriously affect the results of the simulation. Quality control of data sets is important in this context to ensure that beam irradiances are always acceptable for simulation.

The corresponding hourly slope irradiation values were then calculated, hour-by-hour, using the monthly means of the hourly values of the observed hourly global and diffuse horizontal observations. Only the days in each month identified with the selected extreme day global irradiation data were used in obtaining these means. The declination values needed to generate the necessary mean underlying solar geometry were set at the standard clear day design values, see Table 2. This declination selection generates a solar geometry that accords precisely with the standard solar altitude and azimuth methodology underlying the world clear sky solar irradiance tables described in section 3. The diffuse sky irradiation conversions to sloping surfaces were achieved using the Muneer methodology described in section 2.10.5. A ground albedo of 0.2 was assumed.

The resulting tables, with the horizontal values based on observation, may be directly compared with the world clear sky solar irradiance tables described in section 3.3, as they share the same underlying geometry, which aligns precisely with the solar geometry presented in Figure 3.

3 Theoretical estimation of shortwave solar radiation

3.1 Introduction

In many design situations, observed hourly global and diffuse irradiation data for horizontal surfaces are not available and a theoretical approach has to be adopted to provide suitable estimates. In terms of building services engineering design risk, cloudless or near cloudless days are often associated with maximum or near maximum cooling loads, especially in heavily glazed buildings. The solar beam transmission through the local atmosphere at different wavelengths depends on both the amount of absorption due various gases in the atmosphere and the molecular scattering. Water vapour aloft produces strong absorption in the infra-red region and ozone strong absorption in the ultra-violet region. The beam transmittance is also strongly influenced by the amount of atmospheric scattering and absorption due to dust, smoke and water droplets. The basic blue-dominated scattering by the air molecules is complemented by such particulate scattering in the solar path. Water vapour droplets are important scattering agents, especially in the humid tropics. The longer the path length the greater is the absorption and the scattering.

This section concentrates on the estimation of clear sky shortwave irradiance and irradiation on horizontal and inclined planes at any location between latitude 60° N and 60° S. Sections 3.9 and 3.10 deal with the estimation of diffuse irradiance on overcast days under different cloud conditions and also with the estimation of diffuse irradiance on partially clouded days. With high thin clouds, diffuse irradiance levels can be quite high.

A systematic tabulation system has been devised for the presentation of hourly clear sky beam and diffuse irradiance estimates at any season at any latitude based on the CEC ESRA clear sky model[1]. This model can be used for surfaces of any inclination. Tables of predicted clear day beam and diffuse irradiance on vertical and horizontal surfaces have been calculated at 10-degree intervals of latitude from 0 to 60 degrees with a extra tables for latitude 55°N and 52°N (representative of southern England and Wales).

The application of simple, date-dependent numeric conversion factors given in Table 9 below enables these tables to also be applied to the southern hemisphere. A detailed description of the models used and their applications has been published elsewhere[20]. This section considers the application of the tables in engineering design.

A sound approach to the estimation of solar radiation requires some quantitative measure describing the transmission properties of the atmosphere at specific places. It is useful to have single number to describe the combined impacts of the various atmospheric factors on the solar beam transmittance. The atmospheric clarity in this document is described using the Linke turbidity factor. The Linke turbidity factor is the ratio of the observed optical depth of the atmosphere at solar zenith to the optical depth of a perfectly clean, dry Rayleigh atmosphere (also estimated at the zenith). The blue rich scattering in this reference atmosphere depends only on the scattering by the gaseous molecules in the atmosphere. The impact of the Linke turbidity factor on the strength of the beam at sea level at different solar altitudes is set down in Table 8. The tabulation system devised for clear day irradiance estimation allows the application of adjustments for both height above sea level and for variations in the Linke turbidity factor. The tables of predicted clear day beam and diffuse irradiance were generated using a Linke turbidity factor of 3.5 and assuming sea level. This value has been adopted as the standard reference level throughout this section. The tables presented are adjusted to the correct mean solar distances on different dates for the northern hemisphere. An accompanying table provides the detailed correction data for site elevation above sea level and differences in atmospheric clarity from the reference value of 3.5. The use of these two tables is explained later.

The models used take account of the fact that when the clarity of the atmosphere decreases, the clear sky beam radiation becomes weaker and, simultaneously, the clear sky diffuse horizontal radiation from the sky becomes stronger. Furthermore, the slope model used to estimate diffuse radiation from the sky properly reflects the impact of the non-isotropic distribution of the radiance of the clear sky on the inclined surface diffuse irradiance.

Surfaces facing the sun receive significantly more diffuse radiation from the clear sky than surfaces facing away from the sun. The diffuse irradiance in the tables includes both the sky diffuse component and the ground reflected diffuse component. While a standard ground albedo (i.e. reflectivity for solar radiation) of 0.2 has been used to estimate the ground reflected component, it is simple to make adjustments for other ground types using the albedo values given in Table 7.

Table 8 Beam irradiance normal to the solar beam at sea level at mean solar distance as a function of solar altitude angle and Linke turbidity factor; note that the beam normal irradiance is not zero at sunrise and sunset, at which time the resolved component on the horizontal surface is zero

Solar altitude angle (°)	Beam irradiance ($W \cdot m^{-2}$) normal to the solar beam at sea level for stated Linke turbidity factor (for air mass m = 2)							
	1.5	2.5	3.5	4.5	5.5	6.5	7.5	8.5
0	369	154	64	27	11	5	2	1
1	426	195	90	41	19	9	4	2
5	638	384	231	139	83	50	30	18
10	804	564	396	278	195	137	96	67
15	901	683	517	392	297	225	170	129
20	966	766	607	482	382	303	240	191
25	1012	828	677	554	453	371	303	248
30	1046	876	733	613	513	429	359	301
35	1073	913	777	662	563	479	408	347
40	1095	944	814	702	605	522	450	388
45	1112	969	844	735	641	558	486	424
50	1126	989	869	763	671	589	518	455
60	1146	1019	906	805	716	637	566	503
70	1159	1038	930	833	746	668	598	536
80	1166	1049	943	848	763	686	617	555
90	1168	1052	947	853	768	692	623	561

Note: beam irradiance must be corrected to adjust to actual sun–earth distance on specific days (see Table 3)

3.2 *European Solar Radiation Atlas* clear sky irradiance model

3.2.1 General

The theoretical clear sky model developed for the fourth edition of the *European Solar Radiation Atlas*[1] has been used to develop the clear sky irradiance tables provided in this Guide. The scientific basis of the model used is described below.

The beam irradiance given in the tables is estimated as a function of the Linke turbidity factor and solar altitude. A standard reference Linke turbidity factor of 3.5 has been adopted. This value provides beam irradiance estimates that are usually initially conservatively high. The Linke turbidity factor is referred to an air mass of 2, following the recommendations of Kasten[21]. Guidance is given in section 3.5 on the subsequent application of adjustments to the tabulated values to allow for more turbid conditions.

The clear sky diffuse irradiance is estimated separately, beginning with the hourly horizontal diffuse irradiance. These values depend on solar altitude and the Linke turbidity factor. As the Linke turbidity factor increases, the horizontal diffuse irradiance at a given solar altitude rises. The sky diffuse irradiance values for inclined planes are then estimated from the horizontal values, using a validated slope model that reflects the actual radiance distribution of the clear sky.

The actual path length through the atmosphere is very significant. This path length is described in relative terms using the concept of relative air mass. The optical path length is expressed as the ratio of the actual optical path length to the optical path length at solar zenith to sea level for a standard atmosphere. The air mass value thus depends on site elevation and solar altitude.

3.2.2 Clear sky beam irradiance

More detailed descriptions of the model is published elsewhere[1] and a full report with independent tests by Rigollier et al.[20].

Beam normal irradiance

The irradiance normal to the beam is calculated using the Linke turbidity factor as follows:

$$B_n = 1367\ \varepsilon_j \exp\left[-0.8662\ T_{LK}\ m\ \delta_r(m)\right] \quad (38)$$

where B_n is the irradiance normal to the beam ($W \cdot m^{-2}$), ε_j is the correction to mean solar distance on Julian day number J (see equation 13), m is the relative optical air mass corrected for station atmospheric pressure (usually known as the air mass), T_{LK} is the Linke turbidity factor (for air mass m = 2) and $\delta_r(m)$ is the Rayleigh optical depth of clear blue dry sky at air mass m.

The Linke turbidity factor was set at 3.5 for the tables presented in this document.

The relative optical air mass at sea level is approximately equal to ($1 / \sin \gamma_s$) but is calculated accurately as:

$$m_{SL} = 1 / \left[\sin \gamma_s + 0.50572\ (\gamma_s + 6.07995)^{-1.6364}\right] \quad (39)$$

where m_{SL} is the relative optical air mass at sea level and γ_s is the solar altitude (°).

The sea level air mass must be corrected for station atmospheric pressure, as follows:

$$m = m_{SL}\ (p / p_o) \quad (40)$$

where m is the optical air mass corrected for station atmospheric pressure, p is the atmospheric pressure of the station (kPa) and p_o is the atmospheric pressure at sea level (kPa).

As station height increases, the rays of the sun have to pass through less of the atmosphere. The result is mountain sites experience higher cloudless day beam irradiances at a given solar altitude than low-level sites in the same region, see Figure 7.

If observed values of the station atmospheric pressure are available in kPa, the hourly pressure correction is (p / 101.3). If the vapour pressure is in millibars, the correction is (p / 1013). Otherwise, for elevations below 4000 metres, the following expression is adequate:

$$(p / p_o) = 1 - (z / 10000) \quad (41)$$

where z is the site elevation above sea level (m).

Rayleigh optical depth

The Rayleigh optical depth, $\delta_r(m)$, describes the transmission characteristics of a pure, clean dry atmosphere without pollution[21]. It represents the transmission characteristics of the pure blue sky.

The Rayleigh optical depth is a function of the air mass. It's reciprocal is given by:

$$1 / \delta_r(m) = 6.6296 + 1.7513\ m - 0.1202\ m^2 + 0.0065\ m^3 - 0.00013\ m^4 \quad (42)$$

where m is the optical air mass corrected for elevation. (The polynomial limit for reliability is an air mass less than 20. For air mass >20, then $(1 / \delta_r(m)) = 10.4 + 0.718\ m$.)

Irradiance normal to the beam

Table 8 provides calculated sea level values of the beam irradiance normal to the beam at mean solar distance for a range of Linke turbidity factors. This table can be used to adjust the tabulated standard hourly beam values in the world clear sky solar irradiance tables for different Linke turbidity factors, see section 3.6. Site elevation can be considered by using the effective Linke turbidity factor, T_{LK} (p / p_o).

Figure 7 below shows the impact of site elevation on the beam normal irradiance with the sun at different solar altitudes, expressed as a ratio to the beam normal values for the standard Linke turbidity factor of 3.5 at sea level. Elevation is most significant at low solar altitude angles.

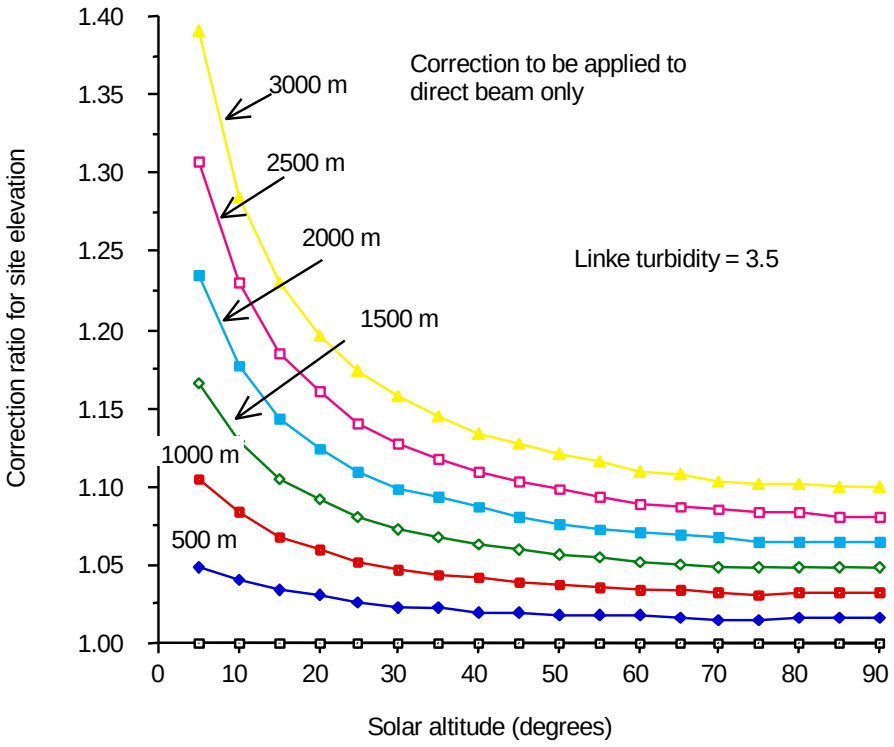

Figure 7 Effect of site elevation in metres on the predicted beam irradiance expressed as a ratio to the sea level beam irradiance at different solar altitude angles

Example 2

Estimate the beam normal irradiance at latitude 50° at 15:30 on Aug 4 for a Linke turbidity factor of 5.5. The solar altitude angle is 36.93°.

From Table 8, a Linke turbidity factor of 5.5 yields an adjusted beam normal irradiance of 580 W·m^{-2}. Correcting to mean solar distance using Table 3 give the irradiance corrected for mean solar distance as (580 × 0.971) = 563 W·m^{-2}.

3.2.3 Clear sky diffuse irradiance on horizontal surfaces

The diffuse horizontal irradiance of the clear sky, D_c, depends on the solar altitude, the site elevation and on the air mass 2 Linke turbidity factor, T_{LK}. As the sky becomes more turbid, the diffuse irradiance increases while the beam irradiance decreases. Figure 8 presents sea level values of the clear sky diffuse irradiance on horizontal

surfaces at different solar elevations for a range of values of Linke turbidity factor. These values are based on mean solar distance. They may be corrected to mean solar distance on specific dates using Table 3. The horizontal diffuse irradiance for any value of Linke turbidity factor may be estimated graphically from Figure 8. The numerical algorithm used may be found in Appendix A3, section A3.3.

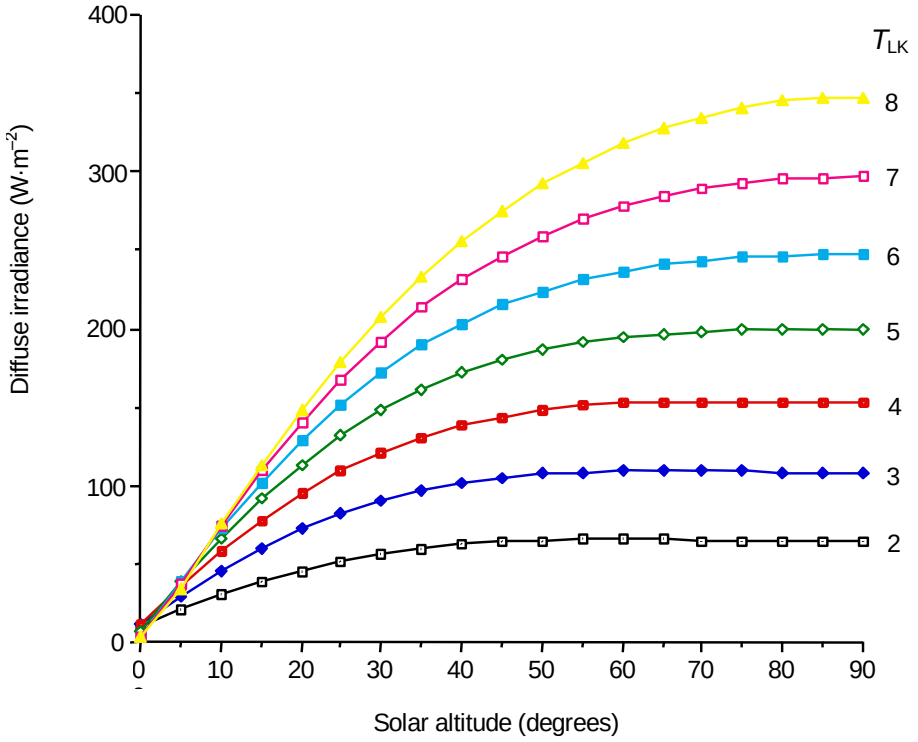

Figure 8 Diffuse irradiance on horizontal surfaces (at sea level) from the clear sky at mean solar distance as a function of solar altitude, for T_{LK} values from 2 to 8

Example 3

Compare the estimated diffuse irradiance at latitude 50° N at 15:30 on Aug 4 for a Linke turbidity factor of 6 with the tabulated values for the standard Linke turbidity factor of 3.5.

From the world clear sky solar irradiance tables, the tabulated horizontal diffuse irradiance at latitude 50° N at 15:30 on Aug 4 for a Linke turbidity factor of 3.5 is 113 W·m^{-2}.

Figure 8 shows that, at the corresponding solar elevation of 36.9°, the diffuse horizontal irradiance for a Linke turbidity factor of 6 is about 180 W·m^{-2} at mean solar distance. Correcting to mean solar distance for Aug 4 using Table 3 gives the irradiance as (180 × 0.971) = 175 W·m^{-2}.

Therefore, the proportional increase in horizontal sky diffuse is (175/113) = 1.55.

3.2.4 Clear sky global irradiance

The clear sky global irradiance on a horizontal surface is simply obtained from beam normal irradiance, the solar altitude and the diffuse horizontal irradiance:

$$G_c = B_n \sin \gamma_s + D_c \quad (43)$$

where G_c the clear sky global irradiance on a horizontal surface ($W \cdot m^{-2}$), B_n is the beam normal irradiance ($W \cdot m^{-2}$) and γ_s is the solar altitude angle (°).

3.2.5 Estimation of clear sky diffuse irradiances on vertical surfaces

The conversion to sloping surfaces needed to generate the clear sky tables has followed the principles set down in section 2.10.5. However, in this case, the CEC ESRA[1] clear vertical surface irradiance algorithm, which is Linke turbidity factor sensitive, was used, rather than the Muneer model. For details, see Appendix A3, section A3.4.

Figure 9 below shows the conversion factors that were applied to obtain the diffuse sky irradiation on vertical surfaces of given orientation from the horizontal diffuse irradiance given in the world clear sky solar irradiance tables. The mathematical algorithm used is given in Appendix A3, section A3.4. The correction to mean solar distance is dealt with implicitly in the estimation of the horizontal value. Note the large departure from the isotropic sky model value of 0.5 for all solar elevations and wall solar azimuth angles. It is clear from Figure 9 that the lower the sun, the greater are the directional effects.

The ground reflected contribution is estimated as explained in section 2.10.6 and then added to the sky component to give the total diffuse component on the different vertical surfaces.

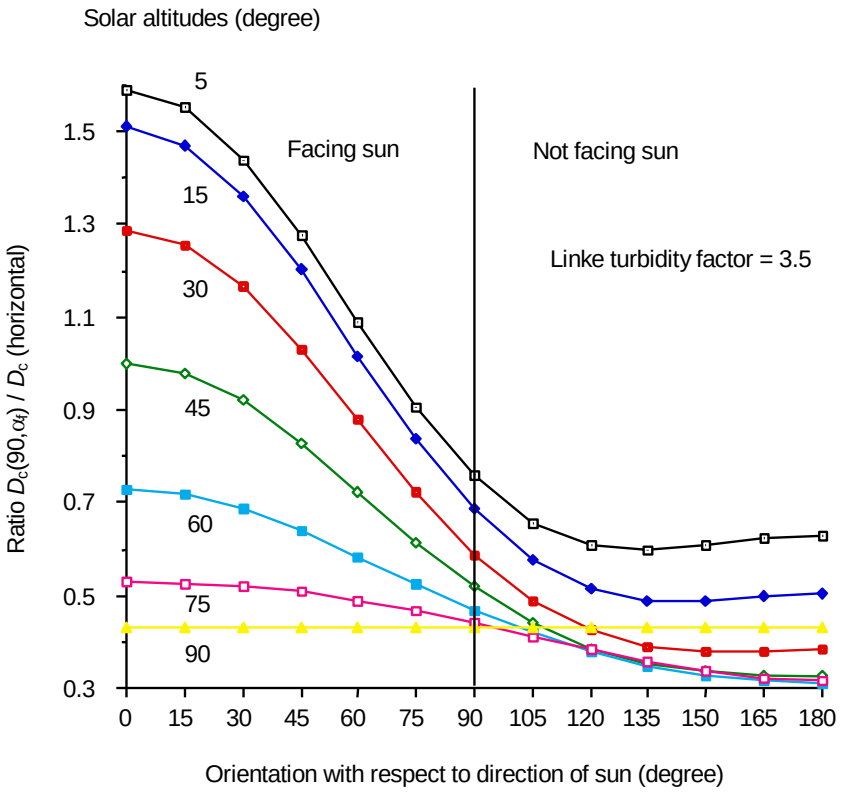

Figure 9 Relative diffuse sky irradiance from the clear sky on vertical surfaces, $D_c(90,\alpha_f)$, for a Linke turbidity factor of 3.5 expressed as a ratio to the sky diffuse horizontal value, D_c, as a function of wall solar azimuth angle α_f and solar altitude angle

3.2.6 Estimation of clear sky diffuse irradiances on non-vertical inclined planes

The clear sky values of the sky diffuse irradiance falling on non-vertical inclined surfaces may be estimated from the clear sky hourly beam and diffuse horizontal surface values using the methods set down in section 2.10.5.

3.3 World clear sky solar irradiance tables

3.3.1 General

The tables of predicted solar irradiance provide calculated hour-by-hour values of the beam and diffuse irradiance on vertical surfaces for a range of surface orientations. These tables are referred to in this document as the world clear sky solar irradiance tables. The diffuse irradiance values given in the tables combine the ground reflected diffuse radiation with the diffuse radiation from the sky. These tables provide irradiances for clear skies for latitudes between 0° and 60°, at intervals of 10°, with an additional table for latitude 55°. The tables were calculated using a Linke turbidity factor of 3.5. Interpolation between the tables is required in order to determine the irradiances for the exact latitude of a specific site.

The tables are corrected to mean solar distance in the northern hemisphere. The underlying solar geometry was calculated using the declination values for the clear sky design days in the year given in Table 2. Therefore, in geometric terms, the world clear sky solar irradiance tables for any given latitude align precisely with values given in the accommpanying world solar altitude angles and azimuths table. The world irradiance tables also include the corresponding horizontal surface irradiance values. The diffuse irradiance received on vertical surfaces from the sky alone may be obtained from the tables by subtracting the tabulated ground component on the slope, see below (section 3.3.3), from the combined tabulated diffuse irradiance value.

In addition to the hourly irradiance values, the tables provide daily mean beam and diffuse irradiance values averaged over 24 hours. These daily mean irradiance values on different planes form the first irradiance data column. Beam and diffuse daily mean irradiances are presented separately.

With the exception of the sunrise and sunset hour, all irradiance calculations were performed on the half hour using local apparent time (LAT), i.e. at the mid-hour of the standard meteorological hourly period adopted, e.g. 10:00 to 11:00, 11:00 to 12:00 LAT etc. In the first hour of sunlight and the last hour of sunlight, a different procedure was used for choosing the calculation time, see section 2.7.5. Values calculated for these partially sunlit hours are shown in italics.

The mean daily irradiance values given in the world clear sky solar irradiance tables were obtained by calculating the daily irradiation (including the adjustments described in section 3.3.6) and dividing the result by 24. Note that, as a consequence of the integration process, the tabulated values of the daily mean irradiance multiplied by 24 do not exactly equal the sums of the corresponding hourly irradiance values.

3.3.2 Adjustment for sky clarity and elevation of site

The irradiances given in the world clear sky solar irradiance tables were calculated for sites at sea level and for a standard value of sky clarity corresponding to a Linke turbidity factor of 3.5. This was chosen as being a conservative base value for examining overheating risks and peak air conditioning design load risks. The value adopted represents a relatively clear atmosphere containing some moisture and a modest level of particulates. The accompanying turbidity tables provide factors to enable the tabulated values to be adjusted for different values of atmospheric clarity and for elevation of the site above sea level. The use of these tables is discussed in section 3.5.

3.3.3 Adjustment for ground albedo

The ground-reflected component on sloping surfaces may be estimated for any selected ground albedo (see Table 7) using the tabulated horizontal global irradiance values. The tabulated ground-reflected component, for a ground albedo of 0.20, is given by:

$$R_{gh} = 0.20\, r_g\, G_c \qquad (44)$$

where R_{gh} is the standard ground-reflected component ($W \cdot m^{-2}$) corresponding to a ground albedo of 0.20, G_c is the horizontal global irradiance ($W \cdot m^{-2}$) and r_g is the ground slope factor, see equation 37. (For vertical surfaces, $r_g = 0.5$.)

The ground-reflected component corresponding to some other value of ground albedo is then given by:

$$R_{gh}' = (\rho_g - 0.20)\, r_g\, G_c + R_{gh} \quad (45)$$

where R_{gh}' is the ground-reflected component ($W \cdot m^{-2}$) corresponding to a ground albedo ρ_g.

3.3.4 Calculation of angles of incidence and solar altitude angles from world clear sky irradiance tables

The world clear sky solar irradiance tables provide the beam irradiance values normal to the beam as well as slope values. As a result, the cosine of the angle of incidence of the beam on any tabulated surface at any selected time may be derived directly as the ratio of beam irradiance on the surface to the irradiance normal to the beam. The sine of the solar altitude angle is given by the ratio of the beam horizontal irradiance to the irradiance normal to the beam.

3.3.5 Application to southern hemisphere

The world clear sky solar irradiance tables have been corrected to solar distance for the northern hemisphere using equation 13. An additional correction factor must be applied month-by-month in order to use the tables for sites in the southern hemisphere. Table 9 provides solar distance ratio correction factors that must be applied as multipliers to both the tabulated beam and the diffuse irradiance values when using the tables for sites in the southern hemisphere.

Table 9 Solar distance correction factors for southern hemisphere

Correction factor for stated design day											
Jul 3	Aug 3	Sep 3	Oct3	Nov 3	Dec 21	Jan 28	Feb 25	Mar 28	Apr 28	May 29	Jun 3
0.938	0.953	0.982	1.015	1.046	1.068	1.066	1.050	1.019	0.985	0.955	0.942

3.3.6 Estimation of irradiation from irradiance values

The world clear sky solar irradiance tables present values of the instantaneous flux ($W \cdot m^{-2}$). Solar irradiation is the flux integrated with respect to time ($W \cdot h \cdot m^{-2}$), see section 2.1. If the sun is on the surface for the whole hour, the clear sky hourly irradiation is approximately equal to the mid-hour irradiance. However, if this is not the case, the approximation is not valid and allowance must be made for the proportion of the hour during which the sun is actually on the surface in order to convert irradiance to irradiation.

The times of sunrise and sunset in LAT need to be known in order to achieve the conversion from irradiance to irradiation for the sunrise and sunset hours. The first and last segments can be treated approximately as triangles. The irradiation is given by the area of the triangle. To estimate the sunrise hour irradiation, the irradiance calculated at the midpoint between sunrise and the end of the sunrise hour is multiplied by half the proportion of the sunrise hour during which the sun is above the horizon: i.e. if sunrise is at 05:15, the proportion of hour with the sun up is 0.75 hours. Therefore, the tabulated irradiance values are multiplied by (0.75 / 2) to obtain the irradiation in the sunrise hour. A similar procedure is used for the sunset hour, but working on a sunset hour-beginning basis. The sunrise and sunset times are included in the world clear sky solar irradiance tables, expressed in hours and minutes.

For the general case for a surface of any orientation, if the surface is irradiated for a period ΔT, the beam irradiance on the surface is given by:

$$B_h(\beta,\alpha) = B(\beta,\alpha,t)\,\Delta T \quad (46)$$

where $B(\beta,\alpha,t)$ is the beam irradiance on the surface at the mid-point time t of the beam irradiated period within the hour, t is the mid-point time of the period of irradiation and ΔT is the period of irradiation (h).

For diffuse radiation, the corresponding integration problem only arises in the sunrise and sunset hour.

3.4 Plotting irradiance curves from irradiance tables

To plot irradiances from the tabular data as time series, it is recommended that the times during which the beam is on and off the surface in different months first be determined. This may done by interpolation from solar altitude/azimuth tables, from solar charts or by direct calculation.

The plot-time for the (italicised) sunrise hour values is midway between the tabulated sunrise time and the end of the sunrise hour. The plot-time for the (italicised) sunset hour values is midway between the beginning of the sunset hour and the tabulated sunset time. Sunrise and sunset are additional plotting points that can be extracted from the tables.

Care must be taken if a spreadsheet program is used to plot irradiances. It is important that the spreadsheet takes account of the exact times at which the solar radiation begins to and ceases to impinge upon the surface.

3.5 Correction factors for site elevation and turbidity

The accompanying turbidity correction table provides numerical factors to adjust the tabulated irradiance values in the world clear sky solar irradiance tables to match the sky clarity conditions appropriate to the site. The table provides separate numerical correction factors for global, beam and diffuse irradiance values for Linke turbidity factors between 2.5 (exceptionally clear) and 6.5 (relatively turbid). These factors are applied as simple multipliers to the tabulated beam and diffuse irradiance values given in the world clear sky solar irradiance tables. The adjustment requires an estimate to be made of the Linke turbidity factor in each month, see section 3.7.

The three factors are identifed as follows:

— daily turbidity correction factor for global irradiation: k_{sg}

— daily turbidity correction factor for beam irradiation: k_{sb}

— daily turbidity correction factor for sky diffuse irradiation: k_{sd}.

The turbidity correction table was established by numerical integration of the hourly values computed by the CEC ESRA clear sky model[(1)] over the day at sea level using Linke turbidity factors of 2.5, 3.5, 4.5, 5.5 and 6.5. The daily correction ratios for each value of the Linke turbidity factor at each tabulated latitude were then obtained by dividing the daily irradiation totals obtained using that Linke turbidity factor by the tabulated daily totals (i.e corresponding to a Linke turbidity factor of 3.5) for each month.

The height correction factor table provides daily height correction factors for different elevations above sea level. The three factors are identifed as follows:

— daily height correction factor for global irradiation: k_{hg}

— daily height correction factor for beam irradiation: k_{hb}

— daily height correction factor for sky diffuse irradiation: k_{hd}.

The height correction factors in the table were calculated using a reference Linke turbidity factor of 3.5 and varying the site elevation above sea level to obtain the daily correction factors.

The turbidity and height correction factor tables are used in combination. Once the appropriate Linke turbidity factors have been established, see section 3.6, the turbidity correction factor table may be used to obtain the daily beam (k_{sb}) and diffuse (k_{sd}) correction factors. The corresponding height correction factors (k_{hb} and k_{hd}) are then obtained from the height correction factor table.

The corrected clear sky design direct beam irradiance on any slope is then estimated as:

$$B_c(\beta,\alpha)' = k_{hb}\, k_{sb}\, B_c(\beta,\alpha) \tag{47}$$

where $B_c(\beta,\alpha)'$ is the corrected design direct beam irradiance ($W \cdot m^{-2}$), k_{hb} is daily height correction factor for beam radiation, k_{sb} is the daily turbidity correction factor for beam radiation and $B_c(\beta,\alpha)$ is the slope beam irradiance ($W \cdot m^{-2}$) interpolated from the world clear sky solar irradiance tables.

In the daily ratio correction method, the beam correction factors are applied uniformly to all tabulated beam values throughout that day in a given month. This method does not take full account of the effect of path length through the atmosphere on the intensity of the solar beam. It is thus a pragmatic correction method of lesser accuracy than using the algorithmic model described in section 3.2. In particular, the daily correction method gives less accurate results for east- and west-facing surfaces than for surfaces facing the equator. This is because a significant proportion of the east and west vertical daily irradiation is associated with low solar elevations, which are less well corrected by the daily horizontal ratio method.

In order to correct the tabulated sky diffuse component, the ground reflected component must first be subtracted from the overall diffuse component to obtain the tabulated clear sky diffuse irradiance falling on the vertical surface. Using the standard ground albedo of 0.2, the design sky component for a vertical surface is given by:

$$D_c(\beta,\alpha)' = k_{hd}\, k_{sd}\, (D_c(\beta,\alpha) - 0.10\, G_c) \tag{48}$$

where $D_c(\beta,\alpha)'$ is the corrected design sky diffuse component for a vertical surface ($W \cdot m^{-2}$), k_{hd} is the daily height correction factor for diffuse radiation, k_{sd} is daily turbidity correction factor for diffuse radiation, $D_c(\beta,\alpha)$ is the sky diffuse component for a vertical surface ($W \cdot m^{-2}$) interpolated from the world clear sky solar irradiance tables and G_c is the tabulated ground reflected component ($W \cdot m^{-2}$).

Finally, the corrected ground reflected component for a vertical surface is added. The basic ground reflected component may be obtained from the tabulated values of beam direct and diffuse and horizontal components using equation 36.

The corrected ground reflected component is obtained from:

$$R_{cg}(\beta,\alpha)' = 0.5\, \rho_g\, G_c' = 0.5\, \rho_g\, (B_c' + D_c') \tag{49}$$

where $R_{cg}(\beta,\alpha)'$ is the corrected ground reflected component ($W \cdot m^{-2}$), ρ_g is the ground albedo, B_c' is the corrected beam direct component ($W \cdot m^{-2}$) and D_c' is the corrected diffuse component ($W \cdot m^{-2}$).

Therefore:

$$R_{cg}(\beta,\alpha)' = 0.5\, \rho_g\, (k_{hb}\, k_{sb}\, B_c + k_{hd}\, k_{sd}\, D_c) \tag{50}$$

where k_{hb} is the daily height correction factor for beam radiation, k_{sb} is daily turbidity correction factor for beam radiation, k_{hd} is the daily height correction factor for diffuse radiation and k_{sd} is daily turbidity correction factor for diffuse radiation.

Thus:

$$R_{cg}(\beta,\alpha)' = 0.5\ \rho_g\ (k_{hg}\ k_{sg}\ G_c) \quad (51)$$

where k_{hg} is the daily height correction factor for global radiation, k_{sg} is daily turbidity correction factor for global radiation and G_c is the horizontal global irradiance ($W \cdot m^{-2}$).

The corrected ground component is added to the corrected sky diffuse component to obtain the overall corrected diffuse component.

Example 4

Athens, Greece (latitude 37° 58' N), is known to have had heavy pollution in the period 1966–75. A study for Athens yielded a representative clear day Linke turbidity factor of about 5.5 in August. By contrast, Porto, Portugal (latitude 41° 8' N) has a very clear atmosphere and a similar study yielded a Linke turbidity factor of about 3.2 for the same month. Estimate the clear day beam, diffuse and global correction factors at Athens and Porto on Aug 4. Determine the clear day daily beam and diffuse irradiation on a south-facing surface at Athens on this day and estimate the three components of the irradiance on this vertical south surface at 11:30 LAT. The effect of site elevation may be neglected since both sites are close to sea level.

Step 1: determine basic correction factors k_{sg}, k_{sb} and k_{sd}

For Athens (approximately 40° N), Linke turbidity factor for August is 5.5. Therefore from the turbidity correction factor table:

— turbidity correction factor for beam irradiation: $k_{sb} = 0.76$

— turbidity correction factor for diffuse irradiation: $k_{sd} = 1.57$

— turbidity correction factor for global irradiation: $k_{sg} = 0.90$

For Porto (approximately 40° N), Linke turbidity factor for August is 3.2. Therefore, by interpolation:

— turbidity correction factor for beam irradiation: $k_{sb} = 1.03$

— turbidity correction factor for diffuse irradiation: $k_{sd} = 0.94$

— turbidity correction factor for global irradiation: $k_{sg} = 1.02$

Step 2: obtain basic irradiance values for latitude of Athens

For interpolation between 30° N and 40° N, the interpolation factor from 40° N is (10° – 7.97°) / 10 = 0.203. Therefore, the global horizontal irradiation at 11:30 LAT on August 4 is obtained from the world clear sky solar irradiance tables as follows:

— for latitude 30° N: global horizontal irradiance = 1009 $W \cdot m^{-2}$

— for latitude 40° N: global horizontal irradiance = 947 $W \cdot m^{-2}$

— for latitude 37° 58' N: global horizontal irradiance = [947 – 0.203 (947 – 1009)] = 959.6 $W \cdot m^{-2}$

The beam and diffuse irradiances are obtained similarly. The sky diffuse irradiance is obtained from the diffuse and global horizontal irradiances using equation 48.

Table 10 shows the irradiances obtained for 11:30 LAT on August 4 at 30° N and 40° N and the interpolated values corresponding to 37° 58' N (i.e. 37.97° N).

Table 10 Example 4: determination of basic irradiances for horizontal and south facing vertical surfaces for 11:30 LAT on August 4

Latitude	Global irradiance on horiz. surface ($W \cdot m^{-2}$)	Irradiance on south facing vertical surface ($W \cdot m^{-2}$)		
		Beam	Diffuse	Sky diffuse
30° N	1009	198	167	167 – (0.1 × 1009)
40° N	947	342	174	174 – (0.1 × 947)
37.97° N	960	313	173	172.6 – (0.1 × 959.6) = 77

Values of daily irradiation for latitudes 30° N and 40° N are estimated by multiplying the appropriate daily mean irradiances by 24. Values for latitude 37° 58' N are then obtained by interpolation, as described above. Table 11 summarises the values of daily irradiation obtained for August 4.

Table 11 Example 4: determination of basic daily irradiation values for horizontal and south facing vertical surfaces on August 4

Latitude	Daily global irradiation on horiz. surface ($W \cdot m^{-2}$)	Daily irradiation on south facing vertical surface ($W \cdot m^{-2}$)		
		Beam	Diffuse	Sky diffuse
30° N	8088	984	1560	1560 – (0.1 × 8088) = 751
40°	7872	1968	1656	1656 – (0.1 × 7872) = 869
37.97° N	7916	1768	1637	1636.5 – (0.1 × 7915.8) = 845

Step 3: application of correction factors to obtain hourly irradiances

Corrected irradiances at 11:30 LAT on 4 August for vertical south facing surface are as follows.

For beam radiation:

— from step 1, turbidity correction factor, $k_{sb} = 0.76$

— from Table 10, beam irradiance for latitude 37.97° N = 313 $W \cdot m^{-2}$

— corrected (design) beam irradiance for latitude 37.97° N = 0.76 × 313 = 238 $W \cdot m^{-2}$

For sky diffuse radiation:

— from step 1, turbidity correction factor, $k_{sd} = 1.57$

— from Table 10, sky diffuse irradiance for latitude 37.97° N = 77 $W \cdot m^{-2}$

— corrected (design) sky diffuse irradiance for latitude 37.97° N = 1.57 × 77 = 121 $W \cdot m^{-2}$

For ground reflected radiation:

— from step 1, turbidity correction factor for global irradiation: $k_{sg} = 0.90$

— from Table 10, global horizontal irradiance = 960 $W \cdot m^{-2}$

— using equation 51, for a ground albedo of 0.2, ground reflected component for latitude 37.97° N = 0.5 × 0.2 × 960 = 96 $W \cdot m^{-2}$

— corrected (design) ground reflected component for latitude 37.97° N = 0.9 × 96 = 86 $W \cdot m^{-2}$

For global radiation:

— corrected (design) global irradiance for latitude 37.97° N = 238 + 120 + 86 = 444 W·m^{-2}

Therefore, the effects of correcting the tabulated data for site turbidity are as follows:

— beam irradiance is reduced by 24%

— overall diffuse irradiance is increased by 19%

— sky diffuse irradiance is increased by 57%

— global irradiance is reduced by 9%

Step 4: application of correction factors to estimate daily irradiation

Corrected daily irradiation on 4 August for vertical south facing surface is as follows.
For beam radiation:

— from step 1, turbidity correction factor, k_{sb} = 0.76

— from Table 11, beam irradiation for latitude 37.97° N = 1768 W·h·m^{-2}

— corrected (design) beam irradiation for latitude 37.97° N = 0.76 × 1768 = 1344 W·h·m^{-2}

For sky diffuse radiation:

— from step 1, turbidity correction factor, k_{sd} = 1.57

— from Table 11, sky diffuse irradiation for latitude 37.97° N = 845 W·h·m^{-2}

— corrected (design) sky diffuse irradiation for latitude 37.97° N = 1.57 × 845 = 1327 W·h·m^{-2}

For ground reflected radiation:

— from step 1, turbidity correction factor for global irradiation: k_{sg} = 0.90

— from Table 11, global horizontal irradiation = 7916 W·h·m^{-2}

— using equation 51, for a ground albedo of 0.2, ground reflected component for latitude 37.97° N = 0.5 × 0.2 × 7916 = 792 W·h·m^{-2}

— corrected (design) ground reflected component for latitude 37.97° N = 0.9 × 792 = 713 W·h·m^{-2}

For global radiation:

— corrected (design) global irradiation for latitude 37.97° N = 1344 + 1327 + 713 = 3384 W·h·m^{-2}

Therefore, the effects of correcting the tabulated data for site turbidity are as follows:

— beam irradiation is reduced by 24%

— overall diffuse irradiation is increased by 24%

— sky diffuse irradiation is increased by 57%

— global irradiation is reduced by 0.6%.

3.6 Estimation of Linke turbidity factors

The assessment of the actual site clarity conditions in different parts of the world is difficult. The following sections offer some practical suggestions for estimating the Linke turbidity factor. A more detailed discussion has been published elsewhere[22].

3.6.1 Temperate areas in the northern hemisphere

Table 12, which is based mainly on European experience, provides initial guidance for north European climates. 'Very clear' refers to mountain top sites. For most cities located in European temperate climates, 'urban atmosphere' values are usually the most appropriate for initial design assessment in the absence of specific information for the site.

Table 12 reveals a seasonal trend in the values of Linke turbidity factor in Europe, from a low in January to a high around July and August. Much of southern Britain is influenced by polluted continental air masses coming from mainland Europe. Clearest conditions in the UK tend to be found in the West Country, Wales, Northern Ireland and in Scotland outside the central industrial belt region.

Table 12 Monthly mean values of Linke turbidity factor for temperate climates (based on Steinhauser[23] and Schulze[24])

Type of atmosphere	Linke turbidity factor for stated month												
	Jan	Feb	Mar	Apr	May	Jun	Jul	Aug	Sep	Oct	Nov	Dec	Year
Very clear atmosphere	1.5	1.6	1.8	1.9	2.0	2.3	2.3	2.3	2.1	1.8	1.6	1.5	1.90
Clear atmosphere	2.1	2.2	2.5	2.9	3.2	3.4	3.5	3.3	2.9	2.6	2.3	2.2	2.75
Urban atmosphere	3.1	3.2	3.5	4.0	4.2	4.3	4.4	4.3	4.0	3.6	3.3	3.1	3.75
Industrial atmosphere	4.1	4.3	4.7	5.3	5.5	5.7	5.8	5.7	5.3	4.9	4.5	4.2	5.00

3.6.2 Areas in lower latitudes

A practical approach is that proposed by Perrin de Brichambaut and Vauge[25]. This formulation takes account of vapour pressure but requires either knowledge of the local climate to assess the colour of the sky, which is a subjective assessment or, alternatively, knowledge about typical visibility ranges in different seasons. The values suggested are shown in Table 13. The advantage of this approach is that it can be applied in regions where there are no observed global radiation data. Also, proper account can be taken of the impact of variations in vapour pressure between different seasons.

A shortcoming of the original formulation was the gap between the 'pale blue' and the 'milky blue to whitish' categories. Page[22] has added an extra peri-urban category affected by traffic pollution.

Table 13 Estimation of Linke turbidity factor (air mass 2) as a function of surface vapour pressure, visibility range or typical sky colour[25]

Typical sky colour	Visibility at surface (km)	Linke turbidity factor for stated vapour presure range (mb)			
		3–5	5–8	9–16	18–30
Deep blue	>100	2.0	2.3	2.6	2.9
Pure blue	60–100	2.6	2.9	3.2	3.5
Pale blue	30–50	3.4	3.7	4.0	4.3
Slightly brownish sky	—	3.8	4.1	4.4	4.7
Milky blue to whitish	12–25	4.9	5.2	5.6	5.8

3.7 Mapped data of monthly mean daily global irradiation

Month-by-month world maps of the monthly mean daily relative global irradiation (i.e. $(KT)_m = (G_d)_m/(G_{od})_m$) have been produced by the World Meteorological Organisation[26].

Increasingly, satellite observations are being used for global radiation mapping, for example Raschke et al.[27] for Africa. Such observations form the basis of the CD-ROM associated with the *European Solar Radiation Atlas*[1], which provides twelve monthly maps of $(KT)_m$ plus an annual (i.e. $(KT)_y$) map for the whole area covered by the Atlas. This publication also provides digital maps of monthly mean daily global, beam and diffuse irradiation on horizontal surfaces plus the three corresponding annual maps. These computer-based maps are based on a combination of ground and satellite observations of global irradiation for the period 1981–1990. The maps cover the area from 30° W to 70° E and from 25° N to 75° N. In the centre of the maps, the pixel size represents an area of approximately 10 km by 10 km.

Digital mapping not only gives the capability of achieving a very high spatial resolution but also implants the capacity to link the physical properties associated with each pixel with the location of the pixel, making data extraction exact.

There is currently very considerable international activity dedicated to making satellite observed solar radiation data available in a mapped form for applications on a worldwide basis using the world wide web for data distribution. More and more mapped global radiation data derived from such sources are becoming available through the Internet. For example, there is a considerable European effort in this field, much of it partially funded by the European Commission and based on the use of irradiation data derived from European satellites such as Meteostat.

Another important area of global mapping activity emerges from international work on world climate change. International work in this area is guided by the Intergovernmental Panel on Climate Change (IPPC) set up by the World Meteorological Organisation and the United Nations Environment programme. Currently, climate change models usually take the 1961–90 climatology as the starting point and so the data for this reference period are often mapped. Their systems have to cover the start-up climate reference period as well as providing predictions concerning future climate under different scenarios. The Climate Research Unit at the University of East Anglia* plays a significant role in data handling for the IPCC programme. This includes the operation of the IPCC Data Distribution Centre (http://www.ipcc-data.org/).

The present rapid rate of progress makes it difficult to incorporate these kinds of advances within this document. These recent advances are clearly welcome, but a key shortcoming is often that the data are not always adequately checked against ground observation. Furthermore, many of these data sources provide only global radiation data streams for horizontal surfaces. The currently available data records from satellites are also very short, which implies limited applicability in the assessment of long-term engineering risks such as the impacts of extremes of heat and cold. Therefore, the work described in this document is likely to remain important in making engineering decisions about heating, cooling and natural ventilation design.

A key step in using such data is the splitting of global irradiation into its two components of horizontal beam irradiation and horizontal diffuse irradiation. The methods used in the *European Solar Radiation Atlas*[1] are both seasonal and latitude dependent. The algorithms that were used in the atlas are set down in detail in Appendix A3, section A3.3, which provides the complete methodology for proceeding from monthly mean daily global irradiation data to hourly values of beam and diffuse irradiance on horizontal surfaces.

3.8 Estimation of hourly global radiation for overcast conditions

The transmittance of an overcast sky varies widely according to cloud type. The influence of different cloud types is considered in section 3.9. Mean irradiance values for an overcast day may be estimated from the solar altitude. An overcast day may be defined as a day with no recorded bright sunshine. Aydinli and Krochmann[28], using observed irradiation data from western Europe for days without sunshine, found the following mean relationship with solar altitude angle:

* Climate Research Unit, University of East Anglia, Norwich NR4 7TJ (http://cru.uea.ac.uk/link/)

$$G_b = \varepsilon_j (2.61 + 182.6 \sin \gamma_s) \quad (52)$$

where G_b is the global horizontal irradiance on overcast days (W·m^{-2}), ε_j is the correction factor to mean solar distance and γ_s is the solar altitude angle (°).

Hourly irradiance data for an overcast day may be obtained from daily (overcast) global irradiation data by deriving daily profiles of overcast day irradiance on horizontal surfaces using the methodology developed by Liu and Jordan[29,1]. The daily irradiation for an overcast day must first be estimated. One approach is simply to assume that the typical overcast day daily KT value is equal to the Angstrom coefficient, a_m (see section 2.9.1). However, overcast days have their own statistical distributions.

Cowley[11] presented annual overcast day transmittance (i.e. $(KT_d)_y$) values for the UK in the form of an annual map. The third edition of the *European Solar Radiation Atlas*[7] presents tabulated 10-year means of monthly minimum KT_d values for several hundred sites in Europe. Provided that overcast days actually occur (which, for example, they do not in many eastern Mediterranean sites during the summer), the monthly mean minimum daily KT_d values tend on average to be about 0.10, with rather lower values in winter. Further guidance may be found in the 3rd *European Solar Radiation Atlas*[7].

3.9 Influence of cloud type during overcast hours

Kasten and Czeplak[9] provide a useful analysis of radiation observations at Hamburg. Among other topics, they reported on the impact of cloud type on the observed transmittance of shortwave radiation during overcast hours at Hamburg. They found that the overcast hour diffuse radiation from a given cloud type was roughly a linear function of the sine of the solar altitude angle. There were, however, strong differences between the cloud types.

The overcast hour horizontal radiation data with different cloud types were expressed as a fraction of the corresponding clear sky global horizontal radiation found at Hamburg for the same solar elevation. Table 14 shows the resulting relative overcast hour cloud transmittances, where 'relative' means relative to the clear sky global irradiances on a horizontal surface. These relative transmittances were found not to vary much with solar altitude. The values in Table 14 can be used in conjunction with the world clear sky solar irradiance tables to provide rough estimates of maximum likely diffuse irradiation values with thin high cloud during overcast periods.

Table 14 Relative overcast cloud transmittances[9]

Cloud type	Transmittance
Cirrus, cirrostratus and cirrocumulus	0.61
Altocumulus and altostratus	0.27
Cumulus	0.25
Stratus	0.18
Nimbostratus	0.16

For example, for latitude 50° N, the clear sky global irradiance at 12:30 LAT on June 21 is 912 W·m^{-2}. Therefore, using Table 14 for an overcast, cirrus-covered sky, the horizontal surface global and diffuse irradiance is estimated as 912 × 0.61 = 552 W·m^{-2}. Observations for Bracknell and Aberporth, see section 3.10, indicate that the maximum observed hourly diffuse horizontal irradiation is approximately equal to 9 γ_s, where γ_s is the solar altitude angle in degrees. For this example, for latitude 50° N, the solar altitude and azimuth table gives the corresponding solar altitude angle as 63°. Hence, the slope is (552 / 63), i.e. $G = 8.76\ \gamma_s$ W·m^{-2}, which agrees well with the Bracknell and Aberporth observations.

3.10 Estimation of diffuse irradiance under partially clouded conditions

Estimation of likely solar radiation loads under partially clouded conditions and their consequent impact on building services design presents considerable practical difficulties without the aid of computer simulation. The maximum hourly diffuse irradiation values on horizontal surfaces tend to occur during hours of broken thin cloud. The diffuse radiation from partially clouded skies is normally substantially higher than the diffuse radiation either from clear skies or from overcast skies. Therefore, attempting to calculate the monthly mean hourly diffuse radiation by linear interpolation between estimated overcast sky and estimated clear sky hourly diffuse radiation values is not valid. Appendix A2 suggests a more appropriate methodology.

The typical hourly sunshine that produces the highest diffuse irradiation conditions is about 0.3 to 0.5 hours during the hour. Surprisingly high global radiation levels can occur under thin high cloud conditions but the radiation is very diffused. The consequent global radiation loads on vertical surfaces are approximately equal over all facades of the building.

Using UK observations, Louden[30] set the cloudy sky diffuse irradiance on a horizontal surface as 5.04 γ_s W·m^{-2}, where γ_s is the solar altitude in degrees. This linear formula was used to produce the diffuse cloudy values in the world solar irradiance design tables. Recent work[1] has shown that this approach overestimates the diffuse irradiance at the higher solar elevations characteristic of the tropics. Appendix A2 suggests that a sine relationship is more appropriate. If consistency with previous practice is desired, a match at 45° degrees between Louden's UK-based linear relationship and the sine relationship given in Appendix A2 suggests that diffuse cloudy irradiances might be set at 321 sin γ_s W·m^{-2} for humid tropical design. However, this would not be an absolute maximum design level and Appendix A2 indicates the higher value of 463 sin γ_s W·m^{-2} as representative of UK maximum diffuse conditions. Such conditions can be expected elsewhere with thin cirrus cloud.

During the preparation of this document, a study of the maximum observed hourly diffuse horizontal irradiation as a function of solar altitude was undertaken over one year for Bracknell and Aberporth. It was found that the maximum valid observed values fell within an envelope which could be approximated by the product 9 γ_s W·m^{-2}, where γ_s is the solar altitude in degrees.

The majority of the observed UK data are associated with solar elevations below 30°. As the sine function does not approximate to a straight line very well for solar elevations above 45°, it would be unwise to project the 9 γ_s relationship beyond solar altitude angles of about 50°. For example, for latitude 0°, the world clear sky irradiance tables gives the clear sky global horizontal irradiance at 12:30 on September 4 as 1042 W·m^{-2}. Using Table 5.14, for cirrus-type clouds, the overcast global irradiance is (1042 × 0.61) W·m^{-2}. The corresponding solar altitude angle of 80° yields (1042 × 0.61) / 80 = 7.95 γ_s W·m^{-2}, which may be compared with the observed UK envelope values at a solar altitude angle of 45°. Adopting the sine relationship suggests that setting diffuse cloudy irradiation equal to 572 sin γ_s W·m^{-2} might be a more suitable expression to define engineering extremes for diffuse horizontal sky irradiance under cirrus cloud conditions at lower latitudes. These suggestions should be regarded as tentative until more detailed research has been carried out datasets for low latitudes.

When considering peak cooling loads in the presence of thin cloud, this approach leads to substantially increased cooling loads due to diffuse irradiation. However, this increase is offset by the corresponding reduction in the cooling load due to beam irradiation.

4 Longwave radiation exchanges at external surfaces of buildings

4.1 Basic principles

Section 4 is based on the decisions made during the development of the 4th edition of the CEC *European Solar Radiation Atlas*[1], funded by DGXII of the European Commission. The key contributors to the improved

scientific analysis of longwave radiation for practical applications have been R. Aguiar (INETI, Portugal), G. Czeplak (DWD Germany), R. Dognieux (IRMB, Belgium) and J.K. Page (University of Sheffield, England).

This section provides quantitative analytical procedures for estimating longwave radiation exchanges with the external surfaces of buildings. Such information is needed, for example, in order to:

— calculate sol-air temperatures, see section 5

— assess the potential of natural radiative cooling

— assess the risks of night time surface condensation.

Longwave radiation is thermal radiation emitted at temperatures at or fairly close to those found at the earth's surface. The waveband range covered is from 4 μm and 100 μm. The major characteristics of longwave radiation are as follows:

— Incoming longwave radiation on external surfaces is received both from the atmosphere and from all other elements to which the surface is radiatively exposed as a consequence of its surface orientation. For inclined surfaces, the incoming longwave radiation sources thus include the ground, the surrounding building elements, landscape elements etc., in addition to the atmosphere itself.

— The longwave radiation exchange at any surface involves a two-way process. Longwave radiation is absorbed at the surface from the radiative environment seen by the surface. Simultaneously, longwave radiation is emitted from the surface to that surrounding environment. This radiative exchange is strongly influenced by the longwave surface emissivity/absorptivity properties of the receiving surface.

— The net longwave energy balance on any surface is the difference between the absorbed incoming long-wave radiation and the emitted outgoing longwave radiation. There is normally a net longwave radiative loss that continues day and night. This net loss is normally greatest from horizontal surfaces.

— In daylighting hours, the incoming shortwave radiation absorbed offsets the net cooling effects of long-wave radiation, so its impact is often concealed. The impact of longwave radiation is more obvious after dark when not compensated for by any incoming shortwave radiation. Nevertheless, these longwave impacts are taken into account in standard design heat loss calculations within the concept of the external surface conductance.

— Cloud cover produces an increase in the incoming longwave downward radiative flux from the sky dome. Increase in cloud cover makes the net longwave radiation balance less extreme compared to clear sky conditions. The greatest reduction in net losses is associated with low cloud but even then there still is normally a net longwave radiation loss from external building surfaces to the outdoor environment. The greatest longwave losses occur from horizontal surfaces under cloudless conditions with a dry atmosphere aloft.

— Under cold winter conditions, the adverse radiative balance found on clear still nights is of particular concern. During calm clear nights, the net outgoing flux can be sufficient to cause the outside surface of insulated lightweight components to cool as much as 10° C below the external air temperature. While this rarely lasts long enough to have a significant effect on energy use, it can cause severe interstitial condensation in, for example, an inadequately sealed sheet metal roof. The practical consequences of these external surface cooling effects, most evident in long clear winter nights, need consideration in their own right, requiring a quantitative analysis of night-time heat balances.

— In hot weather such night-time radiative cooling may be advantageous. It can be harnessed in design through the use of passive cooling techniques.

4.2 Estimating longwave radiation exchanges on horizontal surfaces

The incoming longwave radiation from the atmosphere falling on horizontal surfaces is not a widely measured meteorological variable, so its magnitude must be estimated from other available climatological variables using relationships derived from research. The incoming longwave radiation falling on an inclined surface is made up

of two components: the atmospheric longwave radiation received directly from the sky, $L_{sky}(\beta)$, and the long-wave radiation received from the ground, $L_g(\beta)$. The component $L_g(\beta)$ includes radiation both emitted from and also reflected from the ground and/or from other surrounding surfaces to which the surface is radiatively exposed. In this document the longwave radiation and sol-air temperatures have been computed on the assumption that the exposed surfaces are unobstructed. Figure 3 defines the surface geometry. In the case of an unobstructed site, the two incoming longwave components depend on surface slope (β) alone and not on surface orientation (α). The following analysis deals only with plane surfaces.

The longwave radiation absorbed by any plane surface depends on the amount of incident longwave radiation and on the longwave absorptivity of the surface. The absorptivity at a given wavelength is equal to the emissivity at that wavelength. As the radiative exchange at externally exposed surfaces involves both longwave and shortwave radiation, a distinction has to be made between the longwave radiation surface absorptivity properties and the shortwave radiation surface absorptivity/reflectivity properties of the irradiated surface materials. Typical building materials have longwave emissivity values of about 0.85–0.95. The important exceptions are unpainted/unvarnished bright metal surfaces. Table 15 below provides some examples of absorptivity/reflectivity properties of selected building materials. These data are drawn from CIBSE Guide A: *Environmental design*[32].

Table 15 Longwave emissivity and shortwave absorptivity of typical building materials at about 30° C[32]

Material	Condition	Shortwave absorptivity	Longwave emissivity
Aluminium	Dull/rough polish	0.40–0.65	0.18–0.30
Asphalt	Newly laid	0.91–0.93	0.90–0.98
	Weathered	0.82–0.89	0.90–0.98
Bitumen/felt roofing		0.86–0.89	0.91
Brick:			
— glazed/light		0.25–0.36	0.85–0.95
— light		0.36–0.62	0.85–0.95
— dark		0.63–0.89	0.85–0.95
Clay tiles (red, brown)		0.60–0.69	0.85–0.95
Concrete		0.65–0.80	0.85–0.95
— block		0.56–0.69	0.94
Copper	Highly polished	0.18–0.50	0.02–0.05
	Varnished		0.80–0.98
Glass (hemispherical values)		*	0.84
Iron (galvanised)	New	0.64–0.66	0.22–0.28
	Old, very dirty	0.89–0.92	0.89
Lead	Old, oxidised	0.77–0.79	0.28–0.281
Paint (aluminium)	Bright	0.30–0.55	0.27–0.67
Stone:			
— limestone		0.33–0.53	0.90–0.93
— sandstone		0.54–0.76	0.90–0.93
Slate		0.79–0.93	0.85–0.98
Stainless steel	Oxidised	0.20	0.79–0.82

* Refer to manufacturers' data

Note: coating a bright metallic surface with clear varnish raises the longwave emissivity of the surface to that of the varnish; anodising exerts a similar effect on the emissivity of bright aluminium

Since the longwave absorptivity is equal to the longwave emissivity, ε_l, it follows that the overall absorbed flux is the sum of the absorbed atmospheric based component, $\varepsilon_l L_{sky}(\beta)$, and the absorbed ground based component, $\varepsilon_l L_g(\beta)$.

The outgoing longwave radiation flux emitted by any plane surface, F, may be calculated from the Stefan-Boltzmann law:

$$F = \varepsilon_l \sigma T_{eo}^4 \quad (53)$$

where F is the longwave radiation flux emitted by a plane surface ($W \cdot m^{-2}$), ε_l is the longwave surface emissivity, σ is the Sefan-Boltzmann constant (5.6697×10^{-8}) ($W \cdot m^{-2} \cdot K^{-4}$) and T_{eo} is the (absolute) surface temperature (K).

Note that the outgoing longwave flux does not depend on the orientation of the emitting surface. The consequent longwave radiation energy exchange on a sloping plane may then be expressed as a net balance:

$$L^*(\beta) = \varepsilon_l (L_{sky}(\beta) + L_g(\beta) - \sigma T_{eo}^4) \quad (54)$$

where $L^*(\beta)$ is the longwave radiation energy exchange ($W \cdot m^{-2}$), $L_{sky}(\beta)$ is the atmospheric longwave radiation received directly from the sky ($W \cdot m^{-2}$), $L_g(\beta)$ is the longwave radiation received from the ground ($W \cdot m^{-2}$) and β is the inclination of the surface (°).

For the special case of an unobstructed horizontal surface, equation 53 simplifies to:

$$L^* = \varepsilon_l (L_{sky} - \sigma T_{eo}^4) \quad (55)$$

Various formulae have been proposed to estimate the longwave radiation emitted downwards by the atmosphere and upwards from level ground. The procedure adopted here is closely based on the work of Page et al.[33] which formed the basis of the *European Solar Radiation Atlas*[1] work on longwave radiation.

The daytime sky longwave irradiance from the atmosphere falling on a horizontal surface may be estimated as:

$$L_{sky} = \sigma T_a^4 [0.904 - (0.304 - 0.061\, p_w^{1/2})\, S_h - 0.005\, p_w^{1/2}] \quad (56)$$

where L_{sky} the daytime sky longwave irradiance on a horizontal surface ($W \cdot m^{-2}$), σ is the Stefan-Boltzmann constant (5.6697×10^{-8}) ($W \cdot m^{-2} \cdot K^{-4}$), T_a is the (absolute) ambient air temperature (K), p_w is the water vapour pressure (hPa) and S_h is the hourly sunshine fraction.

Values of p_w can be estimated from dry and wet bulb temperatures using the tables of data given in section C1 of CIBSE Guide C: *Reference data*[34].

During the nocturnal period, S_h is replaced with the term $[1 - (N_h / 8)]$ where N_h is the hourly cloud cover in oktas. As the values of S_h are not very reliable during the first and last hour of daylight, it is best to treat these two hours as lying in the nocturnal period.

Table 16 provides values of the incoming longwave radiation L_{sky} on horizontal surfaces for cloudless and overcast conditions as a function of vapour pressure. Values for intermediate conditions of cloud cover may be estimated from Table 16 by linear interpolation using either the hourly cloud fraction (okta / 8) or the sunshine fraction, or, for improved accuracy, directly calculated using equation 56. Longwave radiation emitted by a blackbody at different air temperatures (σT_a^4) is also provided in Table 16 below. The figures printed in italic type lie above the saturated vapour pressure and are provided for interpolation procedures only.

The daytime ground longwave upward flux is given by:

$$L_g = \sigma \{0.980\, T_a + 0.037\, (1 - \rho_g)\, G_h\}^4 \quad (57)$$

where L_g is the longwave upward flux falling on a horizontal surface ($W \cdot m^{-2}$), T_a is the (absolute) screen air temperature (K), ρ_g is the shortwave ground albedo and G_h is the hourly global irradiation ($W \cdot h \cdot m^{-2}$).

Equation 57 is based on observations at Brussels and makes allowance for the heating effect of the sun on the surface temperature of the ground.

Values for albedo (i.e. ground reflectance for entire solar radiation spectrum) are given in Table 7.

The introduction of the global irradiation in equation 57 allows the warming effect of the rays of the sun on the ground surface temperature to be taken into account in striking the longwave radiative balance. During the night the term associated with G_h becomes zero.

Table 16 Longwave radiation flux from the sky on horizontal surfaces for cloudless and overcast sky conditions

Ambient temperature T_a (K)	Black body radiation ($\sigma\ T_a^4$)	Longwave radiation flux received by horizontal surface from sky, L_{sky} ($W \cdot m^{-2}$), for cloudless and overcast conditions for stated vapour pressure, p_w (hPa)											
		0		5		10		15		20		25	
		C'less	O'cast	C'less	O'cast	C'less	O'cast	C'less	O'cast	C'less	O'cast	C'less	O'cast
313	544	326	492	395	486	423	483	444	481	463	480	479	478
308	510	306	461	370	456	396	453	417	451	434	450	449	449
303	478	287	432	347	427	371	424	390	423	406	421	421	420
298	447	268	404	324	399	347	397	365	396	380	394	393	393
293	418	251	378	303	373	325	371	341	370	355	368	*368*	*367*
288	390	234	353	283	348	303	346	319	345	*332*	*344*		
283	364	218	329	264	325	283	323	*297*	*322*				
278	339	203	306	246	302	*263*	*301*						
273.15	315	189	285	228	281								
268	292	175	264	*212*	*261*								
263	271	163	245										
258	251	151	227										
253	232	139	210										

Example 5

Estimate the longwave radiation balance for a black, non-metallic flat roof having a longwave emittance of 0.9 for a cloudless and an overcast night-time hour with both the screen air temperature and the roof surface temperature at 0 °C (i.e. 273.15 K). The vapour pressure is 2.5 hPa. The longwave emittance of the roof is 0.9.

Using equation 56, for $p_w = 2.5$ hPa:

— incoming radiation for cloudless conditions, $L_{sky} = 217\ W \cdot m^{-2}$

— incoming radiation for overcast conditions, $L_{sky} = 283\ W \cdot m^{-2}$

From Table 15, outgoing radiation for a black body, $(\sigma T^4) = 315\ W \cdot m^{-2}$

Hence, from equation 55, the net loss for a horizontal black body is:

— cloudless sky conditions: $L^*(\beta) = 0.9\ (217 - 315) = 88\ \text{W·m}^{-2}$

— overcast sky conditions: $L^*(\beta) = 0.9\ (283 - 315) = 29\ \text{W·m}^{-2}$

The actual surface temperature depends on the energy balance of the surface. The example illustrates the large longwave radiation losses from horizontal surfaces on clear nights. The impact of these large, continuous losses increases with longer nights and shorter days, which yield less compensating short wave radiation. Low vapour pressure also leads to greater losses.

The night-time longwave radiation emitted from the ground is given by equation 57 as:

$$L_g = \sigma \{(0.98 \times 273.15) + 0\}\ T^4 = 291\ \text{W·m}^{-2}$$

4.3 Longwave radiation exchange for inclined flat planes

The treatment of the longwave radiation from the sky on inclined planes is based on Cole[35]. For a sloping surface of inclination β, $L_{sky}(\beta)$ is estimated from L_{sky} and the cloud cover, N, as follows:

$$L_{sky}(\beta) = L_{sky}\, r_{sky} + 0.09\, k_3\ \{1 - (N / 8)\ [0.7067 + 0.00822\ (T_a - 273.15)]\}\ \sigma T_a^4 \quad (58)$$

where $L_{sky}(\beta)$ is the atmospheric longwave radiation received directly from the sky by inclined surface (W·m^{-2}), β is the inclination of the surface (°), L_{sky} is the daytime sky longwave irradiance on a horizontal surface (W·m^{-2}), r_{sky} is the sky view factor for the inclined plane ($r_{sky} = \cos^2(\beta / 2)$), k_3 is a function of the inclination β, N is the cloud cover (okta), T_a is the (absolute) screen air temperature (K) and σ is the Stefan-Boltzmann constant (5.6697×10^{-8}) $\text{W·m}^{-2}\text{·K}^{-4}$.

Function k_3 obtained from:

$$k_3 = 0.7629\ (0.01\ \beta)^4 - 2.2215\ (0.01\ \beta)^3 + 1.7483\ (0.01\ \beta)^2 + 0.054\ (0.01\ \beta) \quad (59)$$

For vertical surfaces $k_3 = 0.3457$.

If only hourly sunshine data are available, then cloud cover can be estimated using the method given in section 2.9.3.

The ground reflected component is found by applying the ground view factor r_g to L_g, as follows:

$$L_g(\beta) = L_g\, r_g \quad (60)$$

where $L_g(\beta)$ is the ground reflected longwave radiation received by an inclined surface (W·m^{-2}), β is the inclination of the surface (°), L_g is the longwave upward flux falling on a horizontal surface (W·m^{-2}) and r_g is ground view factor for the inclined plane ($r_g = \sin^2(\beta / 2)$).

The total radiative exchange (i.e. shortwave plus longwave) is given by:

$$R^*(\beta,\alpha) = \alpha_{rad}\, G(\beta,\alpha) + \varepsilon_l\ [L_{sky}(\beta) + L_g(\beta) - \sigma T_{eo}^4] \quad (61)$$

where $R^*(\beta,\alpha)$ is the total radiative exchange for an inclined surface (W·m^{-2}), β is the inclination of the surface (°), α is the orientation of the surface (°), α_{rad} is the shortwave surface absorptance, $G_h(\beta,\alpha)$ is the hourly global solar irradiation (W·h·m^{-2}) for a plane of slope β (degree) and orientation α (degree) and T_{eo} is the (absolute) external surface temperature (K),

Example 6

Assuming the same input data as for Example 5, estimate the corresponding night-time longwave radiation balance for vertical surfaces at 0 °C.

From Example 5:

— incoming longwave radiation on horizontal surface for cloudless conditions: $L_{sky} = 217$ W·m^{-2}

— incoming longwave radiation on horizontal surface for overcast conditions, $L_{sky} = 283$ W·m^{2}

— outgoing (vertical) radiation from the ground: $L_g = 291$ W·m^{-2}.

From equation 60, the ground reflected component on a vertical surface is given by:

$$L_g(90) = 291 \sin^2 (90/2) = 290 \times 0.5 = 145 \text{ W·m}^{-2}$$

For a vertical surface, $k_3 = 0.3457$ and for a cloudless sky, $N_h = 0$. Therefore, from equation 58, the sky component of the longwave radiation is given by:

$$L_{sky}(90) = 217 \cos^2 (90/2) + (0.09 \times 0.3457) (1 - 0)\ \sigma\ T_a^4$$

From Table 16, for a screen air temperature of 0 °C (i.e. 273.15 K): $(\sigma T_a^4) = 315$ W·m^{-2}.

Hence:

$$L_{sky}(90) = (217 \times 0.5) + (0.09 \times 0.3457 \times 315) = 118 \text{ W·m}^{-2}$$

The total incoming longwave radiation (cloudless sky) is:

$$L_g(90) + L_{sky}(90) = 145 + 118 = 263 \text{ W·m}^{-2}$$

For overcast conditions, the ground component, $L_g(90)$, is unaltered at 145 W·m^{-2} but, for $N_h = 8$, equation 58 now gives the sky component as:

$$L_{sky}(90) = 283 \cos^2 (90/2) + (0.09 \times 0.3457)\ \{1 - (N / 8)\ [0.7067 + 0.00822\ (T_a - 273.15)]\}\ \sigma T_a^4$$

Hence:

$$L_{sky}(90) = (283 \times 0.5) + (0.09 \times 0.3457)\ \{1 - [0.7067 + 0.00822\ (273.15 - 273.15)]\}\ \sigma T_a^4$$

Again, from Table 16, $(\sigma T_a^4) = 315$ W·m^{-2}.

Therefore:

$$L_{sky}(90) = 141.5 + 2.9 = 144 \text{ W·m}^{-2}$$

The total incoming longwave radiation (overcast sky) is:

$$L_g(90) + L_{sky}(90) = 145 + 144 = 289 \text{ W·m}^{-2}$$

Therefore from equation 54, for an emissivity of 0.9, the net longwave radiation balance for the vertical surface with a surface temperature of 273.15 K is as follows:

— for cloudless conditions: $L^*(90) = 0.9\ (259 - 315) = 50.4$ W·m^{-2} (loss) (cf. 88 W·m^{-2} for horizontal surface, see Example 5)

— for overcast conditions: $L^*(90) = 0.9\ (289 - 315) = 14.4\ W \cdot m^{-2}$ (loss) (cf. 29 $W \cdot m^{-2}$ for horizontal surface, see Example 5)

4.4 Other sources of longwave radiation data

The CD-ROM that accompanies the 4th edition of the *European Solar Radiation Atlas*[1] provides computational procedures for estimating longwave radiation from the sky alone falling on horizontal and inclined surfaces, using the above algorithms. However, these procedures can only be used where the supporting daily sunshine data input needed are available on the CD-ROM. For night-time hours monthly mean night time cloudiness values are estimated from the daily mean sunshine duration, interpolating overnight between the daily sunshine on the preceding day and that on the following day. There are no cloud data on the ESRA CD-ROM. The Inter-governmental Panel on Climate Change (IPCC), established by the World Meteorological Organisation under the United Nations environment programme, has a web site at the Climate Research Unit at the University of East Anglia[*]. This makes accessible the 1961–90 global reference climatology, which includes mean cloud cover data. Monthly mean cloud and sunshine data for the period 1961–90 for 4000 sites worldwide may be found on the WMO 1961–90 Global Climate Normals CD-ROM, produced by the (US) National Climate Data Center[†] on behalf of the World Meteorological Organisation[36]. (WMO 1995)

5 Illuminance and daylight availability

5.1 Introduction

Quantitative daylight illuminance data are needed for daylighting design calculations including the sizing of windows, choice of glazing materials and the design of window shading systems. Daylighting and electric lighting systems must be designed to operate interactively. The quantitative estimation of the energy consumption of electric lighting with different control systems needs knowledge of the statistical availability of the horizontal components of daylight, the global horizontal illuminance and the diffuse horizontal illuminance of the sky vault. A means of assessing the effect of orientation on vertical surface daylight availability is also required. The main climatological requirement for daylight and artificial lighting design is good information about the availability of diffuse illumination.

Cumulative frequency curves of horizontal illuminance are used to assess lighting system design. Separate curves are needed for the frequencies at which different horizontal global illuminance levels (E_{vg}) are exceeded and the frequencies at which different levels of diffuse horizontal illuminance levels (E_{vd}) are exceeded. Statistically-based horizontal beam illuminance data (E_{vb}) are not normally used.

5.2 Preparing cumulative frequency illuminance data

The length of the working day must first be defined. The cumulative illuminance data can be derived on a month-by-month or on an annual basis. Hunt[41] defined the standard UK working day for illumination design purposes as 09:00–17:30 LAT in winter and 08:00–16:30 LAT for the period between April and October to allow for British Summer Time. For practical reasons, the difference between LAT and GMT was considered to be small enough to be neglected for the sites processed. However, when the observed input illumination or irradiation data files are only available for integral hours, it is best to set the working daylength to match the observational periods, presented here for the UK in integral hours defined on an hour-ending basis.

Ideally, illuminance cumulative frequency curves should be prepared from long-term records of illuminance measured at very short time intervals of, say, one minute. Only a few data sets of this sort exist, observed for only for relatively short climatic periods. The cumulative frequency curves in common engineering use are

[*] Climate Research Unit, University of East Anglia, Norwich NR4 7TJ (http://www.ipcc-data.org/)
[†] National Climate Data Center, Ashville, NC 28801, USA (http://www.ncdc.noaa.gov/)

usually based either on hour-by-hour observations of illumination or indirectly derived from hour-by-hour observations of irradiation. These irradiation data are converted into illuminance data by applying the appropriate luminous efficacy values. In both cases, the assumption, implicit in the conversion to cumulative illuminance, is that the mid-hour illuminance in kilolux is equal to the hourly illumination in kilolux hours divided by one hour.

The hour-by-hour conversion process from illumination to illuminance also presents difficulties in the sunrise and sunset hours, see section 2. During these hours, the sun will only be above the horizon for part of the hour, making the accurate estimation of the illuminance from the hourly illumination very difficult. This complication is frequently overlooked. Another important factor is that, in the winter months, the sun will be below the horizon for part of the working day. This influences the maximum possible cumulative frequency of daylight provision in the winter months. The impact of this becomes greater with increasing latitude until, at the Arctic Circle, there is no daylight at all in midwinter.

The values of maximum possible proportion of time that some daylight illumination may expected during a defined working daylength in any month at a given latitudes in the UK have been calculated assuming that there is zero daylight once the calculated solar elevation angle (using equation 6) was less than –4 degrees. This calculation procedure increases the illumination daylength to make allowance for the impact of twilight. The results of these calculations are given in Table 17.

These effective daylength calculations were carried out on a day-by-day basis for each month in 1998. The ‘dark time’ for each working day was then summed to provide a value of the monthly proportional dark time loss for that site. The results obtained agree with the plotted monthly intercepts of the cumulative illuminance curves with the Y-axis (i.e. for X = 0) for the winter, found by Hunt[41].

Table 17 Proportion of working day in each month during which some daylight is potentially available at different UK sites for a working day from 09:00 to 17:30 LAT in winter and 08:00 to 16:30 LAT in summer

Month	Proportion of working day for which daylight is available at stated site (latitude in parentheses)										
	Jersey (49.22 °N)	Bracknell (51.38 °N)	Kew (51.47 °N)	London (51.52 °N)	Aberporth (52.13 °N)	Aughton (53.55 °N)	Eskdalemuir (55.32 °N)	Mylnefield (56.45 °N)	Aberdeen (57.20 °N)	Stornoway (58.22 °N)	Lerwick (60.13 °N)
Jan	0.911	0.896	0.895	0.895	0.891	0.880	0.866	0.856	0.845	0.845	0.818
Feb	0.983	0.977	0.976	0.976	0.975	0.970	0.964	0.960	0.957	0.957	0.943
Mar	1.000	1.000	1.000	1.000	1.000	1.000	1.000	1.000	1.000	1.000	1.000
Apr	1.000	1.000	1.000	1.000	1.000	1.000	1.000	1.000	1.000	1.000	1.000
May	1.000	1.000	1.000	1.000	1.000	1.000	1.000	1.000	1.000	1.000	1.000
Jun	1.000	1.000	1.000	1.000	1.000	1.000	1.000	1.000	1.000	1.000	1.000
Jul	1.000	1.000	1.000	1.000	1.000	1.000	1.000	1.000	1.000	1.000	1.000
Aug	1.000	1.000	1.000	1.000	1.000	1.000	1.000	1.000	1.000	1.000	1.000
Sep	1.000	1.000	1.000	1.000	1.000	1.000	1.000	1.000	1.000	1.000	1.000
Oct	0.997	0.995	0.995	0.995	0.994	0.993	0.990	0.988	0.987	0.987	0.981
Nov	0.934	0.922	0.932	0.922	0.918	0.909	0.897	0.889	0.883	0.883	0.858
Dec	0.886	0.869	0.888	0.888	0 863	0.850	0.834	0.822	0.814	0.814	0.777
Year:	0.976	0.971	0.971	0.971	0.970	0.967	0.962	0.959	0.957	0.954	0.948

Note: the maximum daylength in each day was based on the time between that when the astronomical solar altitude reached –4 degrees and the time when the astronomical solar altitude fell below –4 degrees; this was done to allow for the effects of twilight, see section 5.2 for details

Table 18 Proportion of working day in each month during which the solar altitude at different UK sites is above 5 degrees during a working day from 09:00 to 17:30 LAT in winter and 08:00 to 16:30 LAT in summer; for use with datasets truncated at 5 degrees elevation

Month	Proportion of working day for which daylight is available at stated site (latitude in parentheses)										
	Jersey (49.22 °N)	Bracknell (51.38 °N)	Kew (51.47 °N)	London (51.52 °N)	Aberporth (52.13 °N)	Aughton (53.55 °N)	Eskdalemuir (55.32 °N)	Mylnefield (56.45 °N)	Aberdeen (57.20 °N)	Stornoway (58.22 °N)	Lerwick (60.13 °N)
Jan	0.780	0.757	0.756	0.755	0.748	0.726	0.688	0.656	0.631	0.592	0.498
Feb	0.874	0.860	0.860	0.859	0.855	0.845	0.831	0.821	0.814	0.803	0.782
Mar	0.976	0.972	0.972	0.972	0.971	0.968	0.964	0.961	0.959	0.956	0.950
Apr	1.000	1.000	1.000	1.000	1.000	1.000	1.000	1.000	1.000	1.000	1.000
May	1.000	1.000	1.000	1.000	1.000	1.000	1.000	1.000	1.000	1.000	1.000
Jun	1.000	1.000	1.000	1.000	1.000	1.000	1.000	1.000	1.000	1.000	1.000
Jul	1.000	1.000	1.000	1.000	1.000	1.000	1.000	1.000	1.000	1.000	1.000
Aug	1.000	1.000	1.000	1.000	1.000	1.000	1.000	1.000	1.000	1.000	1.000
Sep	1.000	1.000	1.000	1.000	1.000	1.000	1.000	1.000	1.000	1.000	1.000
Oct	0.914	0.904	0.904	0.903	0.900	0.892	0.883	0.876	0.871	0.863	0.848
Nov	0.808	0.788	0.788	0.787	0.780	0.765	0.741	0.719	0.703	0.676	0.613
Dec	0.748	0.721	0.720	0.719	0.709	0.670	0.607	0.560	0 525	0.471	0.336
Year	0.925	0.917	0.916	0.916	0.914	0.906	0.893	0.883	0.875	0.863	0.835

Note: this table is intended for use with data sets truncated below 5 degrees solar elevation (due to the limits set on equations 68 and 69) in order to provide the intercepts at the left axis; the proportion of the working day meeting this condition is much less than is the case in Table 17

5.3 Processing UK data to determine cumulative illuminance distributions

The only long-term illumination observations available for the UK are those undertaken by the Met Office. Hunt[41] (1979) has reported systematically on these observations, which were made for various UK sites. The observational data periods available varied between sites. The longest time series was for Kew, running between 1964 and 1973. Diffuse illumination data were obtained for only two sites, Kew and Bracknell.

More recently, daylight measurements have been made at five locations in the UK as part of the Commission Internationale de l'Eclairage Daylight Measurement Programme. The reported observational integration periods range from five minutes to half-hourly time series. The data collected from Garston (North London), Sheffield, Manchester, Edinburgh (urban) and Edinburgh (suburban) have been compiled onto a CD-ROM. The CD-ROM, along with a companion report[42], are available to the research community from Napier University.

These recent data series are short-term data series and so provide a weak basis on which to found long-term statistical studies of UK daylight availability. However, Muneer and Kinghorn[43] have developed luminous efficacy models based on the above observed data. The global and diffuse luminous efficacy algorithms given below enable the estimation of a long-term time series of diffuse and global horizontal illuminance from the respective hour-by-hour horizontal irradiation time series data. Kinghorn and Muneer[44] found the following regression relationships for solar altitudes above 5 degrees:

$$K_G = 136.6 - 74.54\ KT_h + 57.34\ KT_h^2 \quad (68)$$

$$K_D = 130.2 - 39.82\ KT_h + 49.97\ KT_h^2 \quad (69)$$

where KT_h is the hourly clearness index.

K_G and K_D are defined as follows:

$$K_G = E_{vg} / G \quad (70)$$

$$K_D = E_{vd} / D \quad (71)$$

where E_{vg} is the global illuminance on the horizontal plane (klux), G is the global irradiance on the horizontal plane ($W \cdot m^{-2}$), E_{vd} is the diffuse illuminance on the horizontal plane (klux) and D is the diffuse irradiance on the horizontal plane ($W \cdot m^{-2}$).

The adoption of a 5-degree sunrise start implicit in rejecting observed data with the sun below 5 degrees implies a different starting point to the frequency distribution. Table 18 presents the proportion of the defined working day for which the sun is above 5 degrees. This definition of working day daylight availability yields lower values in winter than the values obtained using the start of twilight and end of twilight given in Table 17.

Below a solar altitude angles of 5 degrees, the *European Solar Radiation Atlas*[1] recommends a fixed luminous efficacy for diffuse irradiation of 120 $lm \cdot W^{-1}$. Section 5.9 provides algorithms for use when the solar altitude is below 5 degrees. These algorithms cover issues relating to twilight period.

A recent unpublished study by Page has shown that, under clear sky conditions, equations 68 and 69 do not perform in an entirely satisfactory way as a means of estimating beam illuminance normal to the beam when the solar angle is less than about 25 degrees. In this process, the beam illuminance on horizontal surfaces is found by taking the difference of the global and diffuse irrandiance observations using equations 68 and 69. When the sun is low, this means taking the difference of two small numbers.

The beam normal illuminance is then estimated from this difference, which, at low solar altitudes, is divided by another small number, the sine of the solar altitude, to estimate the beam illuminance normal to the beam. The limitations in the accuracy implied in the combination of the two models by difference severely limits the accuracy achievable in the estimation of beam normal illuminance at low solar angles. It is therefore best to restrict the application of the above algorithms to the estimation of horizontal surface beam illuminance data only. In the case of horizontal surface illumination, a low solar angle implies a small beam horizontal contribution, so the implicit shortcomings of the pair of algorithms used in combination make only a small impact on the accuracy of the generated horizontal global and diffuse illuminance data.

5.4 Annual cumulative illuminance frequency distributions in the UK

Cumulative frequency distributions of horizontal illuminance are required in order to assess lighting system design. New UK data have been recently derived using luminous efficacy algorithms for global and diffuse illumination estimation[43]. These algorithms have been based on short time-series of simultaneously observed values of irradiation and illuminance[44]. The algorithms have been applied to the recent observed UK hourly irradiation time-series data sets to estimate the corresponding hourly illuminance time-series. These derived illuminance time-series were then analysed statistically to produce cumulative frequency illuminance data.

Annual global cumulative frequency data[44] for a range of UK sites are given in Table 2.15 in CIBSE Guide A, chapter 2, and the corresponding diffuse cumulative frequency data are given in Table 2.16 in CIBSE Guide A, chapter 2. The tables are arranged in order of increasing latitude. In general, increase of latitude produces a lower proportion of the year during which a given global illuminance is exceeded. Because of the limitations imposed by the 5-degree solar altitude exclusion, the values below 1.0 kilolux are not reliable.

The maximum diffuse illuminances are about 60 klux, except in central London where the illuminance is affected by pollution. Figure 11 shows the range of both the annual global and diffuse data for Aberporth and Stornoway. The influence of latitude is greater on annual global cumulative illuminance than on annual diffuse cumulative illuminance. This is because the high levels of cloud in summer in the north increases the diffuse illuminance, which offsets the substantial reduction in diffuse illumination in winter. Values for other sites can be estimated from Tables 2.15 and 2.16 in CIBSE Guide A, chapter 2, using linear interpolation based on latitude. However, the effects of urban pollution mean that the data for central London data should not be used for latitude interpolation.

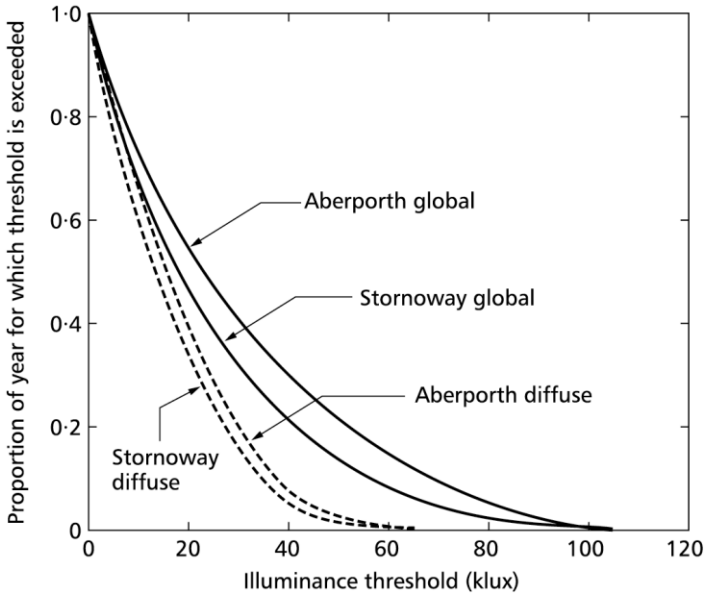

Figure 11 Proportion of year in which different global and diffuse illuminances are exceeded for Aberporth and Stornoway

5.5 Orientation factors

The effect of orientation on the availability of diffuse illuminance can be taken into account by means of an orientation factor, see Table 19.

The diffuse illuminance received on the horizontal plane in a room with CIE sky daylight factor DF (%) is given by:

$$E_v = E_{vd}(c)\ (DF / 100)\ f_o \qquad (72)$$

where E_v is the diffuse illuminance received on the horizontal plane (klux), $E_{vd}(c)$ is the diffuse horizontal irradiance (klux) available for proportion c (%) of the year, DF is the daylight factor (%) and f_o is the orientation factor.

$E_{vd}(c)$ is obtained from Table 2.17 in CIBSE Guide A, chapter 2.

The orientation factor applies only to the annual cumulative diffuse illuminance values.

Table 19 Orientation factor for availability of illuminance[45]

Orientation	Factor, f_o
North	0.97
East	1.15
South	1.55
West	1.21

5.6 Daylighting algorithms for solar altitude angles less than 5 degrees

The analytical difficulties presented by low solar altitudes have been mentioned several times in the foregoing. A practical illuminance treatment has been provided by Tregenza[47], based on illuminance observations made in Nottingham for 15 months between June 1994 and August 1995. The method develops a mean relationship between illuminance and solar altitude. Statistical variation factors are then applied to the mean value curves to estimate the associated range of values falling into different percentile groups around the mean. A feature of this method is the attention given to the period between twilight and the time the solar elevation reaches 5 degrees.

The times of the beginning and the end of twilight are defined as the times when the calculated altitude of the sun is -5^{o}. These are calculated starting with equation 6, inserting the solar altitude of -5^{o}, knowing the declination and the latitude, solving to estimate the corresponding hour angles and converting to a time in the normal way.

For $-5° \leq \gamma_s < 2.5°$:

$$E_{vg} = 0.0105\ (\gamma_s + 5)^{2.5} \tag{73}$$

and for $2.5° < \gamma_s \leq 60°$:

$$E_{vg} = 73.7\ \sin^{1.22} \gamma_s \tag{74}$$

where E_{vg} is the mean global illuminance on the horizontal plane (klux) and γ_s is the solar altitude angle (°).

For $-5° < \gamma_s \leq 5°$:

$$E_{vd} = 0.0105\ (\gamma_s + 5)^{2.5} \tag{75}$$

and for $2.5° < \gamma_s \leq 60°$:

$$E_{vd} = 48.8\ \sin^{1.105} \gamma_s \tag{76}$$

where E_{vd} is the mean diffuse illuminance on the horizontal plane (klux) and γ_s is the solar altitude angle (°)

Figure 15 gives the frequency of occurrence of a given horizontal illuminance as a ratio to the mean illuminance found by Tregenza[47]. By calculating the ratios for all solar altitudes, an average frequency distribution of illuminance may be calculated with the aid of the histogram shown as Figure 15. This may be done for the twilight period as well as for the period when the sun is above the horizon. It should be recognised this approach is based on the climatology appropriate to Nottingham. It has been tested for Belgium (Uccle) and London (Kew), and appears to be representative of north European maritime climates. Currently there are no reports on the applicability of the model outside northern Europe.

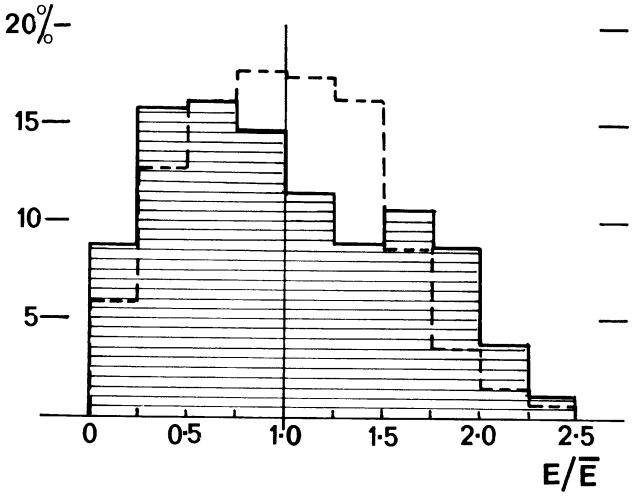

Figure 15 Percentage frequency of occurrence of a given horizontal global and diffuse illuminance on the horizontal plane expressed as a ratio to the mean illuminance at any given solar altitude[47].

5.7 Daylight design information for Europe on the internet

An EU-funded programme called 'SATELLIGHT' has led to the establishment of an advanced internet-based service, geared toward solar energy related applications, with a specific orientation toward the support of daylighting design in western and central Europe[48]. Two years of half-hourly daylight and solar radiation data have been processed on a pixel-by-pixel basis from the Meteosat satellite data. These processed pixellated data have then been placed on an internet server based at the Laboratoire des Sciences de l'Habitat in the Département Génie Civil et Bâtiment* at Vaulx-en-Velin in the suburbs of Lyon (France), as an accessible database. A sophisticated interface has been developed to make it simple for users to access the data and use it for various design purposes.

Facilities include the provision of daylight and solar radiation maps over Europe, as well as climate data for exact locations. Users can thus access a coherent database of daylight and solar radiation information covering Western and Central Europe in a digital form. Users can also request the provision of cumulative illuminance statistical data of the various types set down earlier in this Section 5.6, defining their own time periods. Advanced daylight design methodologies are incorporated and are directly available to users, so users can make specific requests concerning indoor daylight availability, initially supported by test designs at any site in the mapped area. They can then input their own designs for daylighting assessment. The system operates in a very user-friendly way, permitting user defined parameters and user defined statistics. When a design request has been processed, a link to the requested information is fed back to the user via e-mail. The service is currently free and supported by the EU. The site may be accessed at http://www.satel-light.com/

References

1 Scharmer K and Grief J (co-ordinators) *European Solar Radiation Atlas Vol. 2: Database and exploitation software* 4th edn. (Paris: Les Presses de l'Ecole des Mines de Paris) (2000)

2 Littlefair P Correcting for shade ring used in diffuse daylight and radiation measurements *Proc. Symp. on Daylight and Solar Radiation Measurement* (Berlin: Technical University of Berlin) (1989)

* Laboratoire Sciences de l'Habitat (LASH), Départment Génie Civil et Bâtiment, Rue Maurice Audin, 69518 Vaulx-en-Velin, France. Telephone: 0033 4 72 04 70 87; fax: 0033 4 72 04 70 41; e-mail: dominique.dumortier@entpe.fr

3 Bourges B Improvement in solar declination calculations *Solar Energy* **35** 367–369 (1985) (2000)

4 Yallop B D *Algorithm for solar declination angle* (Cambridge: Royal Greenwich Observatory) (1992)

5 Page J K The derivation of hourly KT_h values from observed and computed hourly solar radiation data *Solar Energy* (submitted for publication) (2001)

6 *Measurement of the duration of sunshine* Section 4.7 in *Meteorological aspects of the utilization of solar radiation as an energy source* WMO Report 557 (Geneva: World Meteorological Organisation) (1981)

7 Palz W and Grief J (co-ordinators) *European Solar Radiation Atlas: Solar Radiation on Horizontal and Inclined Surfaces* 3rd edn. (Berlin: Springer for the Commission for the European Communities) (1996) ISBN 3 540611 79 7

8 *Early agrometeorological crop yield assessment* FAO Plant Production and Protection Paper No. 73 (Rome: United Nations Food and Agricultural Organisation) (1986) ISBN 9 251024 19 7

9 Kasten F and Czeplak G Solar radiation and terrestrial radiation dependent on the amount and type of cloud *Solar Energy* **24** 117–189 (1980)

10 Gul M S, Muneer T and Kambezidis H D Models for obtaining solar radiation from other meteorological data *Solar Energy* **64** 99–108 (1998)

11 Cowley J P The distribution over Great Britain of global solar irradiation on horizontal surfaces *Meteorological Magazine* **107** 357–373 (1978)

12 Page J K *Proposed quality control procedures for Meteorological Office data tapes relating to global solar radiation, diffuse solar radiation, sunshine and cloud in the UK* (private communication) (1997)

13 Muneer T Solar radiation model for Europe *Building Serv. Eng. Res. Technol.* **11** (4) 153–163 (1990)

14 Perez R, Ineichen P and Seals R A new simplified version of the Perez diffuse irradiance model for tilted surfaces *Solar Energy* **39** 221–231 (1987)

15 Muneer T *Solar radiation and daylight models* (Oxford: Butterworth Heinmann) (1997)

16 Temps R C and Coulsen K L Solar radiation incident on slopes of different orientations *Solar Energy* **19** 179–184 (1977)

17 Klucher T M Evaluation of models to predict insolation on tilted surfaces *Solar Energy* **23** (1) 111–114 (1979)

18 Saluja G S and Muneer T Estimation of ground-reflected radiation for the United Kingdom *Building Serv. Eng. Res. Technol.* **9** (4) 189–196 (1988)

19 Page J K *The development of monthly near extreme day slope irradiance tables for three UK sites in standard formats, using observed hourly horizontal irradiation data for all days having a 95 precentile exceedence value of daily global irradiation within each month* (private communication) (2000)

20 Rigollier C, Bauer O and Wald L On the clear sky model of the European Solar Radiation Atlas with respect to the Heliostat method *Solar Energy* **68** (1) 33–48 (2000)

21 Kasten F The Linke turbidity factor based on improved values of the integral optical thickness *Solar Energy* **37** 393–396 (1996)

22 Page J K International guidance on the estimation of Linke turbidity factors to use in conjunction with the CIBSE Guide clear sky solar irradiance tables *Building Serv. Eng. Res. Technol.* (submitted for publication) (2001)

23 Steinhauser F Die mittlere trubüng der luft an verschieddenen orten *Gerlands Beiträge zur Geophysik* **42** 110–121 (1934)

24 Schulz R W *Strahklima der Erde* (Darmstadt: Steinkopff) (1970)

25 Perrin de Brichambaut C and Vauge C *Le gisement solaire: evaluation de la ressource energetique* (Paris: TEC/Lavoisier) (1982)

26 *World maps of relative global radiation* annex to *Meteorological aspects of the utilization of solar radiation as an energy source* WMO Technical Note 172 (Geneva: World Meteorological Organisation) (1981)

27 Raschke E, Stuhlmann R, Palz W and Steemers T C *Solar radiation atlas of Africa* (Rotterdam: Balkema/Commission of the European Communities) (1991)

28 Aydinli S and Krochmann J *Prediction of solar radiation on slopes — overcast days with special reference to the EEC region* in Page J K (ed.) *Prediction of solar radiation on inclined surfaces* Solar Energy R&D in the European Community, Series F, vol. 3: *Solar Radiation Data* 213–264 (Dordrecht: Reidel) (1986)

29 Liu B Y H and Jordan R C The interrelationship and characteristic distribution of direct, diffuse and total solar radiation *Solar Energy* **4** 1–19 (1960)

30 Loudon A G *The interpretation of solar radiation measurements for building projects* BRE Current Paper R73 (Garston: Building Research Establishment) (1967)

31 *Weather and solar data* Section 2 in CIBSE Guide A: *Design data* (London: Chartered Institution of Building Services Engineers) (1982)

32 *Environmental design* CIBSE Guide A (London: Chartered Institution of Building Services Engineers) (1999)

33 Page J K, Czeplak G and Dogniaux R *Estimation of longwave radiation exchanges between buildings and the sky and ground* European Solar Radiation Atlas Project Contract JOU2-CT93-305 Internal Task II Report (1998) (available from Prof. J K Page, 15 Brincliffe Gardens, Sheffield, S11 9BG, England)

34 *Properties of humid air* CIBSE Guide C1 (London: Chartered Institution of Building Services Engineers) (1975)

35 Cole R J The longwave radiation incident upon inclined surfaces *Solar Energy* **22** (5) 459–462 (1979)

36 World Meteorological Organisation *1961-1990 Global Climate Normals — version 1.0 Nov 1998* (Ashville, NC: National Climate Data Center) (1998)

37 BS EN ISO 6946: 1997: *Building components and building elements. Thermal resistance and thermal transmittance. Calculation method* (London: British Standards Institution) (1997)

38 Dogniaux R and Lemoine M *Valeurs horaires moyenne mensuelles du bilan radiatif et de ses composantes a Uccle — Periode de reference 1972–1982* IRMB Publications Series A 113 (Uccle, Belgium: IRMB) (1984)

39 Gajzago L *Outdoor microclimates and human comfort* Paper 16 in *Proc. Conf. Teaching the teachers on Building Climatology* (Stockholm: Statens Institut for Byggnadsforsking) (1972)

40 Page J K and Lebens R *Climate in the United Kingdom, a handbook of solar radiation, temperature and other data for thirteen principal cities and towns* (London: The Stationery Office) (1986)

41 Hunt D R G The use of artificial lighting in relation to daylighting levels and occupancy *Building and Environment* **14** (1) 21–33 (1979)

42 Muneer T and Kinghorn D Solar irradiance and daylight illuminance for the United Kingdom and Japan *Renewable Energy* **15** 318–324 (1998)

43 Muneer T and Kinghorn D Luminous efficacy of solar irradiance: improved models *Lighting Res. Technol*. **29** (4) 185–191 (1997)

44 Kinghorn D and Muneer T Daylight illuminance frequency distribution: Review of computational techniques and new data for UK locations *Lighting Res. Technol*. **30** (4) 139–150 (1998)

45 Littlefair P J Predicting annual lighting use in daylit buildings *Building and Environment* **25** (1) 43–54 (1990)

46 Hunt D R G *The availability of daylight* (Garston: Building Research Establishment) (1979)

47 Tregenza P R Measured and calculated frequency distributions of daylight illuminance *Lighting Res. Technol.* **18** (2) 71–74 (1986)

48 Fontoynont M, Dumortier D, Heinemann D, Hammer A, Olseth J, Skartveit A, Ineichen P, Reise C, Page J, Roche L, Beyer H G, and Wald L Satellight: a WWW server which provides high quality daylight and solar radiation data for Western and Central Europe *Proc. 9th. Conf. on Satellite Meteorology and Oceanography, Darmstadt, Germany* vol. EUM P22 434–435 (1998)

Appendix A1: Quality control of global solar irradiation data

During processing of The Met Office synoptic and irradiation data, it was found that significant amounts of hourly data were missing due to the downtimes associated with the measuring stations. This is normal for radiation measuring sites world-wide. In order to produce continuous data sets without gaps, for simulation purposes, the missing data had to be filled using both established procedures and additional methods expressly developed for the present project.

The hour-by-hour solar geometry had to be generated first. The Yallop[(A1.1)] algorithm was used for this purpose. Some observed global data exceeded quality control limits and had to be replaced using the selected 'missing data' procedures. The global radiation data were checked first against the expected values determined by modelling. Consistency between hourly sunshine data and cloud data was first established. The theoretical relationship between the hourly sunshine data and the hourly global irradiation was then used to check the internal consistency of the sunshine data and the irradiation data. Generating the expected global irradiation, using the observed hourly sunshine data, filled gaps in observed global irradiation. Special procedures had to be used at the start and end of the day, when the sun is not strong enough to burn the record card. In these hours, the sunshine used to fill the gaps has to be generated first from the cloud observations. The detailed quality control procedures developed will be published elsewhere[(A1.2)].

References (Appendix A1)

A1.1 Yallop B D *Algorithm for solar declination angle* (Cambridge: Royal Greenwich Observatory) (1992)

A1.2 Muneer T and Page J K Quality control of observed global and diffuse irradiation data and the filling gaps in UK hourly radiation time series records *Building Serv. Eng. Res. Technol.* (submitted for publication)

Appendix A2: Filling gaps in hourly diffuse irradiation records

The hourly diffuse irradiation, D_h, on a horizontal surface can be estimated from the records of the hourly observed global irradiation, G_h, using validated regression equations that relate the two quantities. Dimensionless analysis is usually employed. The two dimensionless quantities usually used are the ratio of hourly horizontal diffuse to hourly horizontal global irradiation (i.e. D_h / G_h) and the hourly clearness index or KT value (i.e. G_h / G_{oh}). Orgill and Hollands[A2.1] were the first to develop a dimensionless regression algorithm linking the two dimensionless quantities at the hourly level. Since then, similar regression relationships have been developed for different locations across the world. Muneer[A2.2], among others, has suggested an hour-by-hour regression algorithm applicable on a world-wide basis. In the absence of a site specific diffuse estimation algorithm for the selected location, equations A2.1 and A2.2 can be used to estimate the horizontal hourly diffuse irradiation from the observed hourly global horizontal irradiation.

If $KT_h > 0.2$ then:

$$D_h / G_h = 1.006 - 0.317\ KT_h + 3.1241\ KT_h^2 - 12.7616\ KT_h^3 + 9.7166\ KT_h^4 \quad \text{(A2.1)}$$

otherwise:

$$D_h / G_h = 0.98 \quad \text{(A2.2)}$$

where KT_h is the hourly clearness index, given by (G_h / G_{oh}).

In case of UK sites, for which observed hourly global horizontal irradiation data are available and hourly diffuse irradiation data are unavailable, the site-specific correlations between the hourly diffuse ratio (D_h / G_h) and hourly clearness index ($KT_h = G_h / G_{oh}$) established by Muneer and Saluja[A2.3] and Muneer[A2.4], may be used to estimate the hourly diffuse and beam irradiance. Equations A2.3 and A2.4 provide a year-round model, suitable for any given location within the UK, and is therefore suitable for hand-held calculators. Equations A2.7 and A2.8, which are a seasonally based model, enable diffuse irradiation estimations for the specific UK locations to be made with a higher degree of accuracy.

For $KT_h > 0.2$:

$$(D_h / G_h) = 0.687 + 2.932\ KT_h - 8.546\ KT_h^2 + 5.227\ KT_h^3 \quad \text{(A2.3)}$$

otherwise:

$$(D_h / G_h) = 0.98\ KT_h \quad \text{(A2.4)}$$

where D_h is the hourly diffuse irradiation on a horizontal surface ($W \cdot m^{-2}$), G_h the hourly global irradiation on a horizontal surface ($W \cdot m^{-2}$) and G_{oh} is the hourly extraterrestrial irradiation on a horizontal surface ($W \cdot m^{-2}$).

G_{oh} is given by:

$$G_{oh} = \varepsilon_j\ 1367 \sin \gamma_s \quad \text{(A2.5)}$$

where ε_j is the correction to mean solar distance and γ_s is the solar altitude (°).

Therefore:

$$KT_h = G_h / (\varepsilon_j\ 1367 \sin \gamma_s) \quad \text{(A2.6)}$$

KT_h is not a reliable dimensionless ratio when the solar altitude is below 5 degrees. Refraction in the atmosphere, ignored in the basic calculation, significantly increases the effective value of G_{oh}, which leads to over-estimation of the KT_h when the elevation of the sun is very low.

If equation A2.3/A2.4 is evaluated as a function of KT_h value, it can be shown that, for any given KT_h value above 0.2, the diffuse irradiation is a simple function of sin γ_s:

$$D_h = (-117.8 + 2450.5\ KT_h - 2598.8\ KT_h^2) \sin \gamma_s = A(0) \sin \gamma_s \quad \text{(A2.7)}$$

Values for $A(0)$ may be easily evaluated from equation A2.7, and these reveal a peak diffuse horizontal irradiance value when the KT_h value is about 0.47, regardless of solar altitude γ_s. The absolute values of $A(0)$ derived are given in Table A2.1. The absolute values for each KT_h value have also been expressed as a ratio to the clear day KT_h value. A reference KT_h value of 0.70 has been selected as the reference clear sky KT_h value. Note that $KT_h = 0.80$ represents exceptionally high global values often linked to fortuitous combinations of unobstructed sunshine and reflective cloudbanks. Note the small variation for KT_h values between 0.4 and 0.5.

Table A2.1 Values of $A(0)$ for equation A2.7

Parameter	Value for stated value of KT_h							
	0.20	0.30	0.40	0.45	0.50	0.60	0.70	0.80
$A(0)$ ($W \cdot m^{-2}$)	266.1	384.9	452.2	462.7	457.9	409.0	329.9	261.8
Ratio to value at $KT_h = 0.7$	0.807	1.167	1.371	1.402	1.388	1.240	1.000	0.794

The existence of a relationship between D_h and the sine of the solar altitude accords precisely with the observation made by Kasten and Czeplak[A2.5] when commenting on their diffuse observations at Hamburg. This relationship contrasts with linear relationship between the cloudy diffuse irradiation and solar altitude used in the 1986 edition of CIBSE Guide A[A2.6], where D_h (cloudy) was set to 5.05 γ_s.

The horizontal beam irradiation B_h at any KT_h value is given by:

$$B_h = KT_h\ (\varepsilon_j\ 1367 \sin \gamma_s) - D_h \quad \text{(A2.8)}$$

where B_h is the horizontal beam irradiation ($W \cdot m^{-2}$).

Thus, for a solar altitude of 30° and a KT_h value of 0.45, at mean solar distance:

$$B_h = 0.45 \times 1367\ (\sin 30) - 462.7\ (\sin 30) = 307.6 - 231.4 = 76.3\ W \cdot m^{-2}$$

This may be compared with a clear sky beam value, using a KT_h value of 0.70:

$$B_h = 0.70 \times 1367\ (\sin 30) - 329.9\ (\sin 30) = 478.5 - 165 = 313.6\ W \cdot m^{-2}$$

The maximum hourly diffuse irradiation on the horizontal surface therefore occurs statistically with the beam irradiation reduced to about a quarter of its clear sky value.

For greater accuracy, using a site-based and season-based approach, the following algorithm may be used with UK observations.

If $KT_h > 0.2$ then:

$$D_h / G_h = a_0 + a_1 KT_h + a_2 KT_h^2 + a_3 KT_h^3 \quad \text{(A2.9)}$$

otherwise:

$$D_h / G_h = 0.98 \quad \text{(A2.10)}$$

where a_0, a_1, a_2 and a_3 are site dependent seasonal polynomial coefficients. Table A2.2 below provides seasonally adjusted coefficients for eleven UK locations.

While covering the wide statistical range of conditions encountered with an acceptable accuracy for many purposes, equations A2.9/A2.10 unfortunately overestimate the diffuse radiation on clear days by 60–70%[(A2.7)]. This leads to a significant underestimation of clear sky beam irradiation (i.e. G_h observed minus D_h estimated). Such extreme beam data are particularly important for cooling load estimates. Therefore, for identifiable clear sky situations, in the absence of diffuse observations, it is recommended that the clear sky model described in section 3.2.3 should be used to estimate missing clear day hourly diffuse horizontal irradiation from hourly global horizontal irradiation observations. This approach can be used only for hours when the clear sky conditions can be identified.

It should be noted, however, that gaps in the Met Office hourly diffuse irradiation data for all UK sites were always filled using equations A2.9/A2.10. The clear day methodology described in section 2.2.3 yields significantly lower clear day diffuse irradiation values. A consequence of the differences between these procedures is that the estimated hourly beam component is higher in the tabulated 97.5 percentile series than that found in the corresponding, individually filled, hourly diffuse values on the hourly datasets.

As the approach described in section 3.2.3 has been shown to align very closely with clear sky observational data [(A2.8)], this method has been retained for estimating the hourly diffuse horizontal irradiances incorporated in the design 97.5 percentile tables. It is the substantially more accurate estimation method for days of high irradiation.

Table A2.2 Seasonal polynomial coefficients for eleven UK meteorological stations and mean values for the UK

Station	Latitude	Period	Number of hours	Winter				Summer				Spring			
				a_0	a_1	a_2	a_3	a_0	a_1	a_2	a_3	a_0	a_1	a_2	a_3
Lerwick	60° 08'	Jan 81–Dec 83	12701	0.617	3.668	–11.197	8.352	0.304	5.768	–14.271	8.840	0.685	3.143	–9.510	6.184
Stornoway	58° 12'	Oct 82–Dec 83	5263	0.539	4.513	–13.254	9.695	0.524	4.056	–10.106	5.766	0.576	4.030	–11.701	7.951
Shanwell	56° 26'	Jan 82–Dec 83	9396	0.456	5.237	–15.718	11.469	0.721	2.722	–7.903	4.614	0.579	4.418	–12.576	8.767
Eskdalemuir	55° 19'	Jan 81–Dec 83	12723	0.559	4.032	–11.715	7.818	0.638	3.228	–9.102	5.621	0.755	2.379	–7.429	4.609
Aldergrove	54° 39'	Jan 81–Dec 83	14107	0.644	3.090	–9.220	5.938	0.513	3.793	–9.739	5.745	0.679	2.800	–8.396	5.279
Aughton	53° 33'	Jan 82–Dec 83	8144	0.758	2.660	–8.839	6.162	0.777	2.142	–6.224	3.317	0.786	2.186	–6.891	4.062
Finningley	53° 29'	Nov 82–Dec 83	5116	0.312	6.614	–19.263	14.472	0.744	2.386	–6.796	3.718	0.572	4.034	–11.966	8.311
Hemsby	52° 51'	Jan 82–Dec 83	9006	0.487	5.055	–14.896	10.476	0.787	2.073	–6.198	3.340	0.790	2.139	–6.922	4.111
Aberporth	52° 08'	Jan 81–Dec 83	11937	0.579	4.093	–12.006	8.058	0.681	2.821	–7.650	4.260	0.741	2.628	–8.162	5.088
Easthampton	51° 23'	Jan 81–Dec 83	14058	0.349	6.085	–17.438	12.387	0.857	1.570	–5.608	3.271	0.784	2.396	–8.306	5.558
Camborne	50° 13'	Jan 82–Dec 83	9109	0.514	4.644	–13.539	9.389	0.632	3.211	–8.730	5.167	0.804	2.145	–6.977	4.198
UK	—	—	111552	0.629	3.549	–10.651	7.098	0.651	3.050	–8.460	5.006	—	—	—	—

References (Appendix A2)

A2.1 Orgill J F and Hollands K G T Correlation equation for hourly diffuse radiation on a horizontal surface *Solar Energy* **19** 357–359 (1977)

A2.2 Muneer T Solar radiation and daylight models for the energy efficient design of buildings (Oxford: Architectural Press) (1997)

A2.3 Muneer T and Saluja G S Correlation between hourly diffuse and global irradiance for the UK *Building Serv. Eng. Res. Techol.* **7** (1) 37–43 (1986)

A2.4 Muneer T Hourly diffuse and global solar irradiation, further correlation *Building Serv. Eng. Res. Technol.* **8** (4) 85–90 (1987)

A2.5 Kasten F and Czeplak G Solar radiation and terrestrial radiation dependent on the amount and type of cloud *Solar Energy* **24** 117–189 (1980)

A2.6 *Weather and solar data* CIBSE Guide A2 (London: Chartered Institution of Building Services Engineers) (1982) (out of print)

A2.7 Page J K Estimation of hourly diffuse horizontal irradiance from global irradiance records under clear sky conditions *Building Serv. Eng. Res. Technol.* (submitted for publication)

A2.8 Page J K The development of monthly near extreme day slope irradiance tables for three UK sites in standard formats, using observed hourly horizontal irradiation data for all days having a 95 precentile exceedence value of daily global irradiation within each month *Building Serv. Eng. Res. Technol.* (submitted for publication)

Appendix A3: Miscellaneous algorithms used in the development of the solar data

A3.1 Introduction

This section brings together various algorithms used in the development of this document, which are not reported in detail elsewhere in the text.

A3.2 Yallop algorithm for the accurate estimation of noon declination for a specific calendar date

This algorithm[A3.1] uses universal time (UT) to calculate the declination. UT is mean time at the Greenwich meridian (longitude 0°). To perform calculations for a site not located on the Greenwich meridian, it is necessary first to calculate what the time would be at longitude 0°.

When working in local clock time (LMT), one simply needs to know the time zone difference from GMT for the site. For example, Germany is 1 hour ahead of Greenwich time. Universal time in Germany is given by ($t_{LMT} - 1$) where t_{LMT} is the LMT expressed as a decimal (i.e. hour + minutes/60 + seconds/3600).

If working in solar time, it is necessary to know the precise longitude of the site. Then:

$$UT = t_{LAT} + (\lambda / 15) \quad \text{(A3.1)}$$

where t_{LAT} is the time of day in solar time (decimal hours) on day d, in month m, in year y and λ is the longitude (^{o}).

Equation A3.1 has astronomical origins and uses the convention that longitudes west of Greenwich are positive. For example, solar noon in Germany will occur earlier in UT than at sites further west in France, even though they share the same legal time framework.

A special time variable for computation is first established as follows:

$$T = \{(UT / 24) + d + [30.6\ m + 0.5] + [365.25\ (y - 1976)] - 8707.5\} / 36525 \quad \text{(A3.2)}$$

where T is the elapsed centuries from a starting reference start time, d is the day in the month, m is the month number and y is the year in full (e.g. 1992). [x] denotes the integer part of x.

If $m > 2$, i.e. potentially after February in a leap year, then $y = y$ and $m = (m - 3)$; otherwise $y = (y - 1)$ and $m = (m + 9)$.

T is first used to calculate the obliquity of eccentricity, e (degrees), i.e:

$$e = 23.4393 - 0.013\ T \quad \text{(A3.3)}$$

T is then used to calculate a quantity G (degrees), i.e:

$$G = 357.528 + 35999.05\ T \quad \text{(A3.4)}$$

If necessary, multiples of 360 degrees are added or subtracted to bring G within the range 0 to 360 degrees.

G is used in turn to calculate quantity C (degrees), i.e:

$$C = 1.915 \sin G + 0.020 \sin 2G \quad \text{(A3.5)}$$

C and T are used to calculate quantity L (degrees), i.e:

$$L = 280.460 + 36000.770\ T + C \quad \text{(A3.6)}$$

If necessary, multiples of 360 degrees are added or subtracted to bring L within the range 0 to 360 degrees.

L is next used to calculate quantity a (degrees), i.e:

$$a = L - 2.466 \sin 2L + 0.053 \sin 4L \quad \text{(A3.7)}$$

The hour angle at Greenwich is then given by:

$$\text{GHA} = 15\ U\ T - 180 - C + L - a \quad \text{(A3.8)}$$

where GHA is the hour angle at Greenwich (degree).

If necessary, multiples of 360 degrees are added or subtracted to bring GHA within the range 0 to 360 degrees.

The declination is given by: $\tan^{-1}$ (tan e sin a) (degrees).

The equation of time is: $(L - C - a) / 15$ (hours).

In very accurate solar calculations allowances have to be made to allow for refraction in the atmosphere. Such refraction corrections have not been applied in this document.

While the declination is a continuously varying function, it is normally satisfactory to estimate the declination at noon for the site under study and adopt it as a constant declination value for the day. The leap year cycle influences the declination found on particular days in the year. This variation is significantly greater than the declination change across a specific day.

A3.3 Algorithm for estimation of monthly mean daily beam diffuse horizontal irradiation and corresponding hourly irradiances from monthly mean daily global irradiation on a horizontal surface

This algorithm was developed by Page and Czeplak in connection with the *European Solar Radiation Atlas*[A3.2]. It is of particular value when presented with satellite-based daily global irradiation data sets on the internet. Such data sets usually provide only monthly mean daily global irradiation values. Additionally, many ground observed radiation data sets from international sources such as the World Radiation Data Centre, St Petersburg, also provide only daily global irradiation data. The use of the Angstrom relationship to estimate monthly mean daily global radiation yields a similar daily global irradiation output (see section 2.9). The algorithms below have been tested on a European-wide basis. They were the basic algorithms used to derive pixellated monthly mean daily diffuse irradiation data from the pixellated monthly mean daily global irradiation for the digital mapping of the monthly mean daily diffuse irradiation climate of Europe for the *European Solar Radiation Atlas*[A3.2].

The daily diffuse horizontal irradiation data can then be broken down into a daily diffuse horizontal irradiance profile. The daily beam irradiation on a horizontal surface, B_d, can be found as the difference between G_d and D_d. The daily beam horizontal irradiation data can then be broken down into a daily beam horizontal irradiance profile. The horizontal global irradiation profile is obtained by addition of the beam horizontal and the diffuse horizontal irradiance profiles. This is inherently a safer algorithmic procedure than estimating the global irradiance profile and estimating the beam by difference. In contrast to the standard global irradiation procedures such as suggested by Collares-Pereira and Rabl[A3.3], it avoids all risk of obtaining negative values of beam radiation. The values obtained in this way at low solar altitudes are always stable and properly defined in physical terms. Estimates based on the differences between two small numbers are avoided, so eliminating errors in beam irradiation when converting to beam normal irradiance at low solar elevations.

Inputs:

— monthly mean daily global irradiation on a horizontal plane, $(G_d)_m$ ($W \cdot h \cdot m^{-2}$)

— latitude, ϕ (^{o})

— solar constant, $I_o = 1367$ ($W \cdot h \cdot m^{-2}$)

— day number in year, J (1 to 365/366); note that mid-month day is used

— hour in day, t (h)

Outputs:

— monthly mean daily global irradiation on a horizontal plane, $(D_d)_m$ ($W \cdot h \cdot m^{-2}$)

— monthly mean beam irradiance on a horizontal plane at time t, $B_m(t)$ ($W \cdot h \cdot m^{-2}$)

— monthly mean diffuse irradiance on a horizontal plane at time t, $D_m(t)$ ($W \cdot h \cdot m^{-2}$)

Stage 1: input mid-month day number; calculate mid-month correction to mean solar distance, ε_l, using equation 5.13:

$$\varepsilon_l = 1.0 + 0.03344 \cos [J (360 / 365.25) – 2.8^o]$$

Stage 2: use mid-month declinations, δ, from Table 2 to calculate mid month sunset hour angle, ω_s, for given latitude ϕ, using equation 9:

$$\omega_s = \cos^{-1} (–\tan \phi \tan \delta)$$

Stage 3: calculate mid-month extraterrestrial irradiation, G_{od}, using equation 14:

$$(G_{od})_m = (24 / \pi)\, e_j\, I_o [(\omega_s\, \pi / 180) \sin \phi \sin \delta + \cos \phi \cos \delta \sin \omega_s)$$

It is important that $(G_{od})_m$ is estimated using the monthly mean declination.

Stage 4: estimate monthly mean daily KT value, $(KT_d)_m$, as $[(G_d)_m / G_{od}]$.

Stage 5: use equation A3.9 below, with coefficients selected according to season and latitude band from Table A3.1 below, to estimate the ratio $(D_d)_m / (G_d)_m$ and hence $(D_d)_m$ from the input value of $(G_d)_m$:

$$(D_d)_m / (G_d)_m = c_o + c_1 (KT_d)_m + c_2 (KT_d)_m^2 + c_3 (KT_d)_m^3 \qquad \text{(A3.9)}$$

Table A3.1 Coefficients of the third-order polynomial for estimation of monthly average diffuse horizontal irradiation(A3.2)

Latitude band	Season	c_0	c_1	c_2	c_3	$(KT_d)_m$ validation range
61° N > ϕ > 56° N	Winter	1.061	–0.397	–2.975	2.583	[0.11, 0.50]
	Spring	0.974	–0.553	–1.304	0.877	[0.24, 0.50]
	Summer	1.131	–0.895	–1.616	1.555	[0.26, 0.60]
	Autumn	0.999	–0.788	–0.940	0.788	[0.21, 0.51]
56° N > ϕ > 52° N	Winter	1.002	–0.546	–1.867	1.490	[0.14, 0.22]
	Spring	1.011	–0.607	–1.441	1.075	[0.22, 0.59]
	Summer	1.056	–0.626	–1.676	1.317	[0.29, 0.64]
	Autumn	0.969	–0.624	–1.146	0.811	[0.23, 0.53]
$\phi \leq$ 52° N	Winter	1.032	–0.694	–1.771	1.562	[0.15, 0.51]
	Spring	1.049	–0.822	–1.250	1.124	[0.23, 0.61]
	Summer	0.998	–0.583	–1.392	0.995	[0.27, 0.63]
	Autumn	1.019	–0.874	–0.964	0.909	[0.22, 0.55]

Stage 6: estimate the diffuse irradiance on a horizontal surface $D_m(t)$ at any time of day t (hours LAT):

(*a*) Convert time of day in LAT to an hour angle using equation 5.5:

$$\omega(t) = 15\,(t - 12)$$

where $\omega(t)$ is the hour angle (°)

(*b*) Then:

$$D_m(t) = r_{om}(t)\,(D_d)_m \tag{A3.10}$$

where r_{0m} given by:

$$r_{0m} = \frac{\pi}{24}\,\frac{[\cos\,\omega(t) - \cos\,(\omega_s)_m]}{[\sin\,(\omega_s)_m - (\omega_s)_m \cos\,(\omega_s)_m]} \tag{A3.11}$$

where $(\omega_s)_m$ is the mid-month sunset hour angle expressed in radians (calculated in step 2).

The daily profile of the beam irradiation can be estimated from the world clear sky irradiance tables in conjunction with the daily turbidity factor correction tables. The first step is to estimate the daily beam horizontal irradiation for the middle day of the selected month. An input value for the Linke turbidity factor for the month must be chosen in order to start the process (see sections 3.5 and 3.6). Four values of hourly mean daily beam horizontal irradiation for the clear sky design day for a given Linke turbidity factor are extracted for the selected month from the world clear sky irradiance tables. These four values provide a basis for linear latitudinal and date interpolation: two values are used to achieve the latitudinal interpolation and two to achieve the date interpolation. The two dates selected must be on either side of the mid-month day.

For example, consider the generation of a mean monthly beam irradiation profile for August for Jersey (latitude 49.22º N). The tables for latitudes 50º and 40º are selected. The design dates of August 4 and Sept 4 are selected.

For a Linke turbidity factor of 3.5, the four daily mean beam horizontal irradiance values extracted are:

— 40º N: Aug 4: 269 W·m^{-2}; Sept 4: 233 W·m^{-2}

— 50º N: Aug 4: 249 W·m^{-2}; Sept 4: 189 W·m^{-2}

The interpolated value for latitude 40º N for the date of August 15 is:

$$269 + [(233 – 269) \times (11 / 31)] = 256 \text{ W·m}^{-2}$$

The interpolated value for latitude 50º N for the date of August 15:

$$249 + [(189 – 249) \times (11 / 31)] = 227 \text{ W·m}^{-2}$$

Hence the interpolated value for latitude 49.22º N is:

$$256 + [(227 – 256) \times (9.22 / 10)] = 229 \text{ W·m}^{-2}$$

This may be converted to a daily irradiation by multiplying by 24, thus:

$$G_{cd} = 229 \times 24 = 5494 \text{ W·h·m}^{-2}$$

A Linke turbidity factor appropriate to the site is now selected from the turbidity correction factot table, say 4.5. The four corresponding daily beam correction ratios together are extracted, along with the values for a Linke turbidity factor of 3.5:

(*a*) For Linke turbidity factor 3.5

— 40º N: correction factors are 0.87 (Aug 4) and 0.86 (Sept 4)

— 50º N: correction factors are 0.86 (Aug 4) and 0.85 (Sept 4)

(*b*) For Linke turbidity factor 4.5

— 40º N: correction factors are 0.76 (Aug 4) and 0.75 (Sept 4)

— 50º N: correction factors are 0.74 (Aug 4) and 0.72 (Sept 4)

For 50º N, for Linke turbidity factor of 3.5 the mean correction factor is 0.855, and for Linke turbidity factor of 4.5 the mean value is 0.73. Hence the daily irradiation for turbidity factor 4.5 is obtained from the value at T_{LK} 3.5 as follows:

$$5494 \times (0.73 / 0.855) = 4691 \text{ W·h·m}^{-2}$$

For 40º N, for Linke turbidity factor of 3.5 the mean correction factor is 0.865, and for Linke turbidity factor of 4.5 the mean value is 0.755. Hence the daily irradiation for turbidity factor 4.5 is obtained from the value at T_{LK} 3.5 as follows:

$$5494 \times (0.755 / 0.865) = 4795 \text{ W·h·m}^{-2}$$

The daily irradiation for latitude 49.22º N is then obtained from the values at 40º N and 50º N by interpolation, i.e:

$$4691 + [(4795 – 4691) \times (9.22 / 10)] = 4787 \text{ W·h·m}^{-2}$$

The clear beam irradiance at any time of day *t* can be calculated using equation 38 in conjunction with equations 39, 41 and 42 as:

$$B_c(t) = 1367\ \varepsilon_j \exp [–0.8662\ m\ T_{LK}\ \delta_r(m)] \sin \gamma_s \qquad \text{(A3.12)}$$

Using the approximation that the mid-hour irradiance equals the hourly irradiation and assuming the average profile has the same relative form as the clear day profile, the monthly mean hourly irradiation, $(B)_m(t)$, can be estimated as as:

$$B_m(t) = (B_c(t) / B_{cd}) \times (B_d)_m \quad \text{(A3.13)}$$

where $B_m(t)$ is the monthly mean hourly beam irradiation on the horizontal at time t ($W \cdot m^{-2}$), $B_c(t)$ is the mid-hour clear sky beam irradiance on the horizontal plane calculated for that mid-hour solar altitude at time t using the selected Linke turbidity factor ($W \cdot m^{-2}$), B_{cd} is the corresponding clear sky daily global irradiation on the horizontal plane calculated for the site turbidity factor ($W \cdot h \cdot m^{-2}$), $(B_d)_m$ is the monthly mean daily beam irradiation on the horizontal plane ($W \cdot h \cdot m^{-2}$).

A3.4 Algorithm for estimation of clear day diffuse irradiances on vertical surfaces for the world clear sky irradiance tables

A3.4.1 Estimation of diffuse irradiance on horizontal surfaces

As the sky becomes more turbid, the diffuse horizontal irradiance increases while the beam horizontal irradiance decreases. The simple model recommended is based on a reformulation of the more complex earlier diffuse model[(A3.5)]. The relationship is now expressed as a polynomial sine function of the solar altitude[(A3.2)].

The diffuse irradiance modeling is carried out in two stages. First, the value of the diffuse irradiance transmittance with the sun at the zenith is calculated using equation A3.14. The diffuse irradiance transmittance, $T_r(D)$, expresses the diffuse irradiance received at sea level with sun at an altitude of 90º as a fraction of the corresponding extraterrestrial irradiation on the horizontal plane. It is calculated using the selected air mass 2 Linke turbidity factor, T_{LK}. The term (p / p_o) in equation A3.14 makes allowance for the effect of site height, taking account of the reduced atmospheric solar path length with increase of site elevation. The diffuse irradiance transmittance is then multiplied by the solar elevation function to correct the zenith value to the actual solar elevation. Finally the correction to mean solar distance is applied.

The following second order polynomial expression is used to calculate the clear sky diffuse transmittance:

$$T_r(D) = (-21.657 + 41.752.(p / p_o)\, T_{LK} + 0.51905\, ((p / p_o)\, T_{LK})^2 / 1367 \quad \text{(A3.14)}$$

(Values of the air mass 2 Linke turbidity factor between 3 and 8 were used in obtaining the regression).

The solar elevation function, $F(\gamma_s)$ is next evaluated using A3.15:

$$F(\gamma_s) = C(0) + C(1) \sin \gamma_s + C(2) \sin^2 \gamma_s \quad \text{(A3.15)}$$

where γ_s is the solar altitude in degrees and $C(0)$, $C(1)$ and $C(2)$ are polynomial regression coefficients, the values of which depend on the air mass 2 Linke turbidity factor, T_{LK}.

The values of the coefficients used to determine $C(0)$, $C(1)$ and $C(2)$ are found from equations A3.16 and A3.17, inputting the product of Linke turbidity factor and site height pressure correction (p / p_o). (See equation 41 in section 3.2.2 for the estimation of (p / p_o) from the site height above sea level.).

$$C(0) = 0.26463 - 0.061581\, (p / p_o)\, T_{LK} + 0.0031408\, ((p / p_o)\, T_{LK})^2 \quad \text{(A3.16)}$$

If $(1367\, T_r(D) \times C(0)) < 3\ W \cdot m^{-2}$, then:

$$C(0) = 3 / (1367\ T_r(\mathrm{D})) \quad \text{(A3.17)}$$

$$C(1) = 2.0402 + 0.018945\ (p / p_o)\ T_{LK} - 0.011161\ ((p / p_o)\ T_{LK})^2 \quad \text{(A3.18)}$$

$$C(2) = -1.3025 + 0.039231\ (p / p_o)\ T_{LK} + 0.0085079\ ((p / p_o)\ T_{LK})^2 \quad \text{(A3.19)}$$

The cloudless sky diffuse irradiance on a horizontal surface at a solar altitude of γ_s is calculated as:

$$D_c = \varepsilon_j\ 1367\ T_r(\mathrm{D})\ F(\gamma_s) \quad \text{(A3.20)}$$

where D_c is the cloudless sky diffuse irradiance on a horizontal surface ($W \cdot m^{-2}$) and ε_j is the correction to mean solar distance on day J (see section 5.2.8.2).

Figure 8 plots the sea level diffuse horizontal irradiance values at mean solar distance against solar altitude for a range of Linke turbidity factors using this simplified turbidity sensitive diffuse horizontal irradiance model.

The diffuse horizontal irradiance is not zero at sunrise. The model uses the following values, which are incorporated in the polynomial coefficients in the equations above. The polynomial fitting process produces a small distortion from the original values used in the fitting process.

Table A3.2 Assumed values of diffuse horizontal irradiance at zero solar altitude used in the fitting process

Air mass 2 Linke turbidity factor	Assumed diffuse irradiance at zero solar altitude ($W \cdot m^{-2}$)	Polynomial values
2	10	9.8
3	9	11.5
4	8	10.5
5	7	7.1
6	6	2.5
7	5	2.8

The model begins to give less reliable results when the air mass 2 Linke turbidity factor rises aboue 7.

A3.4.2 Estimation of clear sky diffuse irradiance on vertical surfaces

The diffuse irradiance from the sky falling on vertical surfaces is combined with the ground reflected component in the world clear sky solar irradiance tables. The sky component is derived from the horizontal surface diffuse irradiance values. It is based on a methodology first developed by Page[(A3.5)]. The original model was improved and simplified by Littlefair[(A3.6)], who followed the original 1986 parameterisation for the Linke turbidity factor. In order to use the formula, the AM2 Linke turbidity factor has first to be corrected for solar altitude. The value of $T_{LK}(\gamma_s)$, the solar altitude corrected Linke turbidity factor at a solar altitude of γ_s, may be found from the air mass 2 Linke turbidity factor by the following expression:

$$T_{LK}(\gamma_s) = T_{LK}(\text{air mass 2}) - (0.85 - 2.25 \sin \gamma_s + 1.11 \sin^2 \gamma_s) \quad \text{(A3.21)}$$

where γ_s is the solar altitude angle (^{o}) and T_{LK} (air mass 2) is the Linke turbidity factor at air mass 2.

Equation A3.21 is not valid below T_{LK}(air mass 2) = 2.5.

Setting $T_{LK}(\gamma_s)$ as T and sin γ_s as s, Littlefair obtained the following equation, which has been used to generate the sky component of diffuse irradiances on vertical surfaces in the world clear sky solar irradiance tables.

$$\begin{aligned} D_c(\alpha_F) / D_c = \{&1.175 - 0.25\, s - 0.164\, s^2 - 0.0947\, T - 0.04\, T\, s + 0.0127\, T\, s^2 \\ &+ 0.0076\, T^2 - 0.0003\, T^2\, s + 0.0005\, T^2\, s^2\} \\ &+ \{0.19 + 0.273\, s - 0.405\, s^2 + 0.106\, T - 0.0043\, T\, s - 0.1\, T\, s^2 \\ &- 0.0029\, T^2 - 0.007\, T^2\, s + 0.0102\, T^2\, s^2\} \cos \alpha_F \\ &+ \{0.157 - 0.068\, s - 0.09\, s^2 + 0.0104\, T + 0.0162\, T\, s - 0.028\, T\, s^2 \\ &- 0.0006\, T^2 - 0.003\, T^2\, s + 0.0026\, T^2\, s^2\} \cos (2\, \alpha_F) \end{aligned} \quad \text{(A3.22)}$$

where α_F is the wall solar azimuth angle (°), see section 2.7, Figure 3.

By trigonometry:

$$\cos (2\, \alpha_F) = 2 \cos^2 \alpha_F - 1 \quad \text{(A3.23)}$$

This expression holds up to a solar elevation of 70 degrees. The values of the ratio with the sun overhead are as follows:

— 0.44 for Linke turbidity factor of 3

— 0.38 for Linke turbidity factor of 4

— 0.34 for Linke turbidity factor of 5

— 0.32 for Linke turbidity factor of 6.

Linear interpolation is used between a solar elevation of 70 degrees and 90 degrees.

Figure 9 plots the values of $D_c(\alpha_F) / D_c$ as a function of solar altitude for a Linke turbidity factor of 3.5.

The ground reflected contribution is added to the sky component to give the total diffuse component. It is estimated as explained in section 3.3.3. The world clear sky solar irradiance tables are based on a ground albedo of 0.2. Corrections for other ground albedos are made as explained in section 3.3.3.

Unlike the Muneer slope radiation algorithm[A3.7] described in section 2.11.5, this algorithm is sensitive to the air mass 2 Linke turbidity factor. It yields values very close to the Muneer algorithms at an air mass 2 Linke turbidity factor of 4.5. However, it is only applicable in this simplified form for estimates for vertical surfaces.

References (Appendix A3)

A3.1 Yallop B D *Algorithm for solar declination angle* (Cambridge: Royal Greenwich Observatory) (1992)

A3.2 Scharmer K and Grief J (co-ordinators) *European Solar Radiation Atlas (4th edn.) Vol. 2: Database and exploitation software* (Paris: Les Presses de l'École des Mines de Paris) (2000)

A3.3 Collares-Pereira M and Rabl A The average distribution of solar radiation — correlations between diffuse and hemispherical, and between daily and hourly insolation values *Solar Energy* **22** 155–164 (1979)

A3.4 Rigollier C, Bauer O and Wald L On the clear sky model of the European Solar Radiation Atlas with respect to the Heliostat method *Solar Energy* **68** (1) 33–48 (2000)

A3.5 Page J K (ed.) *Prediction of solar radiation on inclined surfaces* Solar Energy R&D in the European Community, Series F3: Solar Radiation Data (Dordrecht: Reide) (1986)

A3.6 Littlefair P *A working paper from ESRA project No JOU2-CT—94-03505/P0603* (unpublished) (1996)

A3.7 Muneer T Solar radiation model for Europe *Building Serv. Eng. Res. Techol.* **11** 153–163 (1990)